An investigation into the sensitivity of the performance of an active solar heating system to the control strategy employed.

Reynell, M. J. W.

Award date:
1985

Awarding institution:
University of Bath

AN INVESTIGATION INTO THE SENSITIVITY OF THE PERFORMANCE OF AN ACTIVE SOLAR HEATING SYSTEM TO THE CONTROL STRATEGY EMPLOYED.

submitted by M.J.W.Reynell

for the degree of PhD

of the University of Bath

1985

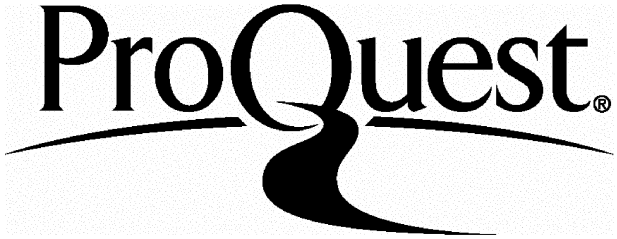

CONTENTS

CONTENTS

CONTENTS page

CONTENTS

CONTENTS page

LIST OF FIGURES

LIST OF FIGURES

LIST OF FIGURES

LIST OF TABLES

NOMENCLATURE

Symbol	Meaning	Units
a,b,c,k	heat capacity	kJ/°K
Cp	specific heat capacity of fluid	J/Kg°K
D	day of year (Jan 1st = day 1)	
dTon,dToff	temperature differentials between solar absorber plate and solar store at which circulating pump is switched on/off	°K
E	pipe loss effectiveness	
F	"shape factor" converting tank volume to surface area	
Fr	"heat removal factor", a constant whose value is related to the effectiveness of heat transfer from the absorber plate to the heat removal fluid	
h	heat capacity flow rate in pipework (m.Cp)	J/s°K
Ibeam	direct irradiation on a normal surface	W/m²
Id	diffuse irradiation on a horizontal surface	W/m²
Ie	extra-terrestrial radiation on a horizontal surf	W/m²
Ig	global solar radiation on a horizontal surface	W/m²
Ir	direct irradiation on a horizontal surface	W/m²
k	thermal conductivity	W/m°K
Kp	pump control index (=1 if pump on)	
Kt	"clearness index" (Ig/Ie)	
L	pipe length	m

NOMENCLATURE

$\dot{m}$	mass flow rate	Kg/s
p	density	Kg/litre
Q	heat flow	W
Qc	rate of heat gain across collector	W/m^2
Qi	incident solar radiation normal to collector plane	W/m^2
Ql	rate of heat loss	W
Qw	hot water load	W
Rs	stable fixed resistance in temperature measuring circuit	ohm
Rt	sensor resistance in temperature measuring circuit	ohm
ri,ro	inner and outer radii of pipe/insulation combination	m
Sc	solar constant	W/m^2
ta	transmittance/absorptance product for glass cover and absorber plate combined	
T	temperature	°K
Ta	ambient air temperature	°K
Tcw	cold water inlet temperature	°K
Ti,To	collector inlet and outlet temperatures	°K
Tp	mean collector absorber plate temperature	°K
Ts	solar store temperature	°K
Tw	hot water tank temperature	°K
U	heat loss coefficient	$W/m^2°K$
UA	overall heat loss coefficient for pipe section	W/°K

NOMENCLATURE

UAs	overall effective heat loss coefficient for solar store	W/°K
Ul	overall effective heat loss coefficient for collector	$W/m^2°K$
V	volume flow rate	litres/s
Vhour	volume of hot water draw-off during hour	litres
Vt	output voltage from temperature measuring circuit	
Vs	excitation voltage in temperature measuring circuit	

ACKNOWLEDGEMENTS

The work reported in this thesis is the result of investigations carried out during my four-year stay at the School of Architecture and Building Engineering of the University of Bath.

The monitoring aspect of the work was supervised by Dr Robin Forrest, Dr Barry Alper and Dr David Bartholemew of ETSU (the Energy Technology Support Unit), AERE Harwell, and their assistance is gratefully acknowledged.

My thanks also to Dr John Rosenfeld and Barry Pye of the Shell Thornton Research Centre who played a significant part in the original development of the computer model, and helped with the considerable task of taking over this valuable research tool.

The work has benefitted from the attention of my supervisor Stephen Edwards, Professor Frank Wallace of the School of Engineering, and of many other colleagues within the School of Architecture and Building Engineering. Special thanks are due to my friend and colleague Richard Lewis, without whose skills in electronics and computing this work could not have been successfully completed.

Finally, thankyou to word processors for making the task of text presentation just bearable.

DECLARATION

The work submitted in this thesis is the result of investigations carried out by the author. Acknowledgement is given by means of a reference where work performed by others is discussed.

The material in this thesis has not already been accepted for any degree, and is not concurrently submitted in candidature for any other degree.

signed: _____

(Candidate)

signed: _____

(Director of studies)

SYNOPSIS

The aim of this thesis was to investigate and challenge current thinking regarding the sensitivity of the thermal performance of active solar water heating systems to the control strategy employed, with particular attention to the effect of the control temperature differential settings between the solar absorber plate and the solar store at which the circulating pump is switched on and off (dTon and dToff).

A mathematical analysis suggested that the performance should be more sensitive to the above parameters than is generally believed. The theoretical appraisal also suggested a relationship for the ratio dTon/dToff required for stable pump control.

Measured data from a large-scale solar heating field trial were carefully correlated with the predictions of a computer model. The calibrated model was then used to carry out a sensitivity analysis into the effect of altering the control criteria.

The results have shown that, contrary to current thinking, the long-term thermal performance of the system is significantly impaired by the use of a pump switch-on criterion (dTon) higher than 6°K, and that the sensitivity to this parameter increases with increasing dTon. The results have also revealed that the heat losses throughout the system are five or six times higher than theoretical calculations based on the insulation manufacturers'

specifications predict. This is not an isolated result, but has been experienced on other monitored installations, and the implication is that the quoted figures for insulation performance (which are derived from tests under tightly controlled laboratory conditions) are extremely difficult to achieve in practice. It is argued that the above two observations are linked, and that a high switch-on criterion leads to significant amounts of collectable solar radiation being wasted as the collector absorber plate loses heat to the surrounding air without reaching a temperature sufficient to turn the circulating pump on.

The effect of the control settings on pump switching stability was also investigated, and, whilst the point at which instability occurred did not agree precisely with the theoretical value, the general relationship between the ratio dTon/dToff and the number of pump switching cycles per year supported the mathematical hypothesis. The discrepancy was attributed to the difficulty of measuring the collector overall heat loss coefficient, Ul, precisely. For the installation under study it was found that a value of dTon/dToff above 8 would ensure stable pump control.

Interpreting optimum performance in terms of both annual solar energy output and pump switching stability, the combination of all the above results led to the general recommendation that a pump switch-on setting of 4-6°K with a switch-off setting of 0.1-0.5°K should be employed to achieve optimum performance of a solar water heating system utilising flat plate solar collectors in the UK.

SYNOPSIS

The switch-on criterion of 4-6°K can be achieved reasonably easily by the use of standard, inexpensive controllers and nickel-based temperature sensors. However, such controllers are not capable of consistently resolving temperature differentials to the degree required to meet the switch-off criterion of 0.1-0.5°K over the full operating temperature range. For large installations, therefore, the use of high quality controllers with calibrated platinum resistance thermometers as temperature sensors will prove cost-effective and is strongly recommended.

1. INTRODUCTION

Most of the research into solar heating system performance to date has concentrated on developing design rules for optimising the major design variables such as collector area, storage volume, collector tilt angle, orientation and so on. There is, therefore, a large and ever-growing body of literature on these topics. A number of design methods have been developed by Duffie and Beckman (1980) and Kenna (1982) for the selection and sizing of the major components of active solar heating systems (e.g collector area, store size), according to the climatic conditions and heating loads imposed on them. There is, however, relatively little previous work on the subject of control strategy and its effect on long-term thermal performance. The latter was therefore selected as the topic for this thesis.

The thermal performance monitoring of a large-scale solar water heating system on the new catering complex at Torbay District General Hospital in Devon provided the experimental basis for this study. However, the measured results alone are of little long-term significance since they are heavily dependent on the particular meteorological conditions and load profile prevailing during the measurement period. Having no control over the meteorological conditions or load profile, it is impossible to assess experimentally the long-term effects of alterations in system parameters such as control strategy. This problem can be tackled in the laboratory, where by means of an artificially controlled

solar input and load profile, the effects of specific design variable changes may be assessed. However, this approach is expensive and time-consuming, requiring several full-length experiments to be carried out before definitive conclusions can be reached. Furthermore, it is well-known that results achieved in the laboratory frequently bear little relation to results achieved in the field.

An alternative approach is to make use of computer simulation. Computer simulation methods were first used in the study of solar processes by Sheridan et al. (1967). Since then, solar process simulation programs have been developed extensively and are now in fairly widespread use. Computer simulations are essentially numerical experiments which can yield the same kind of thermal performance information as can physical experiments, but considerably more quickly and inexpensively. One of the most powerful aspects of computer simulation is that it can provide information on the effects of specific design variable changes on the system performance through a series of experiments all using exactly the same loads and weather conditions.

However, simulations are not substitutes for physical experiments. Full scale physical experiments are necessary to test the mathematical algorithms used, and to bring to light the many practical problems inherent in any complicated system that simulations cannot model. Careful comparisons of experiments and simulations lead to a better understanding of each, and lend

confidence to the mathematical models used. Once simulations have been verified with experimental results, new systems can be designed with confidence using simulation methods. The present study, therefore, places considerable emphasis on the collection of reliable and accurate measured data from the site, and on the correlation of these data with a computer model.

The aim of the present study was not to develop an original computer model from scratch, which would not have been a particularly useful task as there are a number of existing models which have been developed over many years by establishments such as the Solar Energy Unit, University College, Cardiff, the University of Wisconsin, Faber, and the Shell Thornton Research Centre (STRC) in Cheshire. Instead, the thrust of the research has been to take over a model already developed by STRC, calibrate it against measured data from site, and then use it for the investigation outlined above.

This work will contribute to the present state of knowledge in the following areas:

1) the optimisation of automatic control strategies for active solar heating installations.

2) the validation of computer simulation methods for the modelling of solar heating processes.

3) the fundamental design of solar heating installations.

2. LITERATURE REVIEW AND THEORETICAL APPRAISAL.

2.1 Background

Two types of control are commonly used on solar collectors: on/off and proportional. With an on/off controller, a decision is made to turn the circulating pump on or off depending on whether or not useful output is available from the collectors. With a proportional controller, the pump speed is varied in an attempt to maintain a specified temperature level at the collector outlet. Of these two, the former is the simplest and most common form of control, requiring just two temperature sensors, one in the base of the storage tank and one on the absorber plate at the exit of a collector (or on the pipe near the plate), as shown in figure 2.1.

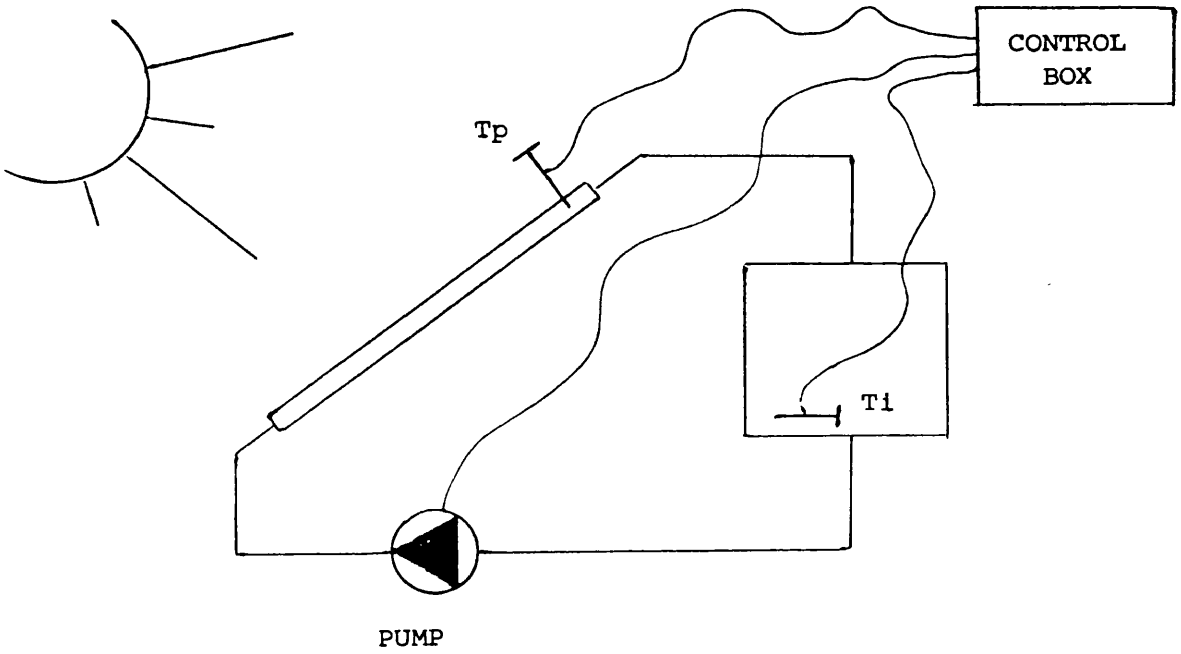

Figure 2.1 Common control method for solar heating systems.

CHAPTER TWO

A considerable amount of research has been carried out to determine the possible benefits of the latter approach, that is optimal control of the flow rate through the panel array. Kovarik and Lesse (1976) have studied this concept, but their numerical results are not suitable for practical application for the following two reasons:

i) the solution requires prior knowledge of the insolation as a function of time

ii) the resulting optimal control is given as a function of time and not as a function of a measurable state (e.g temperature, insolation) of the system, and thus cannot be used as a basis of design for a controller.

Winn and Hull (1978) have further studied the concept of optimal flow rates through collectors, by attempting to maximise the difference between solar energy collected and energy required for pumping fluid through the collector. This is the best criterion for assessing collector performance, since if the pumping energy is ignored the mathematical theory leads to the trivial and impracticable solution that maximum flow rate should be applied whenever the heat gain across the collector is positive.

The results of Kovarik and Lesse (1976) and Winn and Hull (1978), as well as other work by Duffie and Beckman (1980) have shown that,

provided the flow rate through a water collector exceeds the equivalent of 0.01 kg/s per square metre of collector area, the thermal performance of the system is not sensitive to the value chosen. It is not, therefore, proposed to dwell further on the subject of optimal flow control.

2.2 On/off control

Attention now focuses on the simple on/off control system of figure 2.1. The operation is as follows:

Assuming the collector has low heat capacity, then when fluid is flowing transducer Tp senses the collector exit fluid temperature. When fluid is not flowing, this transducer senses the plate temperature. A controller receives this temperature and the temperature at the base of the storage unit. This storage temperature will be called Ti. Assuming lossless connecting pipes, the temperature at the bottom (or exit portion) of the storage tank will also be the collector inlet temperature. Whenever the plate temperature Tp at no-flow conditions exceeds Ti by a set amount (dTon), the pump is switched on. When the pump is on and the measured temperature differential falls below a set amount (dToff), the pump is switched off.

The question is whether the long-term thermal performance of the system is sensitive to the control settings dTon and dToff. Jorgensen (et al) at the University of Denmark (1982) have carried

out some preliminary studies into the effects of variations in these control parameters. However, the emphasis in their work was on the correlation of results from several different solar simulation programs, and so a definitive sensitivity analysis on these parameters was not completed.

Current opinion regarding the importance of the control setting dTon is summed up by Duffie and Beckman (1980) as follows: "Raising the turn on setting (dTon) to 20°K or more will not significantly reduce the useful energy collection." This is stated without evidence or reference to other work, and therefore excited the curiosity and scepticism of the author. On further investigation, recent work by Howells (1984) was found to support the above view. Howells states that "the solar fraction is virtually insensitive to the dTon temperature differential". Howells' work is based on the results of computer simulations, but was carried out without the benefit of a model specifically calibrated using actual measured data. The results are therefore challenged here.

Let us now investigate the effect of choosing various values of the control temperature differentials dTon and dToff.

CHAPTER TWO

THEORETICAL APPRAISAL

2.3 Pump switching stability analysis

When the pump is off, the useful output from the collector is zero and the absorber plate will reach an equilibrium temperature where the heat losses equal the solar heat gains. A comprehensive theoretical analysis of the thermal characteristics of solar collectors is complex and is not part of the scope of this thesis. (For example, heat losses by radiation increase as the fourth power of the absolute temperature, making radiation losses increasingly significant as the plate temperature becomes more than 25°K above the ambient temperature.) The first detailed analysis of these various factors was carried out by Hottel and Woertz (1942). However, a relatively simple equation was developed Hottel and Whillier (1958), Whillier (1977) and Bliss (1959), widely known as the Hottel-Whillier-Bliss equation, which expresses the heat collected per unit area, Qc, in terms of two operating variables, the incident solar radiation normal to the collector plate, Qi, and the temperature difference between the collector inlet temperature, Ti, and the surrounding air temperature, Ta, as follows:

$$Qc = Fr.[(ta).Qi-Ul.(Ti-Ta)] \qquad (2.1)$$

where:

Fr = "heat removal factor", a constant whose value is related to

the effectiveness of heat transfer from the absorber plate to the heat removal fluid.

ta = The transmittance/absorptance product for the glass cover and absorber plate combination. This factor takes account of the complex interaction of optical properties in the solar radiation wavelengths, and is actually some 5% higher than the simple product of the transmittance of the glass and the absorptance of the plate because some of the radiation originally reflected from the collector plate is reflected back again from the inside of the glass cover (the "greenhouse effect").

Ul = the overall effective heat loss coefficient for the collector. This factor takes account of radiative, convective and conductive heat losses.

Ti = collector inlet temperature (or store exit temperature)

Ta = ambient air temperature

Equation (2.1) represents a simplification of a great deal of complex theoretical heat transfer analysis, but Smith and Weiss (1975) have shown that it provides an adequate representation of the performance of flat plate solar collectors.

Under no-flow conditions, then, equation (2.1) reduces to:

$$0 = [S - Fr.Ul.(Tp - Ta)] \qquad (2.2)$$

where $S = Fr.(ta).Qi$

Tp = mean temperature of absorber plate

The value of S when Tp is equal to (Ti+dTon), (i.e sufficient to switch the pump on) is:

$$Son = Fr.Ul.(Ti + dTon - Ta) \qquad (2.3)$$

When the pump does turn on, the useful heat gain is then given by equation (2.1):

$$Qc = [Son - Fr.Ul.(Ti - Ta)] \qquad (2.4)$$

which, when equation (2.3) is substituted for Son, becomes:

$$Qc = Fr.Ul.dTon \qquad (2.5)$$

The collector outlet temperature To, under these conditions is given by:

$$Qc = \dot{m}.Cp.(To - Ti) \qquad (2.6)$$

where:

$\dot{m}$ = mass flow rate of collector fluid (kg/sm^2)

Cp = specific heat capacity of collector fluid (J/kg°K)

The temperature (To - Ti) is the temperature difference measured by the controller after flow begins. If this temperature difference is less than dToff, the pump will immediately switch off again and instability will ensue, with the pump cycling rapidly on and off unless the solar radiation increases to a level significantly higher than that corresponding to Son. (This was a problem with some early controllers installed in solar heating systems during the 1970's, where the controller had no facility for setting different dTon and dToff temperature differentials, but relied on the inherent switching hysterisis which was insufficient to avoid cycling.)

For stable operation at radiation levels around Son, therefore, the following inequality must be satisfied:

$$dToff <= dTon.(Fr.Ul/\dot{m}.Cp) \qquad (2.7)$$

or, re-arranging:

$$dTon/dToff >= (\dot{m}.Cp)/(Fr.Ul) \qquad (2.8)$$

The values of $\dot{m}$, Cp, Fr and Ul for the collector array studied in this thesis are 0.014 kg/sm², 4180 J/kg°K, 0.92, and 5.0 W/m²°K respectively, giving a stability criterion of:

$$dTon/dToff >= 12.7 \qquad (2.9)$$

It should be emphasised that equation 2.8 is the result of a simple steady-state analysis of what is essentially a dynamic problem. Nevertheless, the equation gives an indication of the relationship between the control settings dTon and dToff necessary to ensure stability. Equation 2.8 also shows, rather interestingly, that systems using higher mass flow rates and fluids with higher specific heat capacities will be more difficult to control, while systems with high heat losses will be easier to control. The opposite applies in both cases when the thermal performance of the system is the criterion. Clearly, therefore, a compromise is required between controllability and thermal performance.

2.4 Control settings and thermal performance

The effect of the control settings on thermal performance will now be considered. During periods of medium-level solar radiation, an excessively high switch-on criterion will, it is thought, allow substantial amounts of useful solar energy to go uncollected, since the combined radiative, conductive and convective heat losses from the collector when the aborber plate is at, say, 20°K above ambient temperature may equal the solar radiation absorbed. This equilibrium may persist for considerable lengths of time, although this depends on what happens to the solar radiation. The thermal performance penalty may be more severe in the UK and European climate, where sunny spells are frequently interrupted by passing

clouds, than in the USA, where sunny spells tend to be more prolonged. The thermal capacity of the collector itself will play a part here. A low thermal capacity will minimise the effect of passing clouds and brief, interrupted sunny spells in terms of the long term thermal performance of the system. A high thermal capacitance in such conditions may mean that the switch-on temperature is never attained. The thermal capacity of the collector is, therefore, an important parameter which cannot be ignored in the analysis.

The foregoing qualitative argument gives us some insight into the variables involved, and leads to the suspicion that the effect of the control setting dTon should be more significant than current opinion suggests. The above argument does not, however, lead to any definitive conclusions, and a more quantitative approach is required.

The question is whether the thermal performance of the system is sensitive to the control settings dTon and dToff. For example, a switch-on criterion dTon = 20°K with a switch-off criterion dToff = 1.5°K can be achieved quite easily using standard off-the-shelf analogue controllers, but will such a control strategy give a long-term performance penalty compared to, say, dTon = 6°K, dToff = 0.5°K? Such a question cannot be answered by means of an analytical mathematical treatment of this control function in a solar heating system operating over periods as long as one year, because the differential equations governing the thermal behaviour

of the system are non-linear. The non-linearities result from changes in the system state (e.g pumps switching on, motorised valves switching) and the input irradiance. Computer simulation, however, allows rapid repeated numerical solution of the non-linear equations, and is therefore an invaluable tool for this type of analysis.

A full mathematical treatment, including a statistical survey of meteorological variables would be out of place here since this is exactly what the computer model is designed to do. Before introducing the computer model, however, it is useful to establish factors such as the intensity of solar radiation below which no solar energy will be collected for a given switch-on criterion, and the rate of response of a collector of given thermal capacitance to step changes in solar irradiance.

2.4.1 Collector heat losses.

The combined radiative, convective and conductive heat losses from the collector, Ql, may be expressed by:

$$Ql = Ul.(Tp - Ta) \qquad (2.10)$$

where: Tp = mean absorber plate temperature

Ul = overall effective heat loss coefficient

The value of Ul will vary with factors such as wind speed and

absolute absorber temperature. However, a frequently used mathematical simplification which Smith and Weiss (1975) have shown to be adequate for flat plate collectors is to assume a constant value of Ul. A typical value for a single glazed flat plate solar collector with 50mm of glass fibre wool back insulation is 6 $W/m^2°K$. The heat losses from the collector are then a straightforward linear function of the temperature difference (Tp - Ta), as shown in figure 2.2, reaching a figure of 120 W/m^2 at a temperature difference of 20°K.

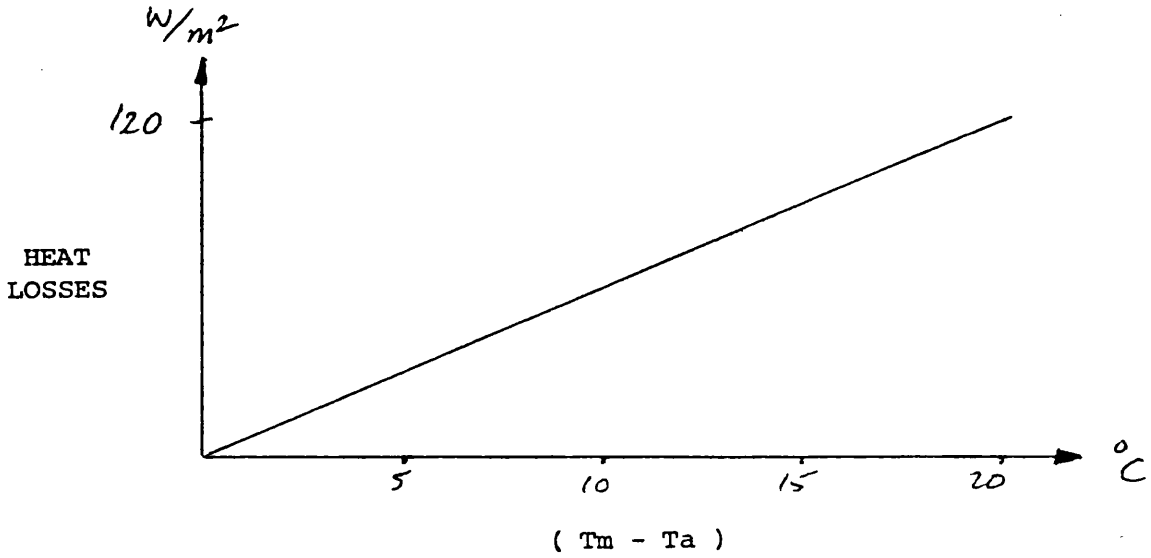

Figure 2.2 Heat losses from typical single glazed solar collector

The proportion of incident solar energy absorbed, from equation (2.1), is Fr.(ta), a factor which takes account of the transmittance/absorptance product of the glass cover/absorber plate

combination, as well as the fin effectiveness. A typical value for a single glazed solar collector with non-selective surface finish is 0.6.

Under no-flow conditions, therefore, with a switch-on criterion dTon = 20°K, the minimum solar irradiance required to switch the pump on is given by:

$$(ta).Qi(min) = Ul.(Ts-Ta+dTon) \qquad (2.11)$$

or, re-arranging:

$$Qi(min) = Ul.(Ts-Ta+dTon)/(ta) \qquad (2.12)$$

Typical values of Ul, and (ta) for a single glazed flat plate solar collector with 50mm of glass fibre wool back insulation are 6.0 $W/m^2°K$ and 0.6 respectively.

Thus, for a given temperature difference between the store and ambient air, Qi(min) is given by:

$$Qi(min) = (6.0/0.6).(Ts-Ta+dTon)$$

When the store is at the same temperature as the ambient air (Ts-Ta = 0), then Qi(min) is directly proportional to the switch-on temperature dTon:

$Qi(min) = Ul.dTon/(ta)$

$= (6.0/0.6).dTon$

And for a dTon setting of 20°K,

$Qi(min) = 200\ W/m^2$

This means that, with dTon set at 20°K, a thermal equilibrium could be set up with the absorber plate temperature up to 20°K hotter than the store and up to 120 W/m^2 of collectable solar energy being wasted. Again it should be emphasised that the foregoing is a simple, steady-state analysis of what is essentially a transient phenomenon. Nevertheless, the result suggests that the choice of the control setting dTon could have a considerable effect on the long-term thermal performance of the system, contrary to the statement by Duffie & Beckman (1980) that "raising the turn on setting to 20°K or more will not significantly reduce the useful solar energy collection". Due to the transient nature of the meteorological variables involved, computer modelling techniques will be required to take this analysis further.

2.4.2 Response to step changes in solar irradiance.

It is also of interest to calculate the approximate rate of response of a typical flat plate solar collector to step changes in the solar irradiance. This is the start of the transient analysis , and the first differential equation is introduced (2.14). (This

transient analysis is taken further when the computer model is introduced in Chapter Three.)

Suppose that a cloud which was obscuring the sun has just passed, causing a step increase in solar irradiance from Qi(1) to Qi(2), as shown in figure 2.3.

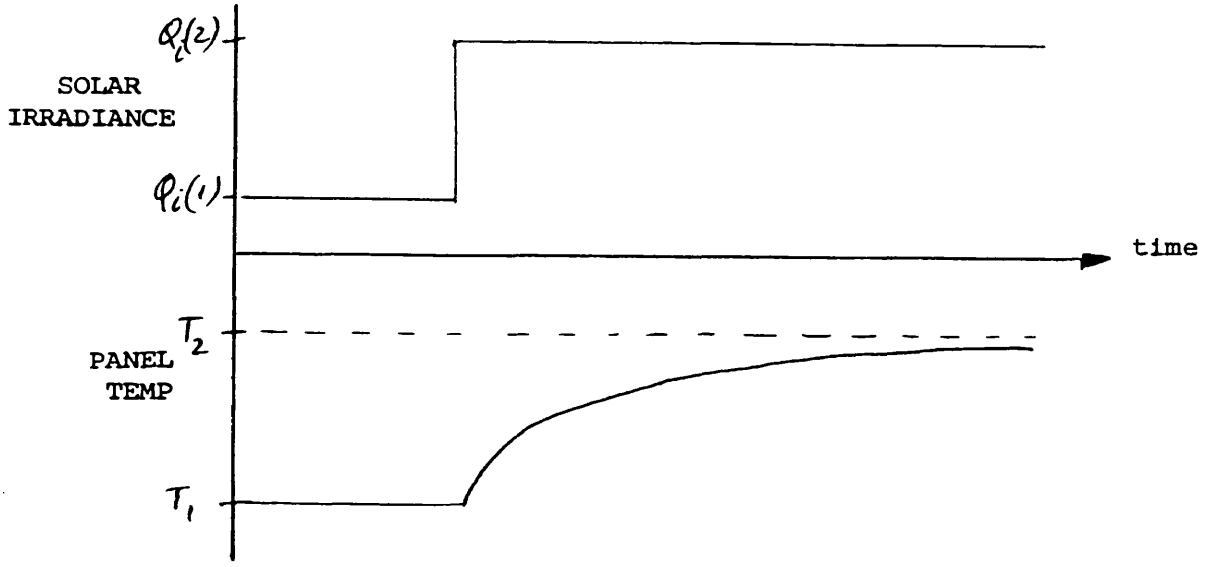

Figure 2.3 Collector response to step change in solar irradiance.

Under no-flow conditions, the absorber plate will have been in thermal equilibrium at a temperature T1 given by:

$$ta.Qi(1) = Ul.(T1-Ta) \qquad (2.13)$$

At the moment of the step change in solar irradiance, the panel temperature will start to increase according to the differential equation:

$$C\ dT/dt = ta.(Qi(2)-Qi(1)) \qquad (2.14)$$

where: C = heat capacity of panel and water content ($J/m^2°K$)

A typical value of heat capacity per unit area for a single glazed solar collector is 5000 $J/m^2°K$. (This includes the heat capacity of the water in the riser tubes.) Using this value, and a step change in solar irradiance of 250 W/m^2, we find that the rate of increase of temperature is given by :

$dT/dt = 0.6 \times 250/5000$

$= 0.03\ °K/s$

$= 1.8°K/min$

Thus it appears that a substantial step increase in solar irradiance causes a relatively slow initial rate of temperature increase of less than 2 °K per minute for a typical flat plate solar collector. This rate of temperature increase will diminish as the temperature increases (under no-flow conditions the collector plate will approach another equilibrium temperature T2 asymptotically as illustrated in figure 2.3). Thus it will take at least 10 minutes for the plate temperature to rise by 20°K. By this time another cloud may have obscured the sun and the opportunity to collect solar energy may have been lost due to a too-high switch-on setting dTon.

The above argument gives a further indication that quantities of collectable solar energy may be wasted by the use of a switch-on criterion which is excessively high. This simple mathematical treatment cannot be extended to give a quantitative prediction of the long-term effect on the thermal performance of the system, since this would require foreknowledge of the meteorological variables involved. Computer modelling techniques are required, therefore, to take the analysis further.

2.4.3 The turn-off setting dToff.

The analysis so far has indicated that the choice of the control setting dTon may have a considerable effect on useful solar energy collection. The choice of the turn-off setting dToff is also important. If the controller of the example above is set at dTon = 6°K, then the turn-off setting dToff should be less than 0.5°K to satisfy the stability criterion of equation (2.8). This is a small temperature difference to detect with standard analogue controllers. The ideal choice of the turn-off setting is such that the pump switches off when the value of the useful solar energy collected is less than the cost of pumping. However, in many cases such a criterion would require a turn-off setting of 0.1°K or less which is impractical using ordinary controllers. The usual criterion is to set the turn-off setting as low as possible, but problems of "drift" with ordinary controllers prevent the use of values less than about 1°K. The computer model will be used to determine the sensitivity of the long-term performance to this

setting, and hence determine whether there is a need for more accurate controllers.

CHAPTER THREE

3. EXPERIMENTAL APPARATUS

3.1 The Solar Heating System

Computer simulations are not substitutes for physical experiments. For this reason, considerable emphasis has been placed on the collection of reliable and accurate measured data from a large scale active solar heating systemt in the UK. The system concerned is described below.

3.1.1 Site location

The solar heating system is situated at Torbay District General Hospital on the south coast of Devon, approximately 3 miles north of Torquay city centre, off the A380.

Latitude = 50 degrees 26 minutes North
Longitude = 4 degrees 15 minutes West
Height = 82 metres above sea level

3.1.2 Local climate

Torbay lies on the highest solar radiation contour for the UK, receiving an annual mean daily insolation of 11.0 MJ/m^2 on the horizontal plane as established by the Meteorological Office (1980) (see figure 4.14). Hourly solar radiation data are not recorded. The wind speed V50 (i.e the wind speed which is exceeded for 50% of the time) is 5 m/s.

Figure 3.1

3.1.3 System type

Figure 3.1 shows a photograph of the solar collector array. 270 m2 of conventional flat plate, single glazed, back insulated solar collectors have been substituted for the south facing wall of the building, at a slope of 53 degrees 30 minutes to the horizontal.

The system is of the indirect, atmospherically vented, pumped circulation type (shown schematically in figure 3.2), and two alternative storage capacities of 3000 litres or 10000 litres may be used, as conditions dictate.

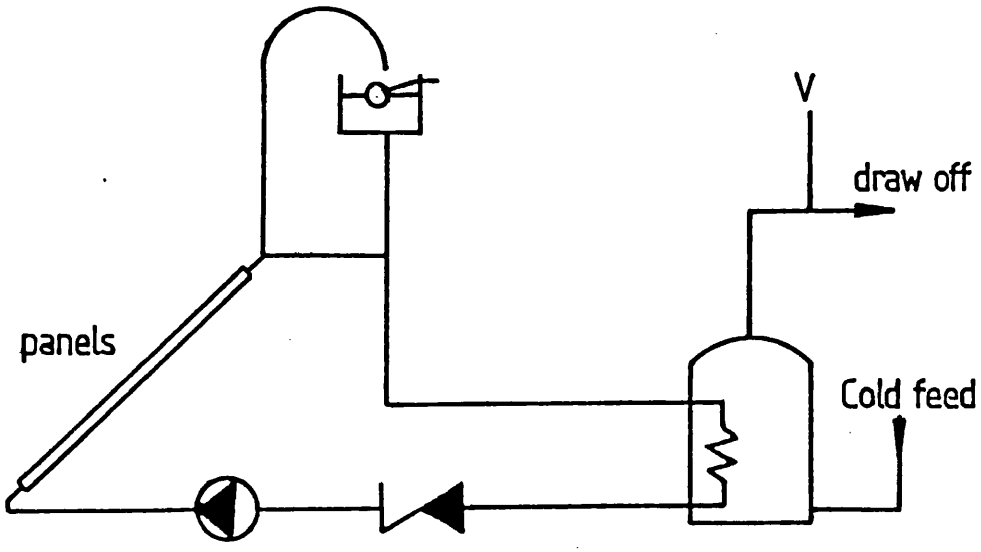

Figure 3.2 Schematic diagram showing solar heating system type.

The heat transfer fluid in the primary circuit is a water / Fernox

mixture. Heat is transferred to the domestic hot water in the 3000 litre solar store via four heat exchanger batteries with a total surface area of 16.88 m2.

The solar preheated water is passed to two conventional steam calorifiers each of capacity 3000 litres, where the auxiliary heat source boosts the water to the required delivery temperature of 65.5 °C.

The layout of the system is illustrated schematically in Figure 3.3.
The control system layout is illustrated in figure 3.4.
Figures 3.5 and 3.6 are reproductions of photographs of various components within the system.

Component details are as follows:

3.1.4 Solar collectors

Type:	Flat plate with waterways
Construction:	Copper fin with 15 mm copper waterways
	Single glazed with 6 mm float glass
	Back insulated with 50 mm "Rockwool"
	Collectors are accessible from inside building for ease of maintenance.

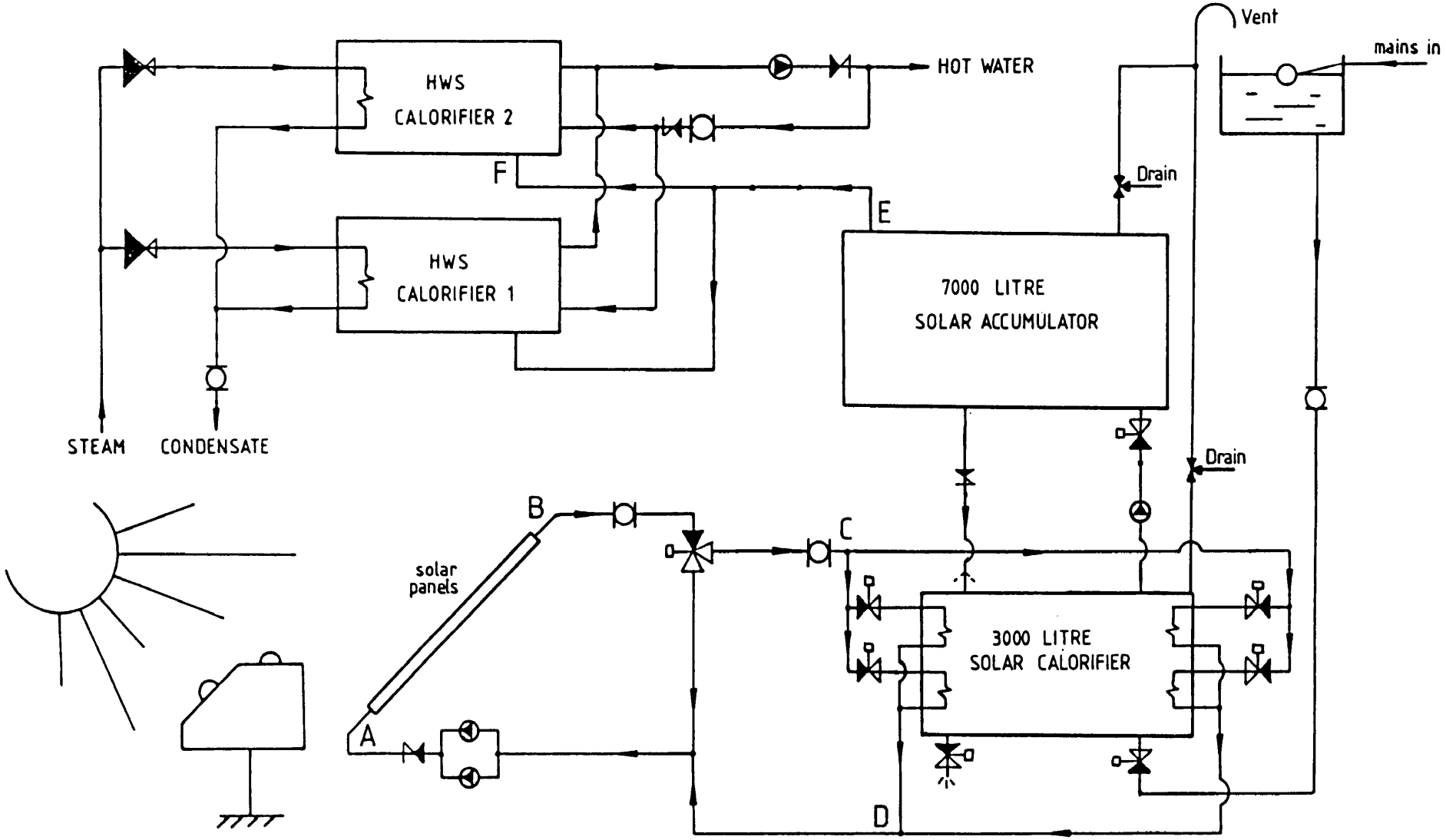

Figure 3.3. Schematic diagram showing solar heating system layout.

TORBAY D.G.H CATERING COMPLEX.

AUTOMATIC CONTROLS FOR SOLAR HEATING INSTALLATION

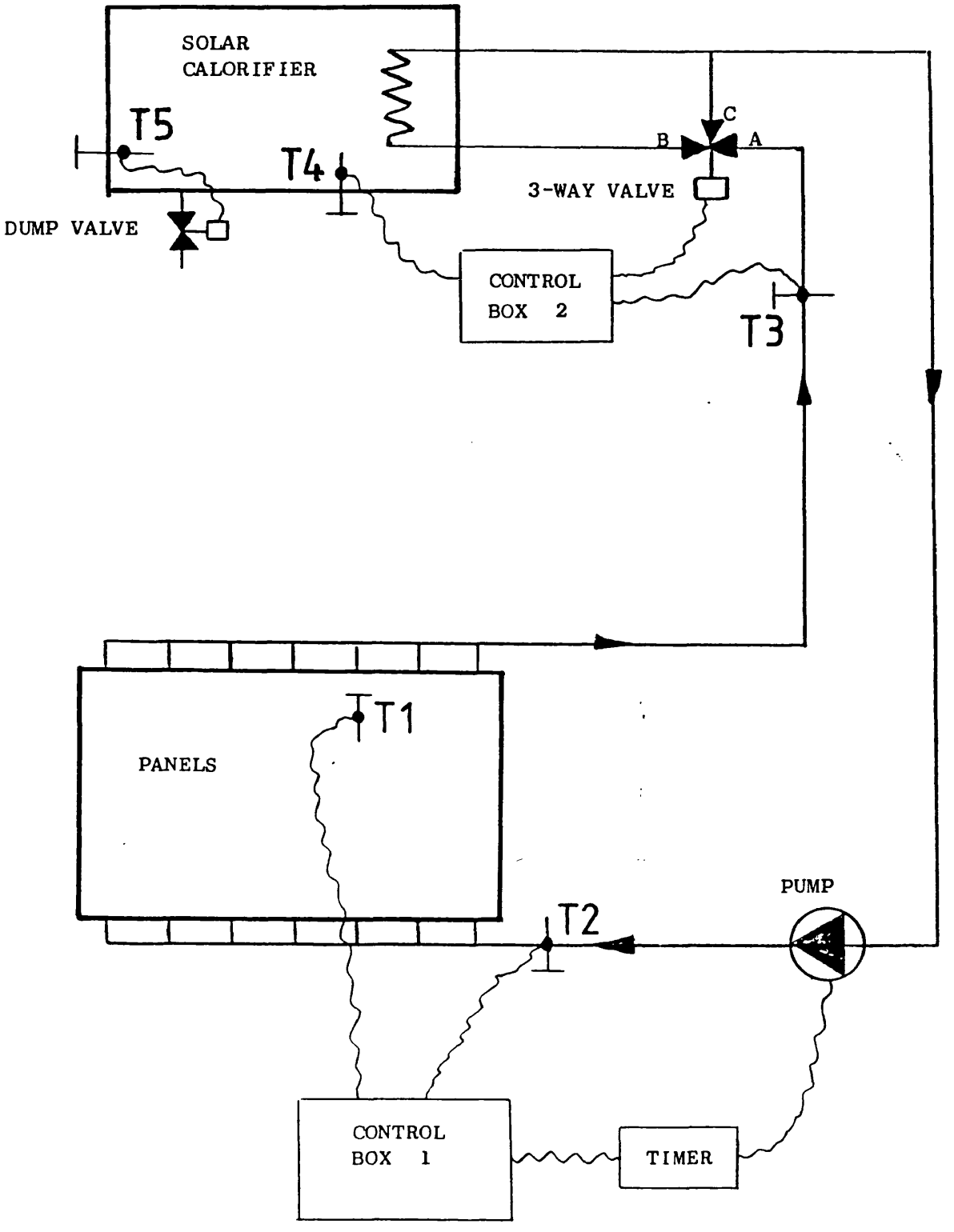

Figure 3.4. Schematic diagram showing control system layout.

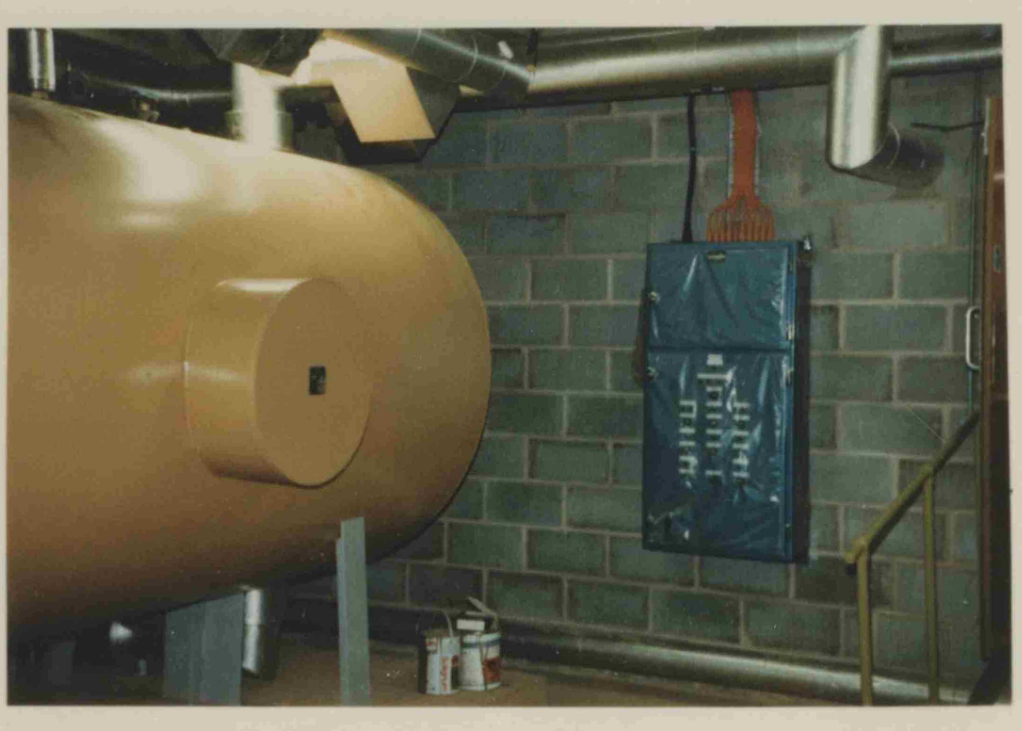

The photograph above shows the 7000 litre solar accumulator, and the solar control panel in the main plant room.

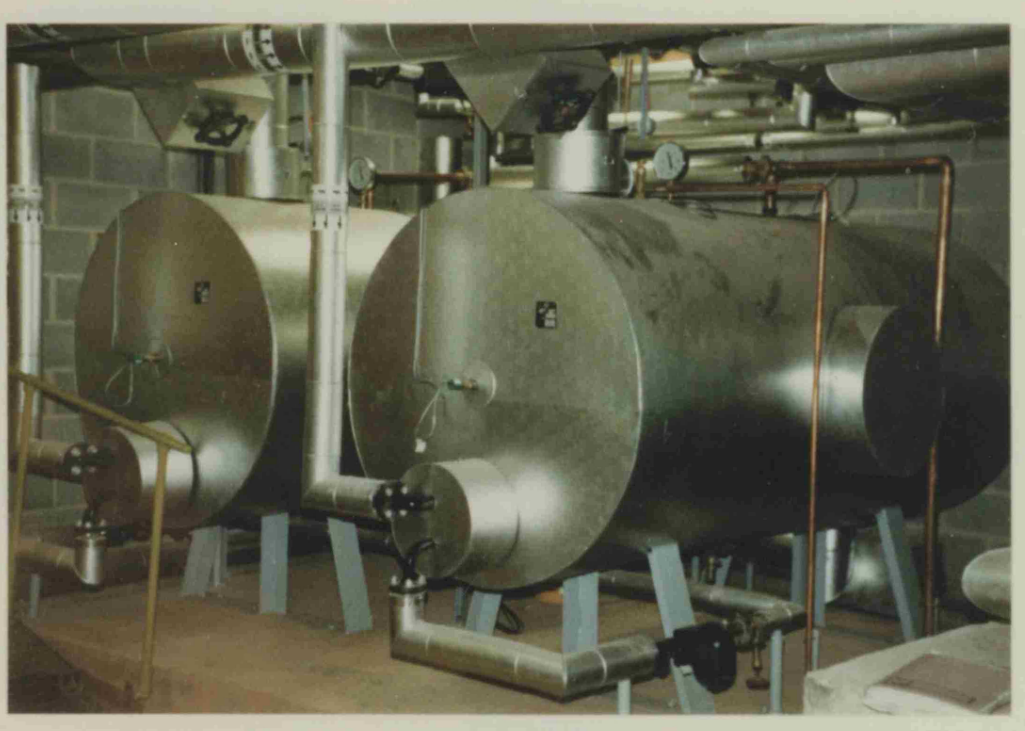

The photograph above shows the two 3000 litre HWS calorifiers, which are also situated in the main plant room. The steam inlet and condensate outlet pipes to the heat exchanger batteries can be clearly seen.

Figure 3.5

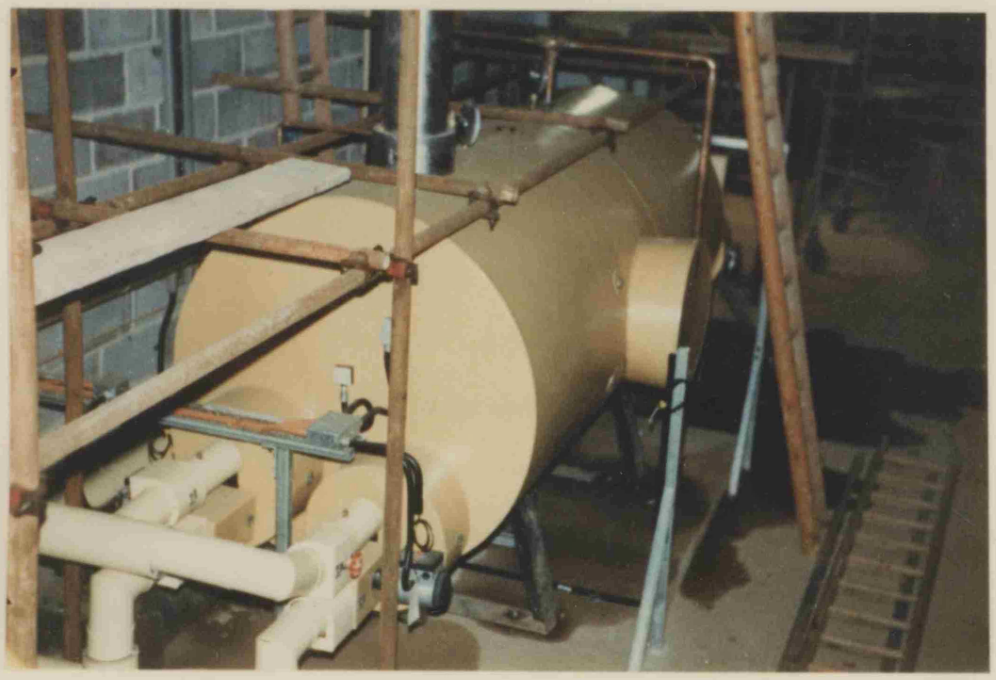

The above photograph shows the 3000 litre solar calorifier shortly before completion of the project. Two of the four heat exchanger batteries can be seen. The solar calorifier is situated at low level behind the solar panel structure.

The photograph on the left is a view of the solar panel array from the inside.

The main header, sub-header and individual riser pipes can be seen.

The diaphragm regulating valve used to control the flow rate through each bank of panels can be seen in the foreground.

Figure 3.6

Manufacturer:	Don Engineering Ltd, Wellington, Somerset.
Area:	270 m2 net
Slope:	53 degrees 30 minutes to horizontal
Orientation:	157 degrees
Surface finish:	Nextel paint (non-selective)
Frost protection:	Primary circuit contains water mixed with Fernox Fp-Cu antifreeze.

3.1.5 Thermal storage

Type:	Sensible heat of water
Capacity:	3000 litres primary, with 7000 litres backup.
Construction:	Copper lined steel cylindrical tanks
Heat exchangers:	Total heat exchange area of 16.88 m2 in four batteries in 3000 litre solar store. (Note: no-flow condition exists in store)
Insulation:	50 mm of glass fibre wool on each tank

3.1.6 Solar primary circuit

Working fluid: Water and Fernox Fp-Cu antifreeze mixture

Flow rate: 3.7 litres/sec (= 0.0137 l/sm²)

3.1.7 Control strategy

Figure 3.4 is a schematic diagram showing the layout and operation of the control system. There are three separate and independent systems which operate as follows:-

System A. This system controls the switching of the pump.

Components: Temperature sensor T1 on solar panel riser pipe
Temperature sensor T2 in flow to solar panels
Control box 1 (TA controls Type TA 211D)
On/off timer
Circulating pump

Operation: The pump is switched on when the absorber temperature (T1) exceeds the temperature in the solar panel inlet pipe (T2) by a set amount (x). When the pump comes on the timer is activated and will keep the pump running for a set period (regardless of sensors T1 and T2). At the end of the set period, if T1 is less

than or equal to T2 the pump is switched off, while if T1 is still greater than T2 the timer is overridden and the pump stays on. When the pump switches off the timer is again activated and will keep the pump off for a set period. (Note: The purpose of the timer is simply to prevent rapid on/off cycling of the pump.)

System B

This system controls the position of the three way diverting valve. The valve does not modulate. The heat exchanger batteries in the solar store either take all the flow in the primary circuit or are bypassed completely.

Components: Temperature sensor T3 in flow from solar panels
Temperature sensor T4 in solar store
Control box 2 (Landis & Gyr Type RSA 22)
Three-way motorised valve

Operation: If the temperature of the flow from the solar panels (T3) is greater than the temperature in the store (T4) by a set amount (y), the three way valve is set open on path A-B so that the hot water from the panels passes through the heat exchanger batteries. If T3 is not greater than T4 + y, the three way valve is set open on path A-C, and the flow from the panels is recirculated.

System C

This system controls the dump valve in the solar store. The purpose is to prevent water boiling in the store.

Components: Temperature sensor T5 in solar store
Dump valve on solar store

Operation: Dump valve opens if store temperature exceeds 95°C.

3.1.8 Auxiliary heat source

Type: Conventional calorifiers heated by low pressure steam from central gas-fired boiler plant.

Operation: The solar pre-heated water is drawn into two conventional calorifiers each of capacity 3000 litres. Here heat is added from the low pressure steam supply to raise the water to the required delivery temperature of 65.5 °C.

CHAPTER THREE

3.2 THE COMPUTER MODEL.

The computer model used in this research was developed by Rosenfeld and Pye (1980) at the Shell Thornton Research Centre over a period of about 15 years. The program suite was written in "Sheltran", (a programming language peculiar to the Shell Corporation) but was machine translated into FORTRAN77 to enable it to be compiled and run on the Bath University mainframe computer (Honeywell "Multics"). The program source code consists of some 11,000 lines of FORTRAN, and is not reproduced in this thesis. Considerable de-bugging and adaptation was required before the program ran successfully on the University computer.

This chapter describes the working of the computer model, and the algorithms and differential equations used to simulate the behaviour of the various solar heating system components.

3.3 Basic strategy of the system simulation.

In order to simulate the energy flows through a solar heating system using a digital computer, one must first derive a set of algorithms which describe the instantaneous heat flows into and out of each system component in terms of certain operating variables (e.g temperatures, flowrates, solar irradiance, load). A set of differential equations can then be set up which describe the state of the system at one time in terms of its state at an earlier time. In a simulation of any phenomenon, a line must be drawn between the

realistic simulation of details and a long and costly calculation. The size of the time step over which the differential equations are solved is therefore important in reaching a proper balance between accuracy and cost. The time step used in the model is automatically adjusted so that when the system is in a dynamic state, with temperatures and flowrates changing rapidly, very short time steps are taken, whereas, when nearly steady-state conditions prevail computing time is saved without loss of accuracy by increasing the time step up to a maximum of 0.2 hours.

A related aspect is the time scale over which fluctuations in the input parameters (e.g solar irradiance) are to be averaged. Ideally these too should be averaged over times short compared with the response time of the system. In practice, however, the shortest period over which meteorological data are readily available is one hour, and so the program is designed to accept input data on this basis. The monitoring system described in Chapter Four was set up to provide meteorological data measured on site on the same hourly basis to facilitate the calibration of the computer model.

If a system component has no thermal inertia (i.e negligible heat capacity), then the rate of heat output at any time can be related to the rate of heat input at the same time by an algebraic expression, or transfer function. This transfer function will involve some of the component's characteristics such as size, surface area, conversion efficiency or heat loss coefficient, and

the flow rate and heat capacity of the heat transfer fluid and may also depend on the instantaneous values of variables such as the temperatures at various points in the system. It would, in principle, be possible to define transfer functions for components whose thermal inertia is not negligible, but then the rate of heat output at a given time would depend on the heat inputs at previous times. Due to the difficulty of defining such transfer functions for components with non-zero heat capacity, a better approach is to write and solve a differential equation which relates the rate of change of the component's temperature, T, to its heat capacity, C, and to the instantaneous energy flows Qin and Qout into and out of the component. The equations are of the form:

$$C\ dT/dt = \sum(Qin) - \sum(Qout) \qquad (3.1)$$

The heat flows Q are expressed algebraically in terms of the flow rate and heat capacity of the heat transfer fluid, the component characteristics and the instantaneous values of the temperatures. Heat losses are simply written as additional terms in Qout. The effect of control elements such as pumps and valves is simulated by indices (one for each element) which multiply the appropriate heat flows and take the value 0 or 1 according to whether the control has switched the heat flow off or on (for modulating control elements such as a mixing valve the coefficient can take any value between 0 and 1). In this way it is possible to simulate control functions which themselves depend on the instantaneous values of system variables (e.g the difference in temperature between the

solar panel and the solar store). This procedure means that switching transients are neglected, that is to say the system variables are assumed to change instantaneously from their values in one state of the system (with the flow on, say), to their value in the other state (flow off) when the control function dictates a switch in the control element. By integrating the set of simultaneous differential equations, the temporal evolution of the temperature at various points in the system is determined. The energy transferred from one part of the system to another, and from the external energy sources are cumulated, to obtain overall system performance. Accuracy is maintained by checking for convergence and shortening the time step if necessary until an acceptable error level is reached.

The heat capacity of pipework is assumed to be negligible by the program. Pipe heat losses are calculated by treating each pipe as a heat exchanger, transferring heat between the fluid inside and the air outside. The effectiveness of the pipe as a heat exchanger can be found from its length, diameter, and insulation characteristics, (see Table 3.1).

The output of the program consists of hourly values of the temperatures at salient points within the system, and of the quantities of energy transferred from one part of the system to another. Also available is information on control elements, for example how often a pump has been switched on and the fraction of time for which it was on. These results can be printed out in

daily, weekly or annual summaries.

The main limitations of the program in terms of its applicability to this particular study are as follows:

a) the program is not equipped to simulate two separate solar stores (though it will simulate a stratified store)

b) the program is not equipped to simulate the action of the three way motorised valve (see section 3.1.7), it utilises the simpler control system illustrated schematically in figure 2.1

c) Switching transients are neglected, i.e the system variables are assumed to change instantaneously from their values in one state of the system (with the pump on, say) to their values in the other state (pump off) when the control strategy dictates a switch in the control element. This neglects the ability of the collector under stagnation conditions to restore some of its heat to the transport fluid when the circulating pump is switched on, which could lead to an over-estimate of the effects of the control settings dTon and dToff.

After consultation with the designers and developers of the program (J.L.J.Rosenfeld and D.B.Pye at STRC) it was decided that the above limitations do not seriously affect the usefulness of the model for this simulation, and can be resolved as follows:

a) When both solar stores are in use, they are kept fully mixed by a 24-hour circulating pump (see figure 3.3). They can therefore be treated as a single isothermal store for simulation purposes, provided the extra surface area of the connecting pipework and two storage vessels is included in the heat loss calculations.

b) When either the three-way motorised valve is closed OR the pump is off in the real system, this may be equated to the "pump off" situation in the model. When the three way valve is open AND the pump is on in the real system, this may be equated to the "pump on" situation in the model.

c) When the pump switches on, and the collector plate temperature is reset to a new starting value, an extra term is calculated which allows for a proportion of the instantaneous heat loss to be transferred to the transport fluid.

CHAPTER THREE

3.4 Algorithms used in the program.

3.4.1 Solar radiation incident on the collector plane.

Most meteorological recording stations in the UK record only daily totals of solar irradiation on a horizontal surface. However, a few record hourly average values of solar irradiance on the horizontal (Meteorological Office, 1980). An algorithm is needed to convert hourly average figures of global solar irradiance on a horizontal plane into direct and diffuse components on the tilted plane of the collectors. A great deal of research effort has been devoted to precisely this end. For example, Heywood (1966) made extensive simultaneous measurements in the London area of total radiation on horizontal and inclined planes under cloudless sky conditions. He developed an empirical method, based on these measurements, for estimating an angular correction factor for total solar radiation. Further work in this field has been carried out by Boes (1976), Collares-Pereira (1979), Mabbs (1980), Liu & Jordan (1966) and others. A detailed comparison of the various correlation methods has been carried out by Pye & Rosenfeld (1984). Their results showed that for computer simulation of solar heating systems in the UK, the best accuracies are obtained using Boes' correlation.

The method given by Boes is based on one year of data (1962) from three US weather stations. His original correlation was a linear relationship between the direct normal irradiation and a "clearness

index", Kt, where Kt is the ratio of hourly global to extra-terrestrial irradiation on a horizontal surface (Ig/Ie). Boes found that the data from each location resulted in a slightly different correlation and that there were also seasonal variations. In an updated version of his correlation (1976) a relationship was developed for the three locations and all seasons combined. This is the correlation used in the model as shown below:

For $Kt \leq 0.29$ $\quad Ibeam = 0$

For $0.29 < Kt \leq 0.84$ $\quad Ibeam = (1.3304\ Kt - 0.3843\ Sc)$

For $Kt > 0.84$ $\quad Ibeam = 0.739\ Sc$

where: Ibeam = direct irradiation incident on a surface normal to the radiation.

Sc = solar constant (1353 W/m^2).

The value of extra-terrestrial irradiation, Ie, used in the calculation of Kt, is given by equation 3.1a

$$Ie = Sc\ [1 - 0.333\sin((360/365)(D + 272.1))](\sin\theta\sin\delta + \cos\theta\cos\delta\cos\omega) \qquad (3.1a)$$

where: D = day of year (jan 1st = 1)

θ = latitude

δ = declination of the sun

ω = hour angle (taken as the apparent solar time at the mid-point of the hour)

The term in square brackets in equation 3.1a accounts for the variation in Ie (of +/- 3.3%) as the distance between the sun and the earth varies throughout the year, and the sin/cos terms in the rounded brackets account for the variation in Ie as the sun's altitude changes throughout the day (variation in ω) and throughout the year (variation in δ).

The direct irradiation on a horizontal surface, Ir, is calculated from the beam radiation using the equation:

$$Ir = Ibeam \times \sin \theta$$

where: θ is the sun's altitude

The diffuse irradiation, Id, on the horizontal is then calculated as a simple subtraction of the direct irradiation from the global irradiation, i.e:

$$Id = Ig - Ir$$

The diffuse and direct components are then converted from the horizontal plane to the tilted plane of the collectors using standard trigonometrical formulae which also allow for the smaller sky area "seen" by collectors at high tilt angles.

CHAPTER THREE

Solar energy collected.

The algorithm used to define the proportion of incoming solar radiation converted into useful heat gain by the collector is that given by equation (3.2). This equation represents the simplification of a great deal of complex theoretical heat transfer analysis, but has been shown to give a good representation of the performance of a flat plate solar collector (Smith & Weiss, 1975).

$$Qc = Fr[(ta)Qi - Ul(Ti-Ta)] \qquad (3.2)$$

The values of Fr, ta, and Ul are constant and are input or calculated once at the beginning of a run. The values of the meteorological variables Qh (solar irradiance on horizontal), and Ta (ambient air temperature) are input each hour and are assumed to remain constant for that hour. The solar irradiance (direct and diffuse) on the plane of the collectors is calculated as described above.

The value of the collector inlet temperature, Ti, is assumed equal to the store temperature, Ts, which is calculated at each time step (max 0.2 hours), subject to the following differential equation:

$$Cs(dTs/dt) = Kp(Qc-Ql) - UAs(Ts-Tas) - Qw \qquad (3.3)$$

where:

Cs = heat capacity of store

Ts = store temperature

Kp = control index (=1 if pump on, =0 if pump off)

Qc = heat gained across collector

Ql = heat losses from collector loop pipework

UAs = overall heat loss coefficient for thermal store

Tas = air temperature around store (= max[15,Ta])

Qw = heat lost due to hot water drawn off being replaced by cold water

3.4.2 Pipe losses

The heat losses, Ql, from each section of pipework are calculated by the program as follows:

$$Ql = h\,(Ti-To) \qquad (3.4)$$

where:

h = heat capacity flow rate through the pipe (J/°Ks)

= mass flow rate (Kg/s) x specific heat capacity of fluid (J/Kg°K)

Ti = inlet temperature

To = outlet temperature

Since To is not known, use is made of the fact that

$$Ql = E \times h \times (Ti - Ta) \qquad (3.5)$$

where:

E = effectiveness of the pipe loss

Ta = temperature surrounding the pipe

[Note: In the program Ta is set to the greater of 15°C and ambient air temperature for pipes inside the building.]

The pipe loss effectiveness, E, is defined as the ratio of heat lost to the maximum heat which could be lost if all the fluid flowing in the pipe were reduced to the environmental air temperature. E is calculated from the standard equation for the effectiveness of an indirect, internal heat exchanger as derived by Kays et.al. (1964):

$$E = 1 - \exp(-UA/h) \qquad (3.6)$$

where UA is the overall composite heat loss factor for the fluid/pipe wall/insulation/environmental air heat transfer.

It will be appreciated that a full treatment of heat transfer in laminar flow in a tube, including effects of boundary layers, entrance length, different thermal boundary conditions and fluid properties which vary with temperature, such as that carried out by Echert & Drake (1959), is complex and is beyond the scope of this

thesis. A simplified model is required for the purpose of simulating pipe losses.

Dane (1980) has shown that the temperature of the outer surface of a thin-walled, well-insulated pipe in which water is flowing varies by not more than 1.5°K from the mean temperature of the fluid under steady-state conditions, for a water temperature range of 10-90°C, surrounding air at room temperature, and over a range of flow velocities covering the full range normally encountered in building services. The above result means that it is a reasonable approximation to treat the pipe/water combination as a single heated element, whose outer surface is at the measured mean water temperature. The situation is illustrated in figure 3.7.

CHAPTER THREE

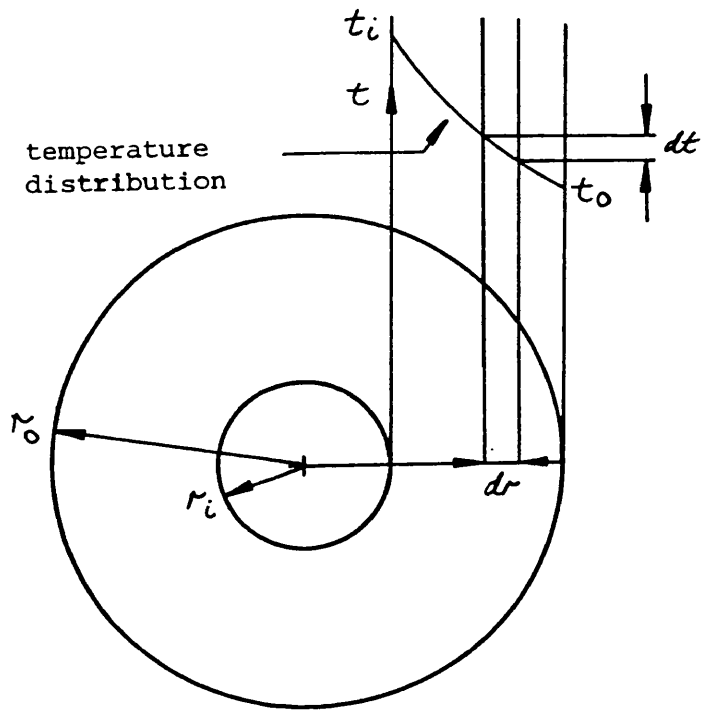

Figure 3.7 One-dimensional pipe losses

Steady-state conduction through the insulating layer.

The inner and outer surfaces ri and ro are assumed to be at a uniform temperature, so that heat flows radially through the tube of insulation. The area of heat flow increases with radius and hence, for reasons of continuity, the temperature gradient must decrease with radius as shown in figure 3.7.

Consider any elemental cylindrical tube of insulation of radius r,

thickness dr, and thermal conductivity k. The area of heat flow per unit length of tube is $2\pi r$, and the temperature gradient normal to the tube is dt/dr. The heat flow, q, is, according to Fourier's law:

$$q = -k\, 2\pi\, r\, (dt/dr) \qquad (3.7)$$

For reasons of continuity, q must be independent of r, and so equation (3.7) can be integrated, giving:

$$q \ln (ro/ri) = -2\pi\, k\, (to - ti) \qquad (3.8)$$

Thus the heat flow per unit length of tube is:

$$q = \frac{-2\pi\, k\, (to - ti)}{\ln(ro/ri)} \qquad (3.9)$$

Thus the composite UA value used in equation 3.6 for the calculation of pipe losses is:

$$UA = 2\pi kL/\ln(ro/ri) \qquad (3.10)$$

where:

k = thermal conductivity of insulation (W/m°K)

ro = outer radius of pipe (m)

ri = inner radius of pipe (m)

L = length of pipe (m)

The details of length, inner and outer radius, insulation k value, and pipe loss effectiveness are shown in table 3.1 below for each of the main pipe runs shown schematically in figure 3.3. (Note: Outer radius - inner radius = insulation thickness).

PIPE SECTION	r(i) mm	r(o) mm	L m	k W/m°K	h J/°Ks	E
B - C	27	52	49	0.033	15466	0.0010
D - A	27	52	98	0.033	15466	0.0020
E - F	54	79	18	0.033	4180	0.0023

Table 3.1 Pipe loss effectiveness details

These were the values for pipe loss effectiveness used in the initial simulations, based on theoretical calculations and the manufacturer's quoted k value for "Rockwool" insulation. As will be explained in Chapter Four, these values required considerable adjustment before agreement could be achieved between the measured results and the predictions of the model.

3.4.3 Heat losses from solar storage tanks and hot water tanks.

The heat loss coefficients, U, for the storage tanks and hot water tanks are input at the start of a run. The heat losses, Ql, from the tanks are then calculated at each time interval from equation (3.11):

$$Ql = U \cdot F \cdot V^{2/3} \cdot (Ts - Tas) \qquad (3.11)$$

where:

U = heat loss coefficient (W/m²°K)

F = "shape factor" converting tank volume to surface area

V = tank volume (m³)

Ts = tank fluid temperature (°C)

Tas= ambient temp around tank (°C)

(Note: As in the case of pipe losses, the ambient temperature around the tanks is set at 15°C or ambient air temperature, whichever is the greater.)

The solar storage tank temperature, Ts, is calculated at each time interval according to the differential equation 3.3.

The hot water tank temperature, Tw, is calculated at each time interval according to a similar equation (3.12)

$$C(dTw/dt) = Qaux - Ql - Qw \qquad (3.12)$$

where:

Qaux = auxiliary heat input

Ql = heat lost through insulation

Qw = heat lost through hot water drawn off being replaced with cooler water from solar store

CHAPTER THREE

The solar storage tanks and the hot water tanks are all flat-ended cylinders lying on their side. The two hot water tanks and the solar calorifier all have a volume of 3000 litres, while the solar accumulator has a volume of 7000 litres. The surface area, A, of a flat-ended cylinder is given by:

$$A = \pi d L + (\pi d^2/2)$$

where d = diameter, L = length.

For the solar calorifier and the HWS tanks, L = 2.9 m and d = 1.2 m, hence A = 13.2 m^2.

For the solar accumulator, L = 3.46m and d = 1.7m, hence A = 23.0m^2.

The shape factor, Fw, for the hot water tanks is therefore:

$$Fw = \frac{\text{total surface area}}{(\text{total volume})^{2/3}} = \frac{26.4}{(6)^{2/3}} = 8.0$$

and for the solar stores:

$$Fs = \frac{36.2}{(10)^{2/3}} = 7.8$$

All the tanks are insulated with 50mm of "Rockwool" glass fibre wool (quoted k-value 0.033 W/m^2°K), giving a theoretical U-value

of 0.66W/m²°K. This was the U-value used in the initial simulations.

3.4.4 Cold water inlet temperature

The seasonal variation in mains cold water inlet temperature is represented by the following equation:

$$Tcw = A - B \cos[(2\pi/365)(D - C)] \qquad (3.13)$$

where:

A,B,C are constants

D = day of year (Jan 1st = day 1)

By suitable choice of the constants A,B and C, the cold water inlet temperature can be made to correspond closely to the measured values, thus allowing for incidental heat gains in the cold water tank. This is part of the computer model calibration process, and is described more fully in Chapter Four.

3.4.5 Hot water load.

24 hourly values of hot water volume draw-off are input to the program each day. The program assumes that this volume is drawn off continuously over the hour, unless a smaller time interval is specified.

The total hot water load, Qw, is calculated each hour from equation (3.14):

$$Qw = (p.Cp).(Tw-Tcw).V(hour) \qquad (3.14)$$

where:

p.Cp = product of density and heat capacity of water (J/l°K)
Tw = control temperature of the hot water tank (°K)
Tcw = cold water inlet temperature (°K)
V(hour) = volume of hot water drawn off (litres)

[Note: The product (p.Cp) is assumed constant at 4140 J/l°K). An examination of the properties of water over the full working temperature range shows that this assumption will produce a maximum error of 1.7% (see table 4.3)]

The total hot water load calculated above is shared by the solar storage tank and the hot water tank, since the hot water tank is fed by the solar pre-heated water. The heat lost from the solar store through hot water draw-off , Qw(s) is therefore given by:

$$Qw(s) = (p.Cp) \times (Ts - Tcw) \times V(hour)$$

where Ts = solar store temperature

which, when combined with equation 3.14 gives:

$$Qw(s) = ((Ts - Tcw)/(Tw - Tcw)) \times Qw \qquad (3.15)$$

Similarly, the heat lost from the hot water tank due to hot water draw-off, Qw(w) is given by 3.16

$$Qw(w) = ((Tw - Ts)/(Tw - Tcw)) \times Qw \qquad (3.16)$$

3.5 Auxiliary heat input

The auxiliary heater capacity is input at the start of the program. The value was initially set at 200kW, but was later increased to correspond with the measured results (see Chapter Four). The hot water supply temperature is set at the start of each run, as is the control thermostat hysterisis. When the hot water tank temperature falls below the set value by an amount greater than or equal to the switching hysterisis, the auxiliary heat source is switched on. The heater then remains on until the hot water tank temperature exceeds the set temperature by an amount greater than or equal to the switching hysterisis. The auxiliary heat source does not modulate, it is either off or fully on.

3.6 Overall simulation set-up

Having discussed the algorithms used in the computer model to

describe the individual system components, we can now present the overall picture of the system "as modelled". Figure 3.8 illustrates schematically the simplified system represented by the model.

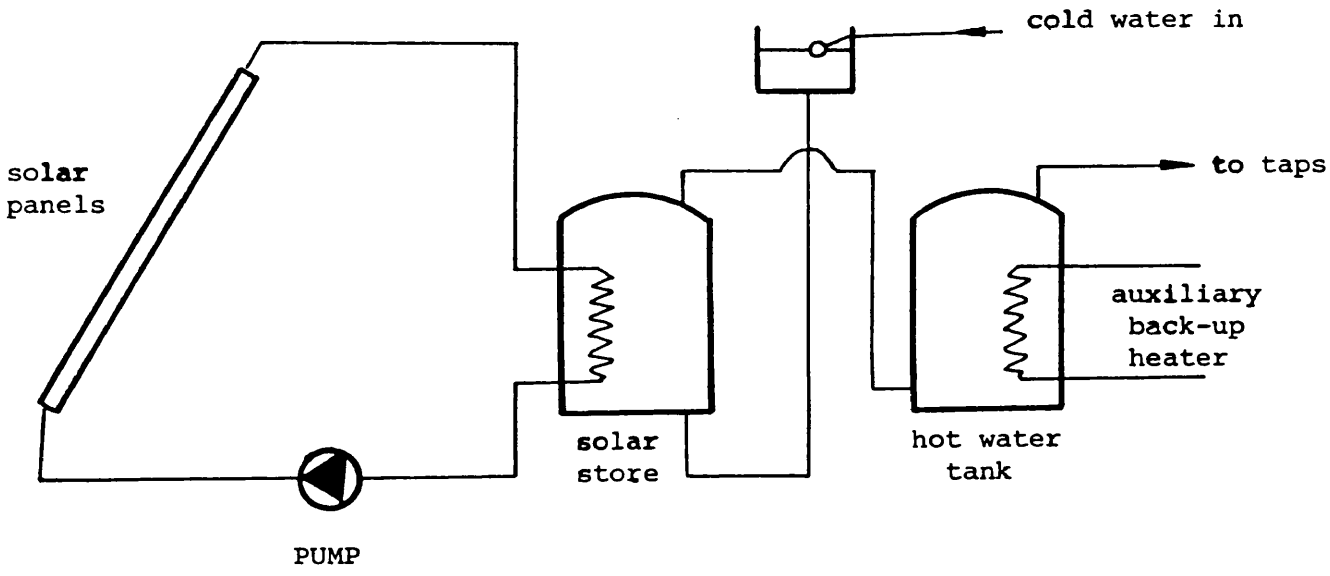

Figure 3.8 Schematic diagram showing system "as modelled"

The "as modelled" system consists of three main components having heat capacity, or thermal inertia; the solar panel array itself, the solar store and the hot water tank. These main components are linked by pipe sections which are assumed to have negligible heat capacity.

The diffuse and direct components of solar radiation falling on the tilted plane of the collectors are calculated from the global solar radiation on the horizontal as described in section 3.4.1. These are assumed constant over each hourly interval.

The energy collected across the panels is calculated at each time step according to equation 3.2. The proportion of this energy transferred to the store is calculated by means of the pipe loss effectiveness values deerived in section 3.4.2 and listed in Table 3.1.

The solar store temperature is calculated at each time step according to equation 3.3. It is a function of the heat input from the solar panels, the heat lost through the insulation, and the heat lost due to cold water replenishing the hot water drawn off during the previous time step.

The heat losses from the pipework section connecting the solar store and the hot water tank is calculated using the pipe loss effectiveness, as above.

The hot water tank temperature is calculated according to equation 3.12. It is a function of the heat lost through the insulation, the heat lost through hot water draw-off, and the heat input by the auxiliary heater during the previous time step.

At each time step the solutions to the above differential equations

are checked for convergence, and if necessary the time step is shortened. All the temperatures and heat flows are accumulated on an hourly, daily and yearly basis and output by the program as required.

CHAPTER FOUR

4. EXPERIMENTAL PROCEDURE

Sections 4.1.1 to 4.1.11 of this Chapter describe how the thermal performance of the solar heating system was monitored. Sections 4.2.1 onwards describe the use and calibration of the computer model.

4.1 The solar heating system.

The determination of the thermal performance of an active solar heating system requires both the system operation and the outside weather conditions to be monitored. There are six basic types of measurement necessary:

a) short wave solar radiation
b) air temperature
c) wind velocity

} meteorological parameters

d) fluid temperatures in pipes and tanks
e) fluid flow rate in pipes
f) plant status

} system parameters

Duffie & Beckman (1980) showed that the recording of meteorological data such as atmospheric pressure, rainfall, visibility and cloud cover is not essential to the evaluation of the thermal performance of solar heating systems. Outside air humidity may be an important

factor if the solar heated building is air-conditioned, but, as the installation with which we are concerned does not use solar energy for air conditioning, this parameter has not been taken into account.

4.1.1 Measuring solar radiation.

This section deals with the short-wave radiation from the sun and the sky, of wavelength less than 3 micrometers. Approximately 98% of the available solar energy lies in this waveband (Duffie & Beckman, 1980), and it is this energy which is being collected in any solar heating system.

4.1.1 Type of sensor.

Kipp & Zonen solarimeters are used for solar radiation measurement throughout the UK. They are recommended by the Meteorological Office (1969) for their accuracy, durability and ease of use. Amongst the establishments using these solarimeters are:

The Meteorological Office
The Open University
BSRIA
University College, Cardiff

It would seem logical, therefore, to standardise on the use of these instruments for the measurement of solar radiation. The type

used in this research was the Kipp & Zonen CM5 solarimeter. The manufacturers' full specifications for the instrument are given in Appendix 1.

4.1.1.2 Principle of operation.

The solarimeter is of the Moll-Gorczynski type shown in figure 4.1. It consists of a thermopile made from alternate strips of manganese and constantan, one set of junctions along the centre line of a blackened surface, the other set in good thermal contact with the relatively massive case. The blackened surface is covered with two concentric hemispherical glass domes to shield the sensitive surface from wind and rain. When the blackened surface is exposed to radiation its temperature will rise until the rate of loss of heat by all causes is equal to the rate of heat gain by radiation. This rise in temperature is detected by the thermopile.

Accuracy.

4.1.1.3 Linearity.

Inaccuracies due to non-linearities in the sensitivity of the instrument are of the order of +/- 1%, as illustrated in Figure 4.2.

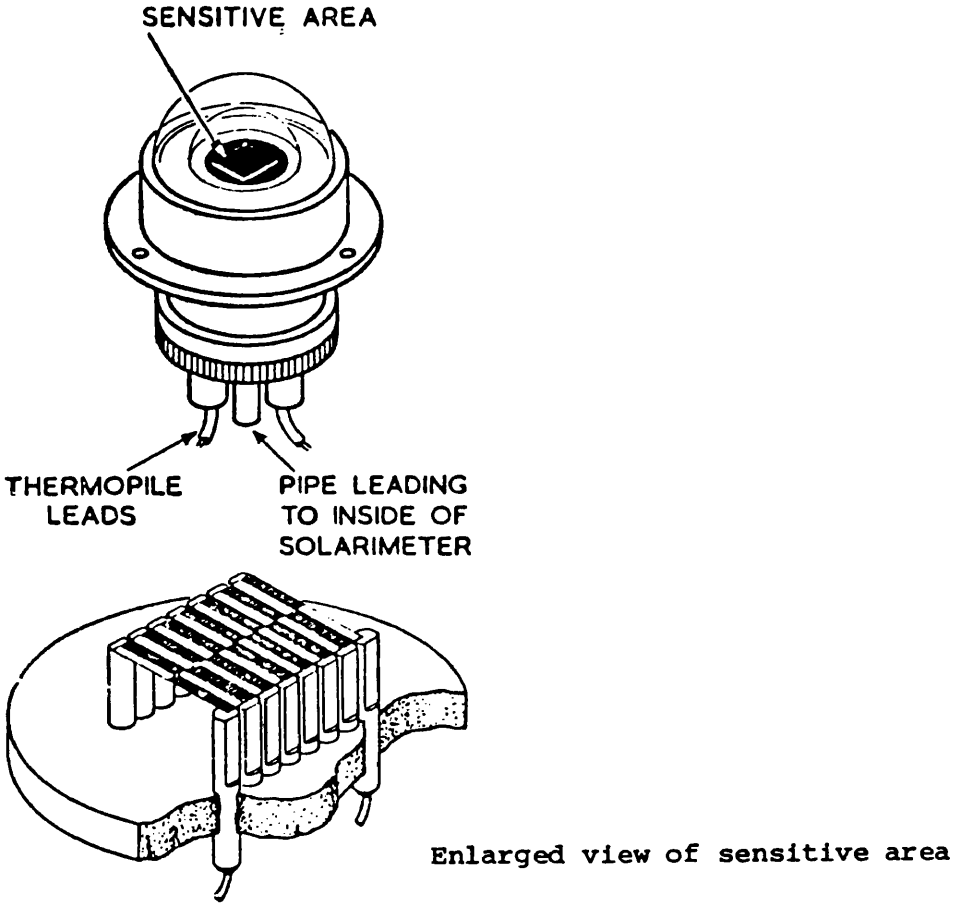

Figure 4.1. Moll-Gorczinski type solarimeter.

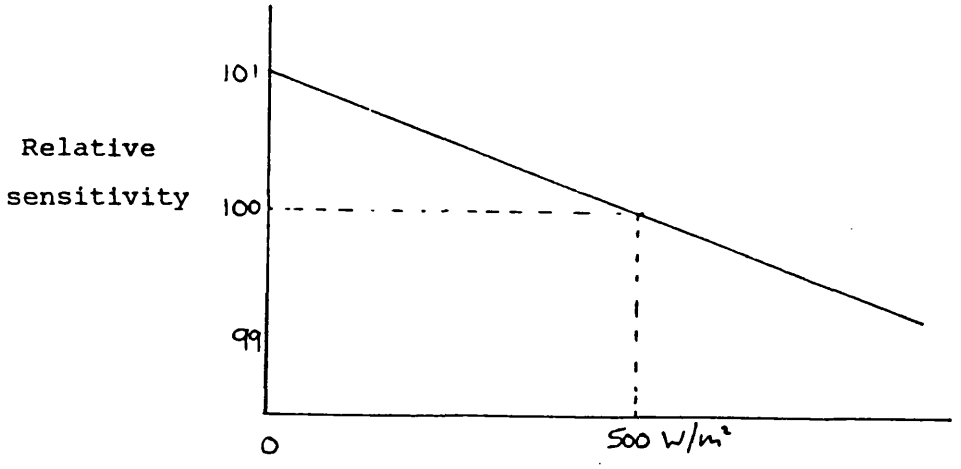

Figure 4.2 Dependence of sensitivity on intensity of incident radiation

4.1.1.4 Temperature dependence.

Inaccuracies due to fluctuations in ambient air temperature are rather higher, of the order of +/- 3% over the range -20 to +30°C, as shown in Figure 4.3. A correction factor has been applied in the data logging process to compensate for this.

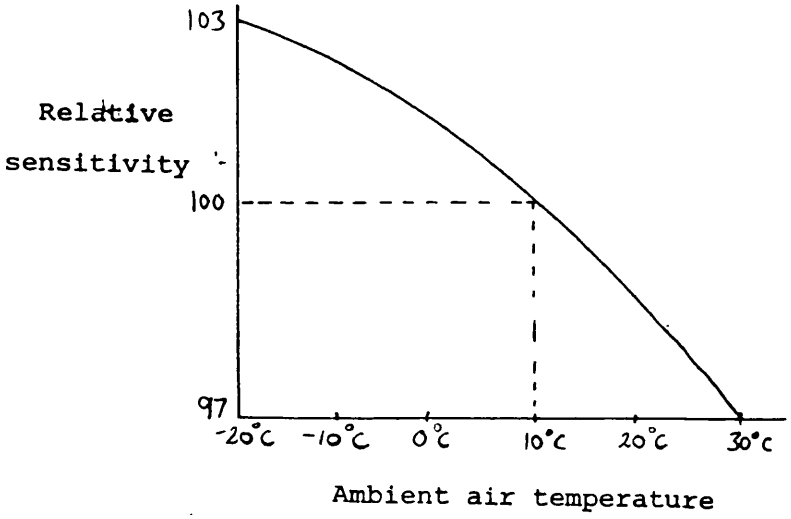

Figure 4.3 Dependence of sensitivity on ambient air temperature

4.1.1.5 Wind speed dependence.

There is a small inaccuracy caused by variations in the wind speed over the instrument. When the wind speed increases the body of the instrument is affected more than the blackened surface (which is protected by two layers of glass), hence the solarimeter output increases. The effect is small, however, typically +/- 0.5%.

4.1.1.6 Cosine response.

There is a further inaccuracy due to the cosine response of the instrument. Ideally, the output voltage V should respond to radiation at altitude angle θ according to equation (4.1):

$$V = K\ I \cos\theta \qquad (4.1)$$

where: θ = sun altitude angle

I = beam radiation intensity

K = constant

However, it has been found that the response of the instrument is dependent on both sun altitude and azimuth angles as shown in Figure 4.4. This response is caused when radiation falling along the line of the thermopile creates localised heating in the vicinity of the thermopile giving an exaggerated reading of up to +12%. Radiation falling perpendicular to the thermopile will give a more accurate reading since the localised heating of the thermopile will now occur at one point only, not along its whole length. Daily peak values of solar radiation will occur most frequently with the sun in the southern quadrant with altitudes between 60 and 15 degrees. If the solarimeter is placed with the axis of thermopiles lying East-West, the greatest inaccuracies will occur in the mornings and evenings when the intensity of solar radiation will be low. Thus the accuracy of peak values and, hence, daily totals of solar radiation are greatest if the instrument is mounted with the line of thermopiles in this direction, and care has been taken to ensure that this is the case.

4.1.1.7 Inclination.

Work carried out at the Meteorological Office, University College

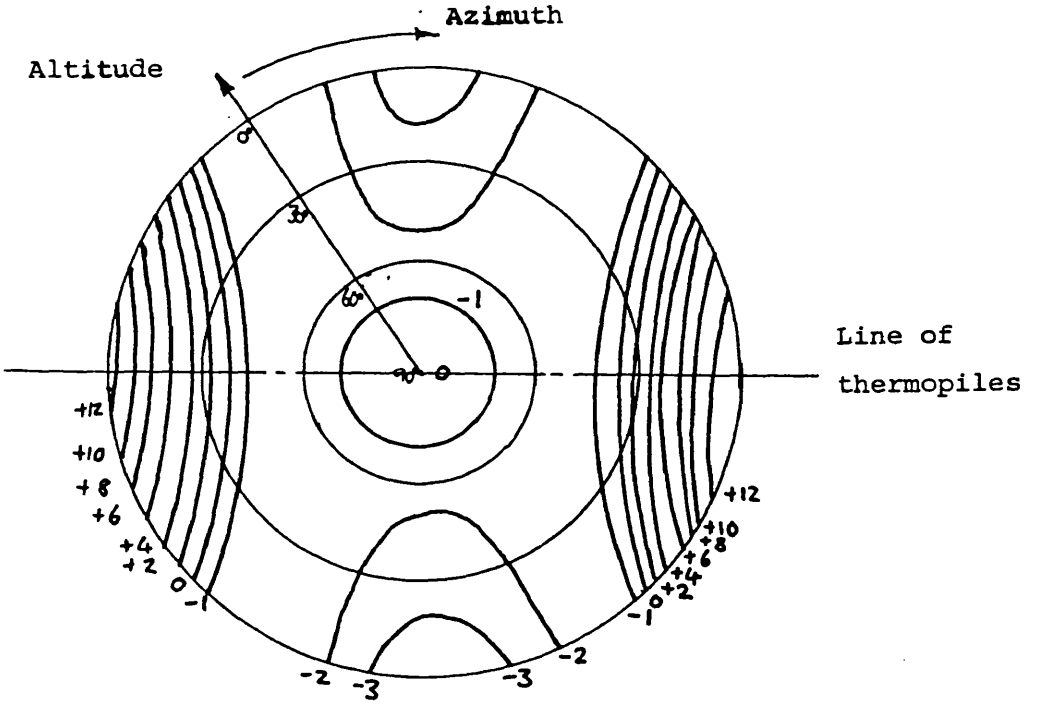

Note: Heavy figures indicate change in sensitivity in per cent relative to sensitivity with radiation source directly above solarimeter.

Figure 4.4. Solarimeter error due to cosine response.

Cardiff and in other countries has shown that the change in sensitivity with inclination is small, of the order of +/- 1.5%, which disproves earlier work by Norris (1974). It has been shown that the least change in sensitivity occurs when the solarimeter is mounted with the heat sinks parallel to the horizontal plane. For a southerly orientated solarimeter, such as will be appropriate for solar heating applications, this is consistent with the criteria previously mentioned, whereby the solarimeter should be mounted with the thermopiles lying in an East-West direction. It is important that inclined solarimeters should have their bodies shielded from direct radiation, and should not be subject to reflected radiation from the solar collectors.

The overall accuracy of the measurement of total solar radiation is therefore in the order of +/- 5%.

4.1.1.8 Calibration.

The two solarimeters used were individually calibrated by the Meteorological Office.

4.1.1.9 Position of sensors.

The intensity of solar radiation incident on the absorber plate of a flat plate solar collector is not proportional to the intensity incident on the panel cover, but is a function of direct radiation, diffuse radiation, angle of tilt of the panel, ground reflection,

and the transmission properties of the panel cover.

The intensity of radiation striking the absorber plate, I, is given by equation (4.2):

$$I = I0.\cos\theta.t\theta + Is.ts.(1+\cos\theta)/2 + Is.rg.tg.(1-\cos\phi)/2 \quad (4.2)$$

where:

I0 = intensity of direct beam radiation

Is = intensity of diffuse sky radiation

θ = angle of the sun to the solar panel

ϕ = angle of the ground to the solar panel

rg = average ground reflectance

$t\theta$ = transmittance of glass to radiation at direct beam angle of incidence

ts = transmittance of glass to diffuse sky radiation

tg = transmittance of glass to diffuse ground radiation

The radiation falling on the absorber could be measured directly by mounting the solarimeter beneath the glass cover of the solar panels. This would pose installation and access difficulties, however, and would subject the body of the instrument to the high local temperatures within the panels. An alternative would be to mount the solarimeter in a separate housing beneath a plate of glass, but this could introduce inaccuracies due to different glass

transmission properties and different dirt deposition rates. In any case, if one accepts that the cover or covers on a flat plate solar collector are an integral part of its construction, it is better to measure the panel efficiency relative to the total intensity of solar radiation striking the panel cover. This is a relatively easy quantity to measure, by simply mounting the solarimeter at the same angle as the solar panel array. The total solar radiation falling on the horizontal plane should also be measured so that comparisons may be made with other sites. Thus, for the installation described in Chapter Three, solar radiation measurements have been made at the angle of tilt of the solar panel array, and on the horizontal plane. The solarimeters were mounted in a well ventilated white-painted box which also shields the body of the instrument from direct radiation.

4.1.1.10 Measurement system.

In the measurement of solar radiation with regard to the performance of solar collectors, it is necessary to determine the total or average radiation falling on a plane in a given time interval. Due to the high short-term variability in intensity of solar radiation (e.g due to passing clouds), it is necessary to integrate the output from the solarimeter over a period of time either by:

a) hardware integration - providing an electrical circuit which will totalise the output from the solarimeter over a given time

interval, or

b) software integration - taking a number of readings during a given time interval to give an average value of solar radiation.

Method (a) requires sophisticated electronic circuitry. Method (b) is easier to achieve in conjunction with a computerised data logging system, and is the method favoured by the Meteorological Office who take readings at one minute intervals to give hourly averages. It must be realised, however, that this method introduces sampling errors which can only be reduced by increasing the number of readings taken in each time interval. As a guide, the Meteorological Office average a total of 60 readings per time interval and it is suggested that this should be a minimum number.

The sampling rate of the data logging system described in Chapter Four is 20-30 seconds. Thus, reliable and accurate measurements of total solar radiation can be made over a minimum time interval of 30 minutes.

The output from a solarimeter will not exactly follow the pattern of solar radiation intensity falling on it. Due to the thermal inertia of the instrument it will tend to smooth out rapid changes in radiation level, giving an apparent decrease in the value of amplitude and in the rate of change of intensity. The effect of this short-term instrument response on the integrated output from a solarimeter when it is subjected to cyclic and step inputs is

evaluated in Appendix II. This analysis shows that the response of the solarimeter will introduce inaccuracies in the measurement of solar radiation, but if the time period over which the readings are averaged or integrated is long enough, the error will be small. For a typical Kipp & Zonen solarimeter of time constant 3 seconds the integrated reading will be within 1% of the total incident radiation, provided the period of integration is greater than 4 minutes. Thus averages of solar radiation made over a period of less than four minutes with a standard solarimeter will not necessarily be accurate, however short the sampling interval. Brinkworth & Hughes (1976) showed that by suitable interfacing the response time of the solarimeter can be accelerated, but this is not necessary for this application.

4.1.2 Measuring air temperature.

The accuracy with which average air temperature can be determined is limited by the variations of the air temperature over short distances and short intervals of time. A period of 10 minutes can show variations in air temperature of as much as 2°C (Meteorological Office, 1969). Variations in air temperature over small areas show similar and sometimes even more striking variations, especially in calm conditions at night. This suggests that, except when dealing specifically with fine structure, it is misleading to state the air temperature to an accuracy greater than +/- 0.5°C.

4.1.2.1 Type of sensor.

There are four basic types of temperature sensor which are compatible with a remote data logging system.

a) Thermocouples.

Until recently the most popular type of sensor for remote temperature measurement, thermocouples have the advantage of being stable over long periods of time, relatively cheap and able to withstand high temperatures. Basically two different metals are joined together to make a continuous circuit. If there is a temperature difference between the two junctions an electromotive force is set up dependent on the magnitude of the temperature difference. Thermocouples can either be used in differential pairs (e.g to measure the temperature difference between two bodies), or can be used individually with an electronic reference junction. They have the disadvantage that their output is low (about 40 microvolts per degC), making them susceptible to radio interference (especially if the output is not being measured close to the sensor). This can be overcome by screening the cable and/or using a low-pass filter. The size of the output can be increased by connection of several thermocouples in series (thermopile).

b) Thermistors.

Thermistors are simply temperature sensitive resistors, generally

with a non-linear characteristic. They have the advantage of being cheap and their resistance can be measured using a standard "Wheatstone bridge" circuit. However, their non-linear characteristics rule out a direct conversion from resistance to temperature, and mean that the accuracy that can be achieved will decrease with increasing temperature.

c) Diodes.

Diodes will pass an electrical current which is a complex function of the junction temperature. By choice of a suitable diode the output can be made proportional to temperature. However, they are prone to electrical noise and are not proven as reliable sensors.

d) Electrical resistance thermometers.

Basically a measurement of the electrical resistance of a mass of metal or other material whose resistance varies in a known manner with temperature can be converted into a temperature reading. Until recently, wire-wound platinum resistance thermometers (PRT's) have been used because their stable and linear resistance characteristics, which give a high degree of accuracy. More recently, however, thick-film PRT's have been developed which are considerably cheaper, equally accurate and reliable, and have a much quicker response time.

After consideration, it was decided that thick-film PRT's were the

best of the above alternatives for the measurement of outside air temperature, and indeed for all temperature measurements in the monitoring system, for the following reasons:

1) The repeatability and long-term stability of PRT's is greater than that of diodes, thermistors or similar electronic devices. Long term stability is particularly important when used in long term performance monitoring systems if frequent recalibration is to be avoided.

2) The voltage output level from PRT's can be made greater than that from thermocouples, thus reducing the risk of interference due to radio pick-up and giving greater accuracy of measurement for a voltmeter of given resolution.

3) Thermocouples, in the form of thermopiles, are well suited to the measurement of temperature differences. However, great care must be taken in the forming of junctions and the installation of thermocouples to reduce spurious thermoelectric effects in the measurement system. Whilst this might be quite possible in a laboratory situation, it was felt that it would be difficult to achieve with on-site installation. By choice of suitable calibration and system of measurement it is possible to achieve the required accuracy for temperature difference measurement with PRT's.

4) The low cost of thick-film PRT's make them an economic solution for multi-point temperature measurement.

Basic types of thick-film PRT's available are:

a) 25mm square flat sensor

b) 25mm long x 5mm wide flat sensor

c) 25mm long x 3mm diameter round sensor

25mm square PRT boards were used for all air temperature measurements because of their large surface area per unit mass characteristic. Full manufacturers' specifications for the various thick-film PRT's used are included in Appendix 1.

4.1.2.2 Accuracy.

The uncertainties inherent in the measurement of absolute temperature and differential temperature using thick-film PRT's and a potential divider network have been analysed in detail by Dane (1980), and are as shown in Table 4.1.

LIMITS OF CERTAINTY	ABSOLUTE TEMPERATURE	TEMPERATURE DIFFERENCE
Absolute calibration of reference detectors.	+/-0.02 ohm +/-0.05 °C	Errors common to both sensors
Calibration of sensor	+/-0.025 ohm +/-0.062°C	+/-0.02 ohm +/-0.05 °C
Accuracy of determination of sensor resistance.	+/-0.025 ohm	Errors common to both sensors.
Net	+/-0.038 ohm +/-0.07 °C	+/-0.02 ohm +/-0.05 °C
Equivalent to:	+/-0.2 °C	+/-0.1 °C

Table 4.1 Limits of certainty for temperature measurement using PRT's

4.1.2.3 Positioning of sensors.

The presence of a large array of solar collectors will alter the micro-climate around the building to which it is attached. On a sunny day, the area immediately in front of the solar collectors will form a "sun trap" and may be considerably warmer than the area behind the panels which will be in shade. The air temperature to which the solar panels are losing heat is therefore not necessarily the same as the ordinary ambient air temperature. For this reason, air temperature has been measured both immediately in front of the solar collectors and in the shade on the north side of the building.

It is also important that the sensors used to measure air temperature should be screened from direct solar radiation,

otherwise an error will be induced. The conditions which an ideal screen should satisfy are:

a) The screen should be a "uniform temperature enclosure".

b) The temperature of the inner walls of the enclosure should be the same as that of the external air whose temperature is required. (i.e the enclosure should be well ventilated)

c) The enclosure should completely surround the sensor.

d) The enclosure should be impervious to radiation.

These criteria are fulfilled reasonably well by a conventional "Stevenson screen". Stevenson screens were therefore used in all measurements of ambient air temperature where there was a possibility of exposure to direct solar radiation.

4.1.2.4 Calibration.

The PRT's were calibrated in groups of twelve by inserting them into a series of metal tubes painted with heat conducting grease. The metal tubes were then immersed in a constant temperature water bath as illustrated in Figure 4.5(a). The bath was then allowed to reach thermal equilibrium at temperatures of approximately 25°C, 50°C and 75°C. At each of these equilibrium points each sensor was calibrated against two reference temperature detectors also

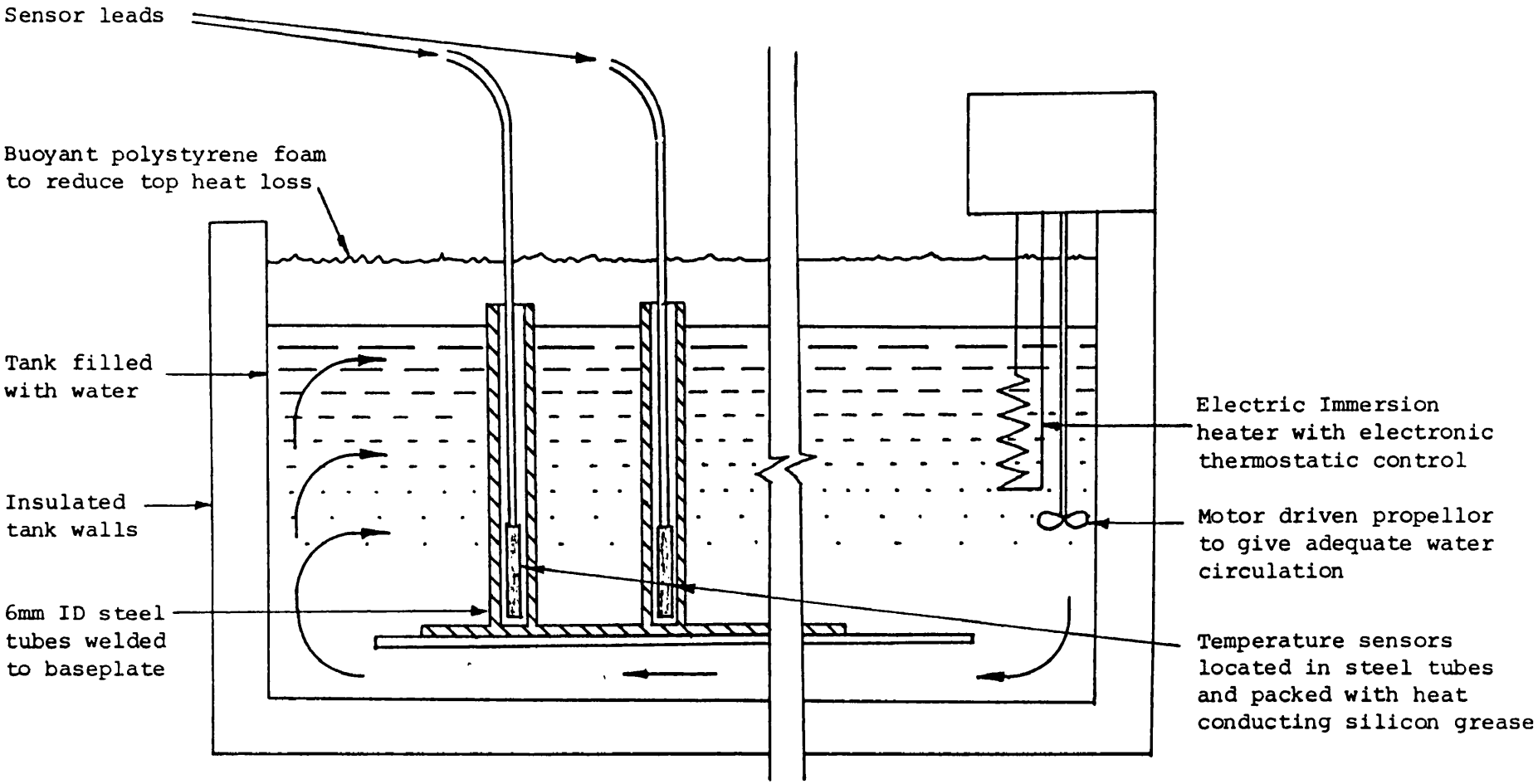

Figure 4.5(a). PRT calibration apparatus.

immersed in the bath. Thus it was not important if the bath was not exactly at 25, 50 or 75°C, as the definitive quantities for calibration purposes are the resistances of the two reference detectors, whose characteristics are known to a high degree of accuracy. Since the calibration is performed against reference detectors of exactly the same mechanical and electrical configuration as the sensors themselves, and within a short space of time, a lot of the possible sources of error such as temperature coefficient of the voltmeter, resistance of lead and connections, etc are common and therefore introduce only second order error terms which can be ignored. The overall accuracy of the calibration process is +/-0.025 ohm, or +/-0.06 °C for each sensor.

4.1.2.5 Measurement system.

The voltage across each PRT is measured using the basic circuit shown in figure 4.5(b).

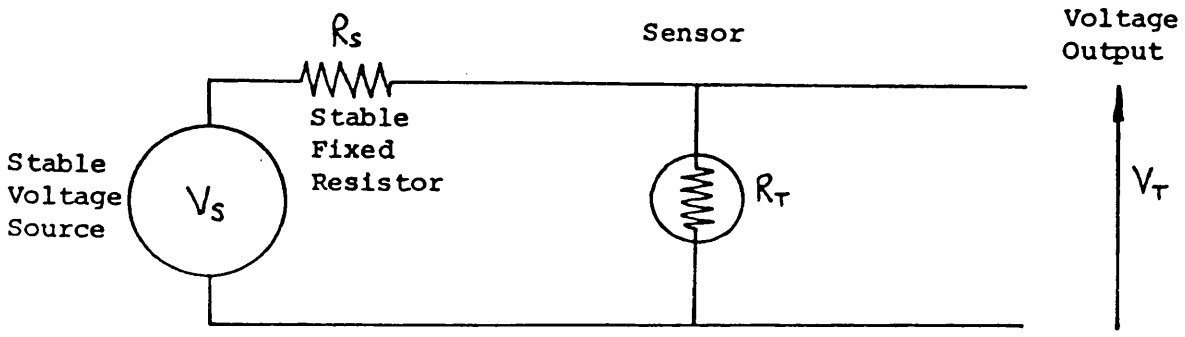

Figure 4.5(b) Basic PRT measuring circuit

The voltage output from the circuit, Vt, is given by equation (4.3):

$$Vt/Rt = Vs/(Rs+Rt) \qquad (4.3)$$

where: Rt = resistance of sensor at temperature T

Vs = circuit excitation voltage

Rs = circuit fixed resistance

Re-arranging:

$$Rt = (Vt/Vs)(Rs + Rt)$$

$$= Rs(Vt/Vs) + Rt(Vt/Vs)$$

Therefore:

$$Rt(1-(Vt/Vs)) = Rs(Vt/Vs)$$

Mutiplying through by Vs:

$$Rt(Vs - Vt) = Rs(Vt)$$

Hence the resistance of the sensor, Rt, is given by equation (4.4):

$$Rt = Rs \times (Vt/(Vs-Vt)) \qquad (4.4)$$

The nominal value of the temperature stable fixed resistor Rs is

6000 Ohms. However, there is a wide variation in the lengths of cable needed to run from the data logger to the various sensors, which meant that it was possible for the total fixed resistance in any measuring circuit (i.e fixed resistor plus cable resistance) to vary between 6000 and 6006 Ohms, introducing an unnecessary source of inaccuracy into the measurement of temperatures. This uncertainty of circuit resistance has been reduced to 0.6 ohms by calibrating each measuring circuit individually using fixed resistors (which correspond approximately to the ice point and boiling point for PRT's) in place of the PRT's.

4.1.2.6 Curve fit for PRT's.

Due to restraints of time, the PRT's were calibrated at only three temperatures of 25,50 and 75°C, as described above. Some method of representing the resistance-temperature curve over the full operating range (say, -10 to +150°C) must therefore be found. It can be shown that the best curve fit is obtained by a quadratic representation of the type:

$$Rt = aT^2 + bT + c \qquad (4.5)$$

where: Rt = resistance of the sensor at temp T

a,b,c are constants.

The constants a,b,c are calculated for each PRT from the three calibration points according to the following equations:

$$a = 1/1250\ (R25 - 2R50 + R75) \qquad (4.6)$$

$$b = -1/50\ (5R25 - 8R50 + 3R75) \qquad (4.7)$$

$$c = 3R25 - 3R50 + R75 \qquad (4.8)$$

where: R25 = resistance of PRT at 25°C

R50 = resistance of PRT at 50°C

R75 = resistance of PRT at 75°C

The temperature T can then be calculated from the PRT resistance Rt by finding the positive root of the quadratic equation (4.5) as follows:

$$T = (-b + \sqrt{(b2 - 4a(c-Rt))})/2a \qquad (4.9)$$

The constants a,b and c are held in the computer memory for each PRT. The voltages Vt and Vs (from equation 4.4) are both measured by the data logger at each scan. Hence the temperature T can be calculated from equations (4.4) and (4.9).

4.1.3 Measuring wind velocity.

Whillier (1967) showed that the air velocity across a solar collector will affect the convective heat loss coefficient of the

collector, and hence will have an effect on the overall heat gain of the collector, though the effect is small in all but very strong winds. If it were desired to determine accurately the dependence of collector performance on wind velocity, it would be necessary to take measurements of air velocity on a grid basis over the entire collector area. This type of research is best done under laboratory conditions, and it was thought inappropriate for the long-term monitoring of a large scale active solar heating field trial to be concerned with such fine details. For this purpose, it was sufficient to use a single anemometer to give a qualitative indication of wind velocity.

4.1.3.1 Type of sensor.

Vane anemometers, hot wire anemometers, and cup anemometers were considered. It was decided to use cup anemometers since these are used universally in weather stations and are best suited to outside use.

4.1.3.2 Accuracy.

A detailed discussion of the accuracy of wind velocity measurement using cup anemometers would be out of place here, since it has already been observed that only a qualitative indication of wind speed is required. However, it is worth mentioning that the cup wheel of the anemometer tends to accelerate more quickly with an increase in wind than it decelerates in a falling wind. This leads

to an overestimate of the true mean wind speed in variable wind conditions. Deacon (1951) showed that for large (100%) fluctuations in wind speed over short time intervals (a few seconds) the error in reading may be as high as 25%. However, for a 10% sinusoidal variation in wind speed the error will be less than 1%. Full specifications for the instrument used for wind speed measurement are included in Appendix 1.

4.1.3.3 Position of sensor.

Since only a qualitative indication of local wind speed was required, the position and height at which the anemometer was mounted was not critical. It was decided to mount the anemometer at a height of 3 metres above ground level at a distance of approximately 3 metres in front of the solar collector array.

4.1.3.4 Measurement system.

As in the case of solar radiation measurements it is more accurate to record the integrated output from the anemometer over a period of time, rather than taking instantaneous readings which would be subject to momentary gusts or lulls at the time of measurement. Cup anemometers are available with pulsed or analogue outputs. Pulsing instruments were chosen since they make the integration of the output much simpler. It is then only necessary for the data logger to count the number of pulses at the end of each time interval in order to produce an average figure of wind speed.

4.1.4 Measuring fluid temperature in pipes and tanks.

The accurate measurement of fluid temperature in pipes and tanks is clearly of vital importance in assessing the performance of a solar heating system.

4.1.4.1 Type of sensor.

Thick-film platinum resistance thermometers were chosen for all temperature measurements for the reasons described in section 4.1.2. The types of thick-film PRT's used were:

a) 25mm square sensors.

These were used for air temperature measurement due to their high surface area to mass ratio.

b) 25mm long, 3mm diameter sensor.

These were used for temperature measurements within bodies (e.g cross-tubes in pipes, thermowells in tanks).

c) 25mm long, 5mm wide flat sensor.

These were used for surface temperature measurements.

Details of these sensors are included in Appendix 1.

4.1.4.2 Positioning of sensors.

The measurement of fluid temperatures in tanks has been made using standard engineering practice of inserting thermowells into the body of the tank, as illustrated in Figure 4.6.

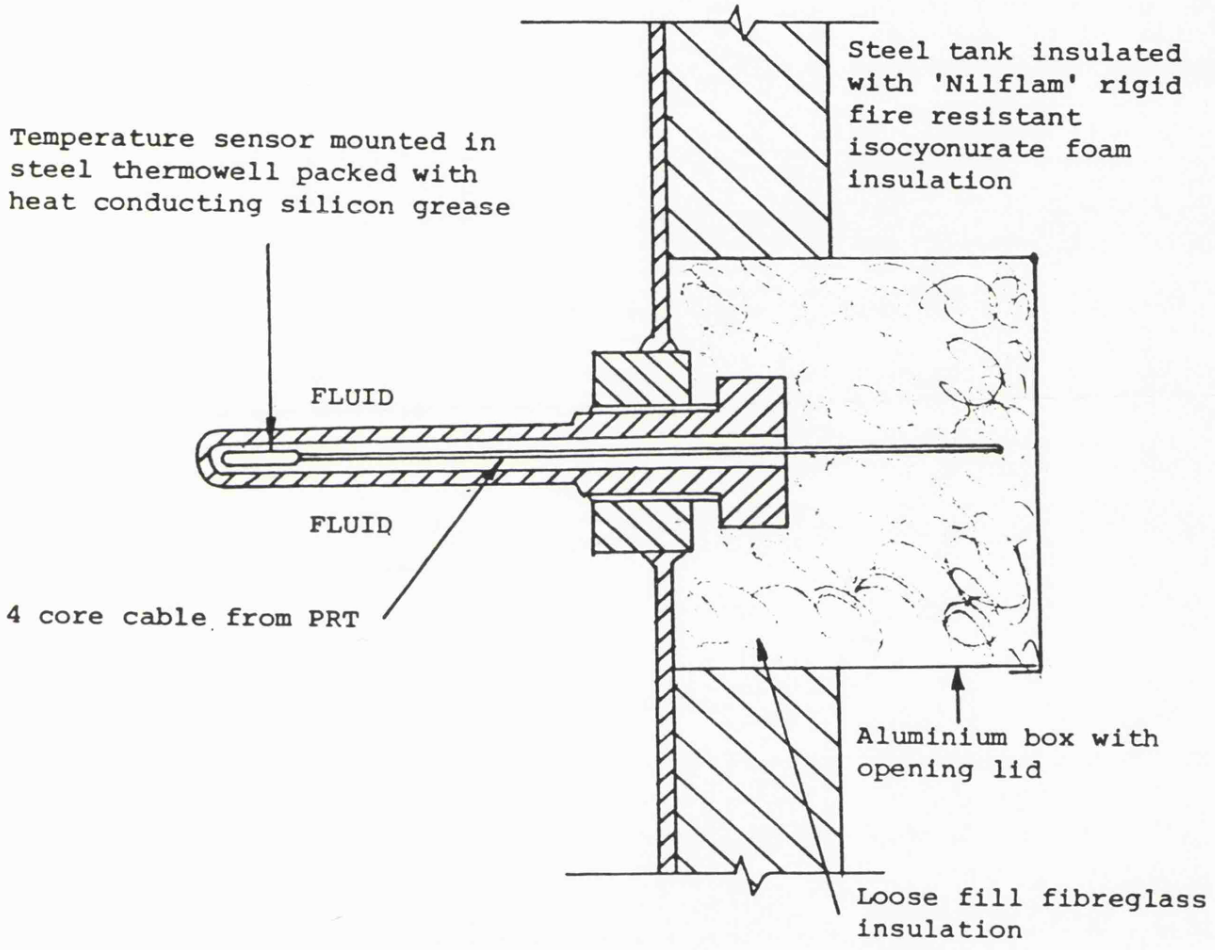

Figure 4.6 Measurement of fluid temperature in tanks

A 3mm diameter PRT has been placed in each thermowell, packed with heat conducting grease to ensure good thermal contact.

CHAPTER FOUR

The effect of sensor mounting on the accuracy of fluid temperature measurement in pipes has been investigated in detail by Dane (1980). The results of this investigation may be summarised as follows:

a) Significant innaccuracies of the order of several degrees Celsius can result if the sensor is placed on the outer wall of the pipe, even if the thermal contact is good and the pipe is well insulated. The response time is also slow with this type of measurement.

b) A sheathed sensor inserted directly into the pipe through a pipe gland gives excellent response time and approach to fluid temperature. However, this method has the important practical disadvantage that access to the sensors involves draining the pipework.

c) Sensors mounted in thermowells (as is common practice in the heating, ventilating and air conditioning industry) give a rather slow response time due to the thermal inertia of the thermowell itself. Installation costs are also relatively high.

d) The recommended method is to weld or solder a cross-tube (preferably of similar material to the pipe) of 5-6mm internal diameter into the pipe, as illustrated in Figure 4.7.

The cross-tube should be blanked off at one end. The length and angle of insertion of the cross-tube should be such that the complete length of the sensor can be mounted within the fluid stream. The sensor is inserted into the cross-tube, which is packed with heat conducting grease. The exit point of the sensor cable is insulated to minimise temperature gradients along the cross-tube.

Method (d) above gives excellent response time due to the relatively low thermal inertia of the cross-tube, and also has the advantage that access to only one side of the pipe is required for installation. Method (d) was therefore used for all pipe fluid temperature measurements.

The choice of positions for the cross-tubes themselves was an important factor. Near pipe junctions, the cross-tube was positioned at least 10 pipe diameters upstream or downstream of the junction (whichever is the temperature required), to allow a proper mixing length.

4.1.4.3 Calibration, accuracy and measurement systems.

These topics have been fully covered in section 4.1.2.

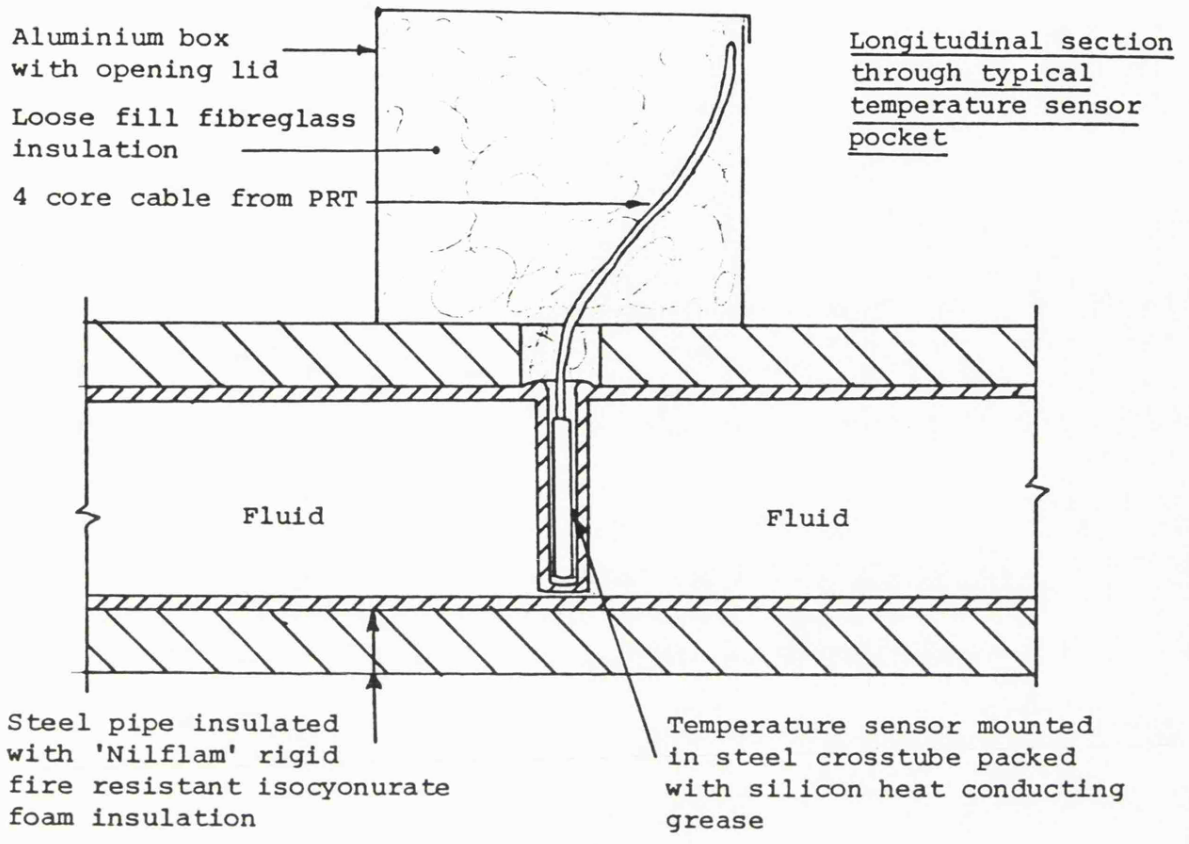

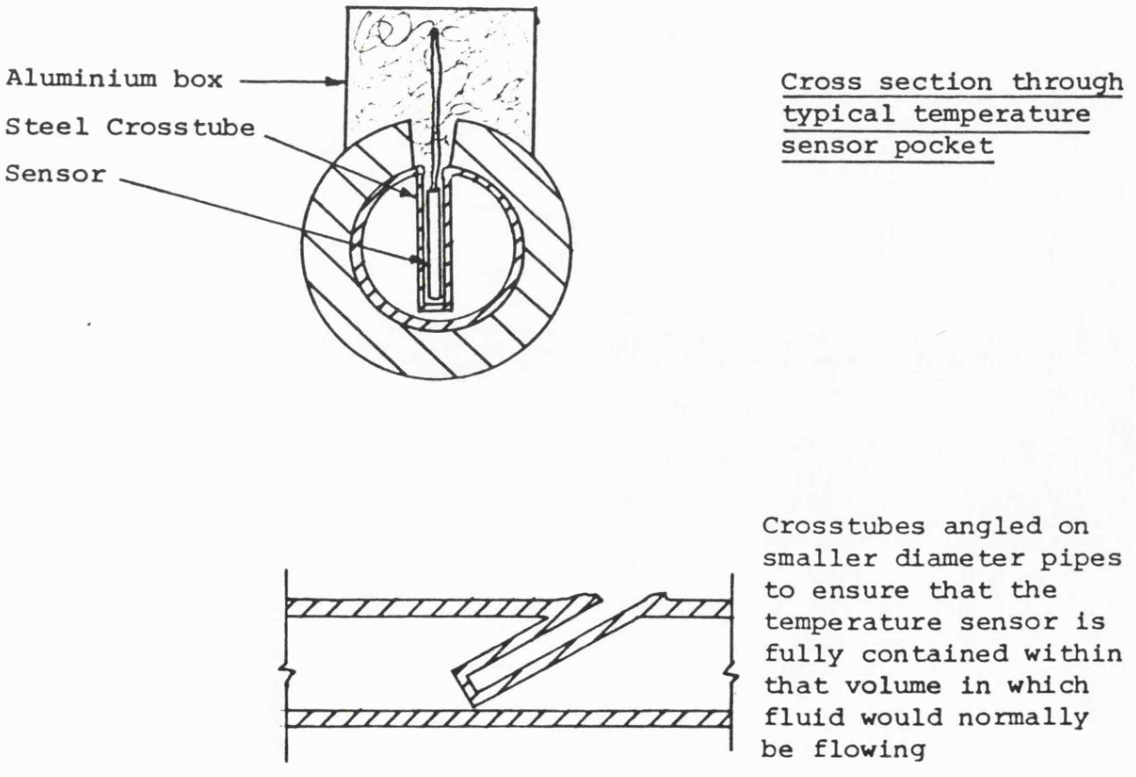

Figure 4.7. Typical temperature sensor installation details.

4.1.5 Measuring fluid flow rates in pipes.

All fluid flow rates to be measured were those of pressurised, incompressible fluids contained within fully flooded pipes. Open channel and volumetric flow metering techniques could not have been implemented without extensive modifications to the fluid network and such methods were therefore ignored.

4.1.5.1 Type of sensor.

There is a wide variety of flow metering systems commercially available, including pressure meters, ultrasonic meters, turbine meters, magnetic meters and thermal devices. This section looks briefly at each of the possible methods, and explains the reasons for the final choice of turbine meters. References are made to a number of papers contained within conference proceedings edited by Wendt (1977) and Spencer (1977).

Pressure meters.

Orifice plates and venturi meters both work on the principle of producing a differential pressure output, p, which is dependent on the average velocity, v, of the fluid passing through the meter such that p is proportional to v^2.

The manufacture and calibration of these meters is covered by British Standards (BS1042), giving a common standard for all meters. The meters require careful installation including flow straightening to ensure that the fluid conditions at inlet and outlet are suitable to give a valid reading. The meters will also introduce a hydraulic resistance into the fluid circuit which should be considered during the system design. The disadvantage of these meters when used with a remote data logging system is that the differential pressure must be converted to an electrical signal using an additional pressure transducer. The accuracy of this transducer will reduce the overall accuracy of the meter unless the combination can be calibrated as a single unit. Also, because of the nature of the meter output (i.e pressure proportional to v^2), an accurate reading over a 10:1 flow rate range will require an accurate reading over a 100:1 differential pressure range. This meter characteristic imposes a serious limitation on the range of flow rates which can be measured with acceptable accuracy.

Ultrasonic flow meters.

Three basic methods underlie nearly all the specific techniques that have been used in ultrasonic flow meters:

a) The travel time difference method. Sound waves are transmitted in opposite directions relative to the flow and the difference in travel times is measured.

b) The beam deflection method. The deflection of an acoustic beam transmitted transversely to the flow is measured.

c) The Doppler shift method. Sound waves are projected along the flow path and the frequency shift in the returning signal from scatters in the fluid is measured.

Ultrasonic flow meters have unique advantages in that they are non-obstructing, linear, and are suitable for any fluid through which sound can be transmitted. Their major disadvantage is their comparatively high cost.

Turbine flow meters.

Turbine flow meters operate by the action of the moving fluid striking the angled blades of a rotor causing the rotor to spin. The speed of rotation is directly proportional to the velocity of the fluid, and is detected by a magnetic pickup. These meters have the advantage of excellent repeatability, linearity, accuracy and response with relatively low meter cost. Turbine meters should have a stable calibration over long periods of time provided they are installed correctly (see later). The Pelton wheel flow meter is a variation on the straightforward turbine meter. A proportion of the flow is diverted to form a jet which impinges on a rotating

paddle wheel. These meters have the disadvantage that the slightest obstruction in the diverting path can cause a significant measurement error.

Magnetic meters.

Magnetic flow meters work on the principle of induced current in a conductor which is put in motion through a magnetic field. Thus the fluid whose flow rate is to be measured must be conductive, although in practice the fluid in any pipe network will probably contain enough impurities to enable the meter to operate. The repeatability of these meters is high though the output is not truly linear. Hence they may have a flow range of less than 10:1 at the 1% accuracy level. Like ultrasonic flow meters, they have the advantage of being non-obstructing but they do require careful pipework design upstream of the meter. Their high cost may be prohibitive in many applications.

Thermal devices.

Thermal devices for measuring fluid flows are essentially of two types. One type depends on the cooling of a heated body exposed to the flow and is generally unsuitable for continuous flow metering because of the discontinuous nature of the output. The other type depends on heating the stream and relating the heat input and the temperature rise of the fluid. Commercially available meters are for use mainly in gas anemometry and are unsuitable for measurement

of liquid flow rates in pipes.

The final choice of sensors for the measurement of fluid flow rates in pipes was made on considerations of accuracy, reliability and cost, resulting in AOT turbine flow meters being used for all flow rate measurements. Various meter sizes were used corresponding to the range of flow measurement required. These meters have the advantages of excellent repeatability, linearity, accuracy and response with relatively low cost. Output is generally independent of temperature over the range 0-100 ^{o}C, and accuracies of +/- 0.5% can be obtained with a turn-down ratio of 10:1. Full manufacturers' specifications for the turbine flow meters used are included in Appendix 1.

4.1.5.2 Mounting and positioning of sensors.

The correct mounting and positioning of turbine flow meters is of vital importance if accurate readings are to be obtained. Typical installation details are illustrated in Figure 4.8. The pipework inner diameter must be reduced to the flowmeter inner diameter for a minimum distance of 15 pipe diameters upstream and 10 pipe diameters downstream from the meter (unless special flow straightening devices are used), and must run perfectly straight for this total distance of 25 pipe diameters. A strainer should be positioned upstream of each meter, as shown in Figure 4.9, to minimise the risk of damage to the delicate rotor assembly. If water is the fluid in question, excessive hardness will lead to

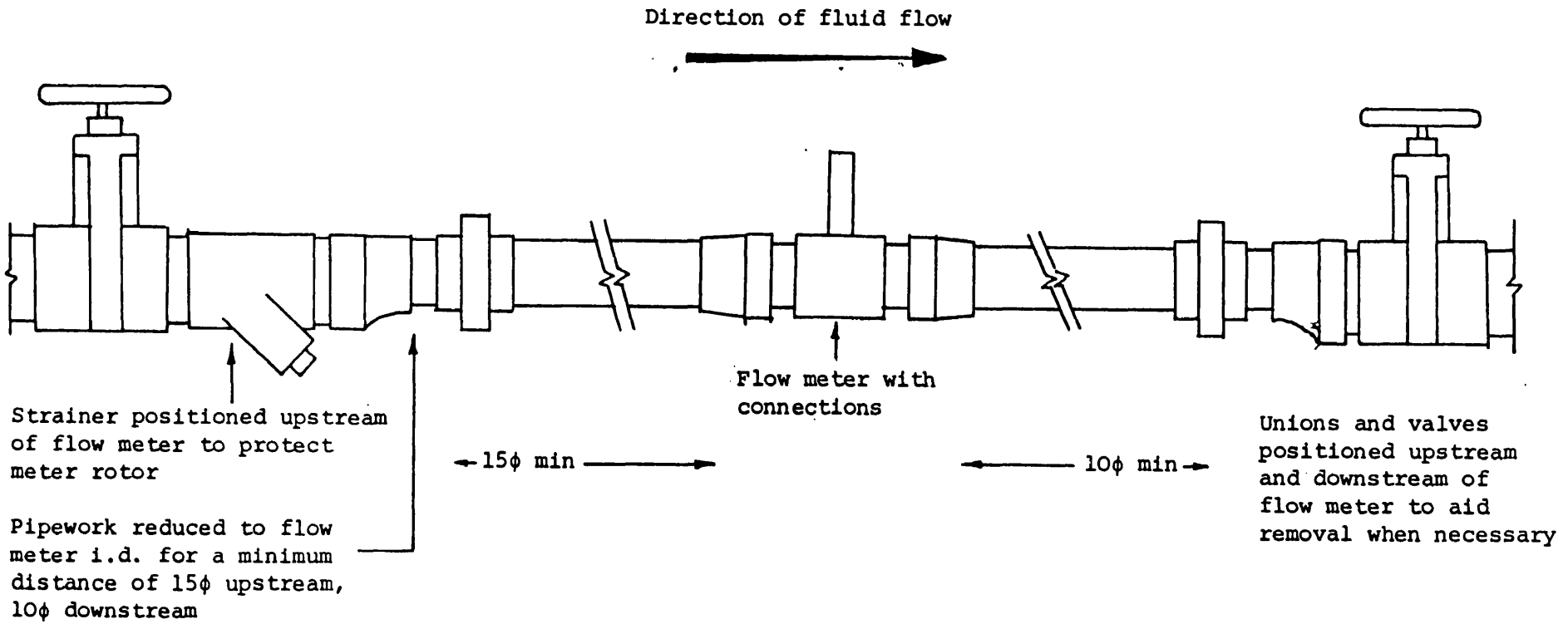

Figure 4.8. Typical flow metering station.

deposition within the meter which will have an adverse effect on the meter performance. The meters may be mounted horizontally or vertically, the vertical position being favoured if there is any air in the system.

4.1.5.3 Calibration and accuracy.

All flowmeters used were supplied ready-calibrated by the manufacturers. The meters are calibrated at five points over the full working range (turn down ratio = 10:1), and an average pulses per litre figure is derived from the five values obtained.

4.1.5.4 Measurement system.

The output from an AOT turbine flowmeter is a sinusoid whose frequency varies in direct proportion to flow velocity. This is fed into the signal conditioning circuit shown in Figure 4.9, which produces a square wave type output of the correct amplitude for input to the data logging system. These pulses are counted and averaged to give flow readings.

4.1.6 Measuring plant status.

It was important to monitor the status of certain plant items (e.g pumps, valves, boilers). This was achieved by simply placing a relay in the circuit with a 240 volt coil operating a switch in the

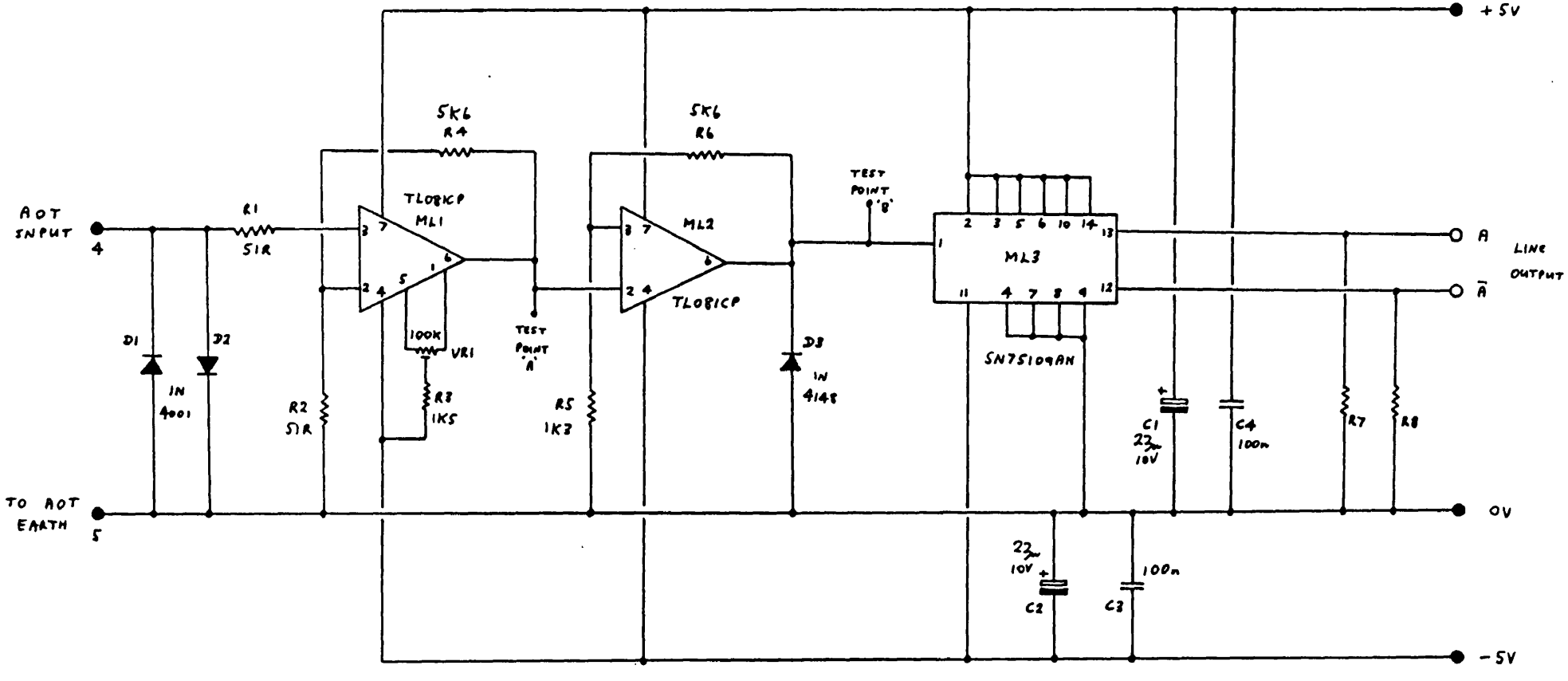

ALL RESISTORS :- 0·25W, 2%, METAL FILM.

R7/R8 - S.O.T.

A.O.T. CIRCUITRY

TYPICAL CURRENTS :- ± 40mA

MAX CURRENTS :- ± 65mA

Figure 4.9. Signal conditioning circuit for AOT flow meters.

low voltage monitoring circuit, as shown in Figure 4.10.

4.1.7 Parameters monitored.

The objective of the monitoring programme was to collect and analyse data in sufficient detail to enable the following tasks to be carried out:

a) To calculate the primary performance factors for the solar heating systems, as laid down by the International Energy Agency (1979) and the Commission of the European Communities (1980).

b) To collect data in sufficient detail to enable a computer model of the system to be calibrated, and meaningful comparisons drawn between measured and modelled performance.

The choice of the parameters to be monitored was made with the above considerations in mind. A full list of the parameters monitored, together with a system schematic diagram showing the positions of the main monitoring points, is given in Appendix 3. All the required energy flows, Q, are calculated by combining two temperatures (flow and return) and a flow measurement, according to equation 4.10.

$$Q = \dot{V}.p.Cp.(Tf-Tr) \qquad (4.10)$$

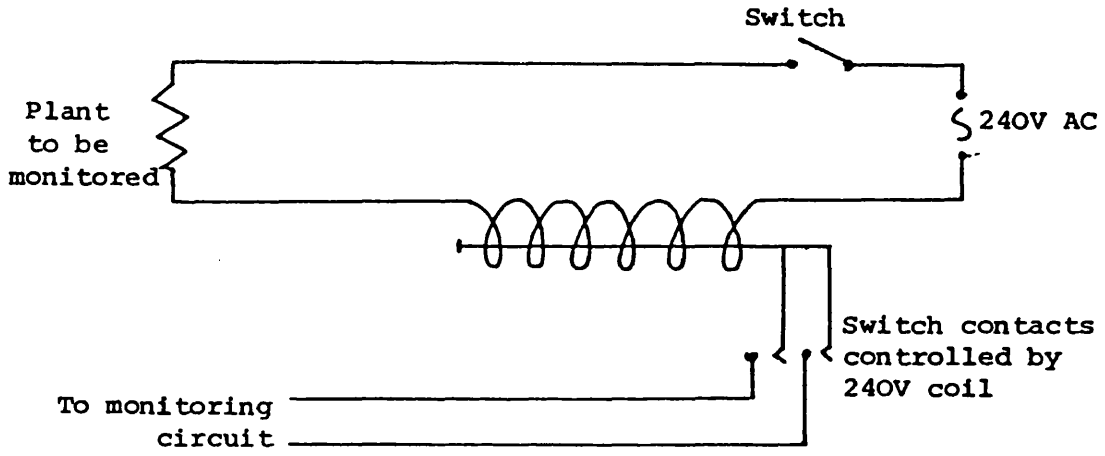

Schematic diagram showing relay operation for status channels

Figure 4.10. Plant status measurement.

where:

$\dot{V}$ = volume flow rate (l/s)

p.Cp = product of density and S.H.C for water (J/l°K)

Tf = flow temperature

Tr = return temperature

4.1.8 Data logging system.

Figure 4.11 shows the layout of the main hardware components of the data logging system. The system is based on a Hewlett-Packard 9825T desk-top computer for which software has been specially written by Lewis (1980).

In addition to the computer, the system consists of a Hewlett-Packard (HP) 3495A 80-channel thermal dry reed relay scanner, HP3455A digital voltmeter, HP2240A measurement and control processor, HP98035A Real Time Clock, and a Perifile 6041 tape cartridge recorder (Perex Ltd).

4.1.8.1 Signal conditioning.

Section 4.1 described the considerations given to sensor choice, installation, calibration and accuracy. This section deals with the consideration given to all sensors to ensure that each type of signal output was transmitted accurately, and in intelligible form,

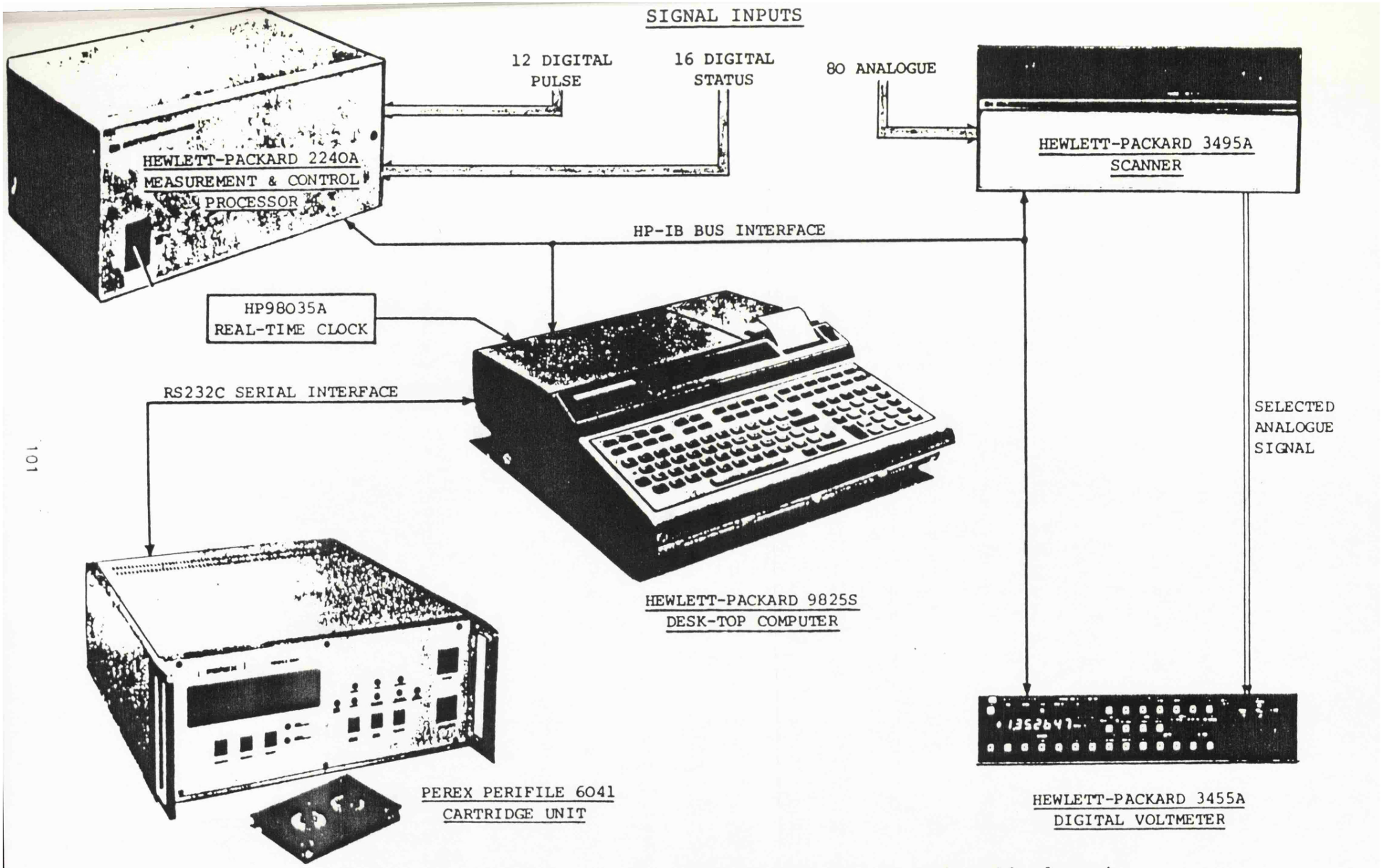

Figure 4.11. Data logging system schematic layout.

to the central data logger.

The data logging system required analogue or digital signal inputs to conform to the following specifications:

Analogue:	max voltage	42 volts (on highest range)
	resolution	1 microvolt (on lowest range)
	reading to	5.5 significant digits
Digital:	levels	5 volt to 12 volt TTL or CMOS

4.1.8.2 Analogue signals.

Solarimeters and temperature sensors give an analogue voltage output as described in Chapter Three. The voltage level from the sensors is sufficient for the accuracy required, without the need for amplification. Attenuation of the signals down the long lengths of cable was found to be negligible, as shown in Appendix 4. Some induced noise can occur in the signal cables, in spite of their screening, but due to the relatively long sampling time of the digital voltmeter used (20 milliseconds) this was effectively smoothed out. Thus it was possible to wire direct between the sensors and the data logger.

4.1.8.3 Digital signals.

The different output devices used (status relays, flow meters and

anemometers) give a variety of waveforms, voltage levels and frequencies. It was necessary to provide signal conditioning for each device to accurately transmit the signal a distance of up to 50 metres and to generate an output within the range 5-12 volts TTL or CMOS levels. Examples of the various signal conditioning circuits used to achieve this are shown in figures 4.9 and 4.10.

4.1.8.4 Capability of data logger.

The capability of the data logging system used may be summarised as follows:

Number of analogue channels = 80
(e.g temperatures, solarimeters)

Number of pulse counting channels = 12
(e.g flow meters, anemometer)

Number of plant status channels = 32
(simple on/off signals)

Data storage capacity of one cartridge = 1.8 Megabytes

Computer memory capacity = 64 kbytes

4.1.8.5 Software development.

The software for the data logging system has been developed over a period of five years, and is still under development at the time of writing.

4.1.8.6 Software version "SABER1".

The letters "SABER" are a mnemonic for School of Architecture and Building Engineering Research. The original version of the data logging software, SABER1, was first implemented in October 1979. This early version of the software recorded the conditioned signal from each sensor (i.e voltage levels and pulse counts) directly onto the tape cartridges. These readings had to be converted into engineering units (i.e ^{o}C, litres/sec), using the appropriate calibration data for each sensor, before any analysis could be carried out. The output from all the sensors was measured at each scan interval (which varies from 15-30 seconds depending on how much work the computer is doing). However, not all the readings were recorded at each scan, since this would result in an unnecessarily large amount of redundant data being recorded. Instead, each reading was compared to the previous mesurement, and would only be recorded if the reading had changed by a significant amount. What constitutes a "significant" change for each parameter is defined by the user and contained in the computer set-up data. This selective data recording greatly reduces the amount of redundant data recorded when little is changing within the system,

but retains the necessary accuracy by making frequent recordings when rapid changes are taking place.

4.1.8.7 Software version "SABER2".

Between 1980 and 1982 a second, more powerful version of the data logging software was developed. The computer memory was increased from 16 to 64 kbytes. The calibration data for all the sensors could now be stored in the computer memory so that the input signals (i.e voltage levels and pulse counts) could be converted directly into engineering units and recorded in this form on the tape cartridge. The extra memory also enabled the computer to combine signals (e.g two temperatures and a flow rate) in order to calculate the energy flows into and out of the various system components. These energy flows are totalled at hourly and/or daily intervals, and recorded on the tape cartridge along with the detailed data.

These improvements have greatly facilitated the analysis of data both on site and in house, enabling the overall system performance to be summarised quickly. The detailed data are recorded on the same selective basis as before, though the minimum scan interval has increased to 30 seconds as a result of the extra computation. The longer scan interval will not lead to significant measurement errors, because the interval is still short compared with the typical transient response time of the installation.

4.1.9 Data analysis.

There would have been no point in developing the powerful, flexible and sophisticated data logging system described in Chapter Four unless facilities for analysing the recorded data were developed concurrently. This section describes the early analysis facilities which were already available, the limitations of these facilities, and the subsequent mainframe computer analysis facilities developed by the author.

4.1.9.1 Early analysis facilities.

Early facilities for analysis of data recorded by the "SABER1" version of the data logging software consisted of a Hewlett-Packard 9825T desk-top computer, a Perifile 6041 cartridge recorder and an HP 9862A calculator plotter. Using this equipment, selected single parameters or compound parameters (e.g energy flows) could be averaged, integrated and plotted over a selected period of time. The analysis programs were written in "HPL", a programming language exclusively for Hewlett Packard equipment. The software has been fully documented by Dane (1980).

The limitations of these early analysis facilities were severe. Due to the sheer size of the database it would take approximately 3 hours of computer time to plot, average and integrate a compound parameter over a period of one week. Many such computations were

necessary for a complete analysis of one week's system operation, and it was found that one week's full analysis took one man-week. Clearly, therefore, it was not practicable to proceed with these limited analysis facilities.

4.1.9.2 Data transfer to mainframe computer.

In view of the serious limitations of the original analysis facilities developed by Dane (1980), it was decided that the recorded data should be transferred to the University mainframe computer for analysis. A Tandberg TDC3000 digital cartridge reader/recorder was purchased for this purpose, and a line driver for the unit was developed by Lewis. Correct operation and interfacing of the unit was achieved in September 1982. One week's recorded data could then be transferred to disk on an intermediary computer (a PDP11) in about eight minutes, and checked. Thence the data are transferred to the "Multics" mainframe computer system via an interface known as "Mulink", and checked again. This secondary transfer takes about thirty minutes. Once transferred, the data are edited into a form more susceptible to analysis (one line per data record). The size of the database built up was too large to be stored on public disk space on the University mainframe computer. Arrangements were made, therefore, to purchase a private volume disk with a data storage capacity of 160 Megabytes. This disk is kept at Bristol University computer centre and is mounted when requested, subject to the availability of an appropriate disk drive. The data are also archived to 9-track 1600 bpi magnetic

tape for safe keeping.

4.1.9.3 Mainframe computer data analysis.

This section describes in detail the software developed for mainframe computer analysis of the recorded data. The programs are written in full-language FORTRAN77. The only non-standard features of the programs are:

a) Variable names are not restricted to 6 characters, but may be up to 32 characters in length.

b) "Encode" and "Decode" statements have been used, which are peculiar to the "Multics" FORTRAN system, and are equivalent to the internal file read and write statements of standard FORTRAN77.

4.1.9.4 Aims of analysis.

The basic aim of the programs was to provide the user with the facility to examine selected items of data over selected periods. This enables the overall thermal performance of the system to be evaluated, and any operational problems to be identified and diagnosed. With this general aim in mind, the analysis programs were written to enable the following specific tasks to be carried out:

a) To reduce the size of the raw data block down to a few parameters of interest, for a specified period, prior to detailed analysis. (This operation is essential to avoid wastage of computer processing time reading repeatedly through large amounts of redundant data.)

b) To produce a neatly formatted printout showing the values of certain parameters of interest, as well as the time and date corresponding to each value.

c) To overlay graphs of up to six parameters of interest, each with a separately scaled and labelled vertical axis, on a common time axis. Each graph should have identifying symbols to avoid confusion where lines cross. (This facility provides an extremely useful analysis tool, in that it gives a quick pictorial representation of the interdependence between certain parameters, and hence gives a valueable insight into the overall system operation.)

d) To calculate the average value of a particular parameter or parameters over a specified period of time.

e) To calculate the total (i.e sum of recorded values) of a particular parameter or parameters over a specified period.

f) To find the number of changes of state of a particular plant item (e.g on/off switchings of a pump) over a specified period.

g) To find the total time spent in one or other state by a particular plant item within a specified period (e.g the total running time of a pump, or total time spent closed for a motorised valve).

h) To find the maximum and minimum recorded values for a particular parameter or parameters over a specified period.

4.1.9.5 Assumptions necessary for data analysis.

Before describing the data analysis programs in detail, it is necessary to give a brief description of the method and format used by the data logging system to record data, as this will obviously have an influence on the analysis process.

4.1.9.6 Form of recorded data.

The data logger scans all the monitored parameters once every 20-30 seconds (depending on the total number of parameters). In order to minimise the amount of redundant data recorded, the data logger will normally record the value of a parameter only if its value has changed by a significant amount since the previous recorded value

(what constitutes a "significant" change for a particular parameter is specified by the user in the computer set-up data). There is, however, a default time interval (normally three hours) after which all the monitored parameters are recorded, regardless of their values. Whenever the computer records a parameter value, it also records the time. Thus, a typical file of raw recorded data will look like that in Table 4.2.

```
D200683 ——— — date ddmmyy (20th June 1983)
T000130 ——— — time hhmmss (1.5 minutes past midnight)
Q64  15.72 — — value of parameter Q64
Q68  47.62
T000500 ——— ————————— (5 minutes past midnight)
Q64  16.22
Q31  19.97
T001230
Q64  16.72
Q68  46.46
P 3  3.16
S12  1
   etcetera
```

Table 4.2. Typical file of raw recorded data

4.1.9.7 Analysis assumptions.

The recording method described above means that, for data analysis purposes, it must be assumed that the value of a particular parameter is constant between two recorded values, and changes in discrete steps. If one attempts to interpolate between recorded values by assuming a steady linear change then a significant error can be generated. This is adequately demonstrated by the following simple example:

Suppose that the temperature of fluid in a pipe has been essentially constant, at the surrounding air temperature of 12°C, for a period of one hour. Suddenly a boiler or pump comes on, and the temperature rises rapidly to 80°C (within 30 seconds, say). The temperature remains at about 80°C for approximately five minutes, after which the pump switches off and the fluid temperature reverts asymptotically back to 12°C over a period of an hour or so. Let us suppose also that the user has specified a temperature change of 1°C to be "significant" for this parameter. The situation is illustrated in Figure 4.12.

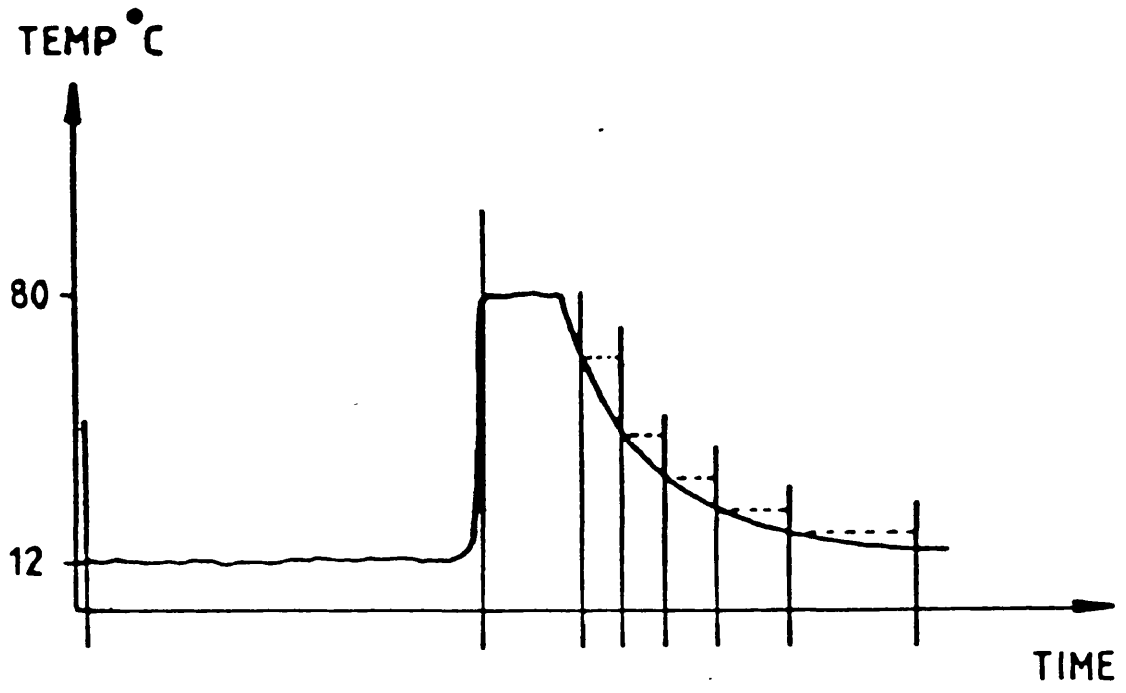

Figure 4.12 Example of data recording operation

Vertical lines indicate the approximate times at which the computer might record the pipe temperature. Clearly it makes no sense to interpolate linearly between the first and second recorded values. It is a much better approximation to assume that the first recorded value of 12°C is valid for the whole time interval up to the next recorded value.

A contrary situation arises when the pipe temperature begins its slow asymptotic return to the environmental temperature. If each recorded value is assumed to be valid for the subsequent time interval, the result will clearly be a slight overestimate of the true average fluid temperature.

There are two possible assumptions for the purposes of data analysis:

1) Assume a steady linear change between recorded values.

2) Assume each recorded value is valid for the subsequent time interval (i.e until next recorded value).

Let us examine these assumptions in the light of the above example with regard to the four possible situations below:
(Note: the terms "rapidly" and "slowly" are relative to the scan interval of 20-30 seconds.)

a) Measured quantity usually increases rapidly and decreases

rapidly.

b) Measured quantity usually increases rapidly and decreases slowly.

c) Measured quantity usually increases slowly and decreases rapidly.

d) Measured quantity usually increases slowly and decreases slowly.

Assumption 1 will give a large systematic error in cases (a),(b) and (c). Assumption 2 will give a small systematic error in cases (b) and (c) only. Assumption 2 is, therefore, clearly the better approximation, and this is the assumption that will be used throughout the analysis process. The scan interval is, in any case, so short that any such measurement errors will be small.

Full details of all the analysis programs written are given in Appendix 5.

4.1.10 Experimental programme.

Before presenting the results to date it is important to note that, during the monitoring period, a number of changes have been made to the system. For example, three of the four heat exchanger batteries in the solar calorifier were valved off for a period of time. The storage volume was also reduced from 10000 litres to 3000 litres for a short period, and some changes were made to the settings of the differential temperature controller governing the

collector circulating pump. Such changes will have an effect on the performance of the solar heating system, though it is not yet known to what extent.

The experimental sequence of events during the monitoring period was as follows:

DATE	ACTION TAKEN
13.4.83 - 19.6.83	System fault-finding and re-commissioning.
19.6.83 - 13.7.83	Full storage volume, all four heat exchanger batteries in use. Controller settings : dT(on) = 6°C, dT(off) = 1°C.
13.7.83	Three of the four heat exchanger batteries in the solar calorifier valved off.
9.8.83	All four heat exchanger batteries back in circuit. Controller settings altered to dT(on) = 12°C, dT(off) = 1°C, but operation incorrect (pump ran continuously till 31.8.83).
23.8.83	Unsuccessful attempt to valve off 7000 litre solar accumulator (thermosyphoning effects caused tanks to mix).
31.8.83	Re-adjusted controller settings to dT(on) = 20°C, dT(off) = 2°C.
6.10.83	Further unsuccessful attempt to valve off solar accumulator.
25.10.83	Valved off 7000 litre solar accumulator properly.
16.11.83	Solar accumulator back in circuit, but mixing pump left off to allow tanks to thermosyphon naturally.

4.1.11 Accuracy.

Before presenting the results to date, it is important to include some general notes on the overall accuracy of the measurements.

The nature of energy monitoring is such that one is generally attempting to measure a parameter which is varying with time. In this situation it is not possible to take a statistically valid sample of measurements, since it is likely that the true value of the parameter one is trying to measure will be changing during the period in which the sample is taken. Thus for any one measurement there will be systematic uncertainties present which cannot be reduced by randomising the conditions. It is important that these systematic uncertainties are evaluated and this work has been carried out by Dane (1980-EG7). The method of calculation of the limits of certainty for each type of measurement is that put forward by Campion et. al.(1969) at the National Physics Laboratory. In the majority of cases one is reliant upon manufacturers' specifications for the various instruments used. The results are summarised in Table 4.3.

Parameter measured	Systematic uncertainty
Solar radiation	+/- 5%
Temperature difference	+/- 0.1 ^{o}C
Fluid flow rates	+/- 2% at 10:1 turndown +/- 5% at 20:1 turndown

Table 4.3 Systematic uncertainties in measurement

By combining the limits of certainty quoted above it is possible to calculate the limits of certainty for a measured heat flow at a specified temperature difference and flow rate:

The heat flow into a particular area within the system, Q, is given by equation 4.11.

$$Q = \dot{m} \cdot Cp \cdot (Tin - Tout) \qquad (4.11)$$

where:

$\dot{m}$ = mass flow rate of fluid entering or leaving the area (Kg/s)
Cp = specific heat capacity of the fluid (kJ/Kg°K)
Tin = fluid temperature in (°K)
Tout = fluid temperature out (°K)

The flow meters used in this project measure volume flow rate, $\dot{V}$ (litres/sec), and so the reading must be multiplied by the density, p (Kg/l), to give mass flow rate $\dot{m}$ (Kg/s).

Hence, $$Q = \dot{V} \cdot (p \cdot Cp) \cdot (Tin - Tout) \qquad (4.12)$$

The working fluid used throughout the system is water, whose density and specific heat capacity vary with temperature. However, by considering the product (p . Cp) as a single fluid property, and taking its value as being a constant at the midpoint of the working

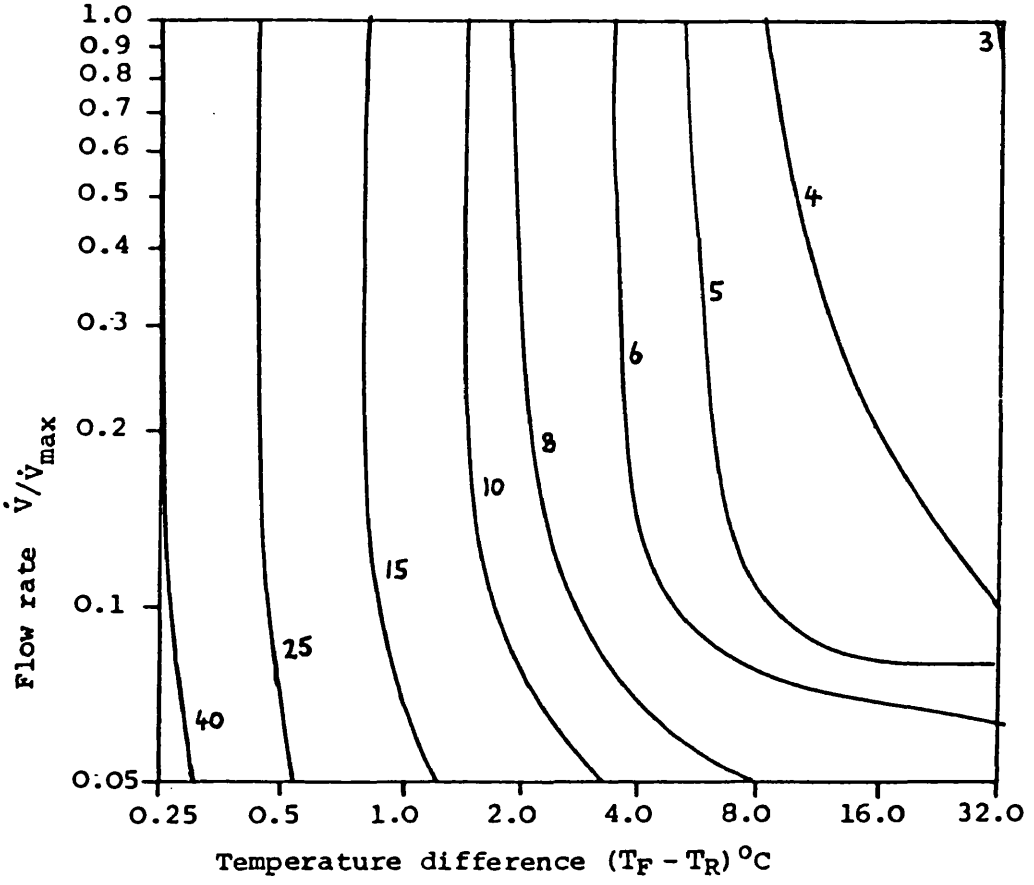

Percentage error in measurement of heat flow
under varying flow rates and temperature differences

$\dot{V}$ - actual measured volume flow rate

$\dot{V}_{max}$ - maximum rated flow rate of flow meter

T_F - Temperature of fluid flowing from system component

T_R - Temperature of fluid returning to system component

Figure 4.13. Overall measurement accuracy.

(1) Temperature °C		(2) Density of water (p) Kg/L	(3) Specific heat of water (C_p) KJ/Kg°K	(4) $p.C_p$ KJ/L
0		.9998	4.2100	4.209
5		.9999	4.2040	4.204
10		.9997	4.1930	4.192
15		.9990	4.1860	4.182
20		.9982	4.1830	4.175
25		.9970	4.1810	4.168
30		.9956	4.1790	4.161
35		.9940	4.1780	4.153
40	Likely range of systems operating temperatures	.9922	4.1790	4.146
45		.9902	4.1810	4.140
50		.9880	4.1820	4.132
55		.9857	4.1830	4.123
60		.9832	4.1850	4.115
65		.9805	4.1880	4.106
70		.9777	4.1910	4.098
75		.9749	4.1940	4.089
80		.9718	4.1980	4.080
85		.9686	4.2030	4.071
90		.9653	4.2080	4.062
95		.9619	4.2130	4.052
100		.9583	4.2190	4.043
$\frac{\text{Max + Min}}{2}$		.9826	4.193	4.133
Range		±1.8%	±0.4%	±1.7%

Figures taken from IHVE

Properties of water between 0°C and 100°C

Table 4.3.(a)

temperature range 5 - 90°C (4.14 kJ/litre), the analysis is simplified and the maximum error introduced is +/- 1.7%, with considerably smaller errors for normal system operating temperatures (see Table 4.3a).

Hence the limits of certainty in the measurement of heat flow are given by:

$$Q + dQ = (\dot{V} + d\dot{V}) \cdot (p.Cp + d(p.Cp)) \cdot ((Tin - Tout) + d(Tin - Tout)) \quad (4.13)$$

Which, when combined with equation (4.12) and ignoring second order error terms gives:

$$dQ/Q = d\dot{V}/\dot{V} + d(p.Cp)/(p.Cp) + d(Tin - Tout)/(Tin - Tout) \quad (4.14)$$

Using the values given in Table 4.3, this function yields the relationship shown in figure 4.13. Thus, for a temperature difference of 6°K and a flow rate of 50%, the limits of certainty are +/- 5%. For a temperature difference of 1°K and a flow rate of 10%, the limits of certainty are +/- 15%. It must be emphasised that these limits of certainty apply to specific temperature differences and water flows. It is a very complex procedure to estimate limits of certainty when varying heat flows are integrated over a period of time. It is anticipated that the limits of certainty will be between 5% and 10% for most measured heat flows.

It is important that these limits of certainty are not ignored when interpreting the data.

CHAPTER FOUR

4.2 THE COMPUTER MODEL.

The basic strategy of the computer simulation, and the algorithms used in the program have been described in section 3.2. This section describes the mounting of the computer model on the Bath University mainframe computer, and the model calibration procedure.

4.2.1 Mounting the computer model.

The programs were originally written in "Sheltran", a programming language peculiar to the Shell Corporation, and not supported by the Honeywell "Multics" mainframe computer system at Bath University. The original "Sheltran" source code was therefore machine translated into standard FORTRAN77 using a Shell translating program. The advantages of this type of machine translation over human translation are that it is much quicker and less error-prone. The disadvantages are that the source code produced is bulky, with many redundant CONTINUE statements, logical expressions are inverted and comment lines are lost, making the code extremely difficult to read and understand.

A copy of the machine translated FORTRAN source code was obtained from the Shell Thornton Research Centre on standard half inch, 9 track, 1600 bpi magnetic tape in IBM format (EBCDIC). The tape was read down at SWURCC (the South Western Universities Regional Computer Centre) and transferred to "Multics" via the network.

The lengthy process of de-bugging the programs then began. At STRC the programs were run on an IBM machine which permitted certain lax programming techniques such as un-initialised local variables. These and various other problems had to be ironed out before the programs would compile successfully to produce object code.

When the programs had been compiled successfully, and the first run was attempted, many run-time errors emerged. Some of these errors were caused by inconsistent format statements, and some were divide-by-zero errors which (though allowable on the IBM machine) are fatal on the "Multics" system. These errors were eventually cured by correcting the relevant format statements and inserting "IF" statements of the type:

```
IF [denominator = 0] THEN SET RESULT = 1E99 AND JUMP 1
```

before each occurrence of a divide by zero error. In this way, correct operation of the programs was eventually achieved.

4.2.2 The Input Data.

The first task was to construct an input file to describe the system to be simulated. The program required input data on the following system components:

Solar collectors

Solar stores

Hot water cylinders

Auxiliary back-up heat source

and on the heat exchange loops connecting them.

4.2.2.1 Solar collectors.

Most of the parameters for the solar collectors were taken directly from the specifications given in Chapter Three. However, no data were available for the specific heat capacity of the collector (plus water content), so this had to be calculated. The heat capacity was calculated as 4.1 kJ/m²°K. Details of the calculation are given in Appendix 6.

4.2.2.2 Solar stores.

The program was not equipped to simulate the two separate solar stores, though it was equipped to simulate a store with temperature stratification. For the week commencing 27th June 1983, the two stores were both in circuit and the mixing pump ran continuously. The two stores can therefore be treated as a single, isothermal store of capacity 10,000 litres for this period. The "shape factor" (see equation 3.8) was modified to take account of the extra surface area of two stores. The heat loss coefficient was initially set at 5.0 W/m²°K. This is considerably higher than the figure calculated using insulation thicknesses and manufacturers quoted performance figures for the insulation, but it agrees with

the measured results. More will be said on this subject later.

4.2.2.3 Hot water cylinders.

The two 3000 litre HWS calorifiers were also treated as a single cylinder, with a suitably modified "shape factor". The heat loss coefficient was calculated from insulation thickness and quoted conductivity, and was 0.75 $W/m^2{}^\circ K$.

4.2.2.4 Auxiliary back-up heat source.

The power of the auxiliary back-up heat source (in this case steam) was required. This was initially set at 200 kW.

4.2.2.5 Pipe loops.

The pipe loss effectivenesses for each section of pipework were calculated according to equation 3.4 (et.seq), and were input initially as shown in Table 3.1.

4.2.3 Weather data.

The program required hourly values of global solar radiation on a horizontal plane, and ambient air temperature. For calibration purposes, the meteorological data used were the actual data measured on site for periods of one week. For the long-term (one year) simulations access was obtained to the SERC meteorological

database at the Rutherford laboratories. There was a choice of six stations in the UK where hourly solar radiation data were available. Aberporth, on the north coast of Wales was chosen as the station whose climate corresponds most closely with that at Torbay. The annual mean daily global solar irradiation on a horizontal surface is 10.5 MJ/m² at Aberporth, which is close to the 11.0 MJ/m² recorded at Torbay (see figure 4.14). The micro-climate is also similar, due to the coastal site.

A "standard year" of weather data was constructed by extracting months for which the solar radiation figures were closest to the long-term averages for that month, as shown in Table 4.3b.

MONTH	YEAR SELECTED	ACTUAL DAILY MEAN SOLAR IRRADIATION ON HORIZONTAL (MJ/m2)	AVERAGE DAILY MEAN SOLAR IRRADIATION ON HORIZONTAL (MJ/m2)
JANUARY	1978	2.48	2.45
FEBRUARY	1976	4.84	4.86
MARCH	1975	9.06	9.12
APRIL	1980	14.59	14.49
MAY	1978	18.42	18.14
JUNE	1974	19.22	19.83
JULY	1976	18.09	17.95
AUGUST	1977	15.79	15.21
SEPTEMBER	1978	10.88	10.88
OCTOBER	1978	5.83	6.05
NOVEMBER	1975	3.07	3.02
DECEMBER	1981	1.99	2.02
YEAR		10.44	10.34

Table 4.3b "Standard year" of weather data from Aberporth

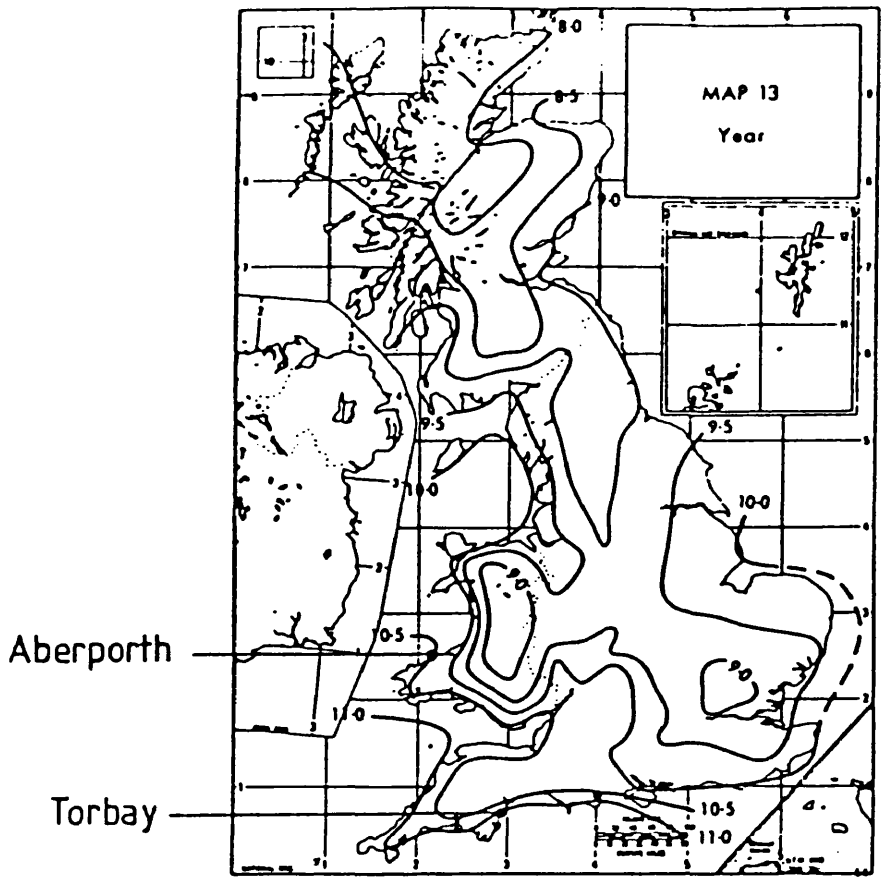

Map 13. Variation over the United Kingdom of the annual mean daily global irradiation on a horizontal surface (in MJ m^{-2})

Figure 4.14. Solar radiation map for the UK.

4.2.4 Calibrating the computer model.

The computer model must be "calibrated" against measured data from the site, to ensure that a faithful and accurate representation of the performance of the real system is being obtained.

The process of calibrating the computer model involves making careful comparisons between the measured results and the model's predictions for at least two different periods of system operation. The reasons for any discrepancies must be analysed, and the parameters of the model altered if necessary.

The importance of this phase of the work can hardly be over-emphasised. As was stated in the introduction, a great deal of research using computer simulation of solar processes has been carried out without the benefit of measured results from a full scale solar heating system to act as a control. The fact that this research has been carried out in conjunction with measured results lends confidence to the mathematical models used and gives extra weight to the results obtained.

4.2.4.1 Comparing modelled vs measured results

Several computer programs were written to facilitate the process of comparing the modelled and measured results. The program produces hourly, daily and annual printed summaries of the temperatures and energy flows at salient points in the system. Running the program, even for short periods, produces a substantial amount of printed

data which it is not practical to reproduce in this thesis. A simple graphical means of comparing the predictions of the model with the measured results was clearly required.

A program called "MODOUT.FORTRAN" was therefore written which reads the output files generated by the modelling program, and writes out hourly values of the six most important parameters in a format which is comparable to the data logger format described in section 4.1.9 (Table 4.2). The parameters selected were:

Solar energy incident on collectors	(MJ/m^2)
Solar energy input to store	(MJ)
Solar energy output to hot water system	(MJ)
Auxiliary energy to hot water system	(MJ)
Hot water load	(MJ)
Store temperature	(°C)

A further program "MERGE.FORTRAN" was then written which merges the output from MODOUT with a file of data recorded by the monitoring system, so that the predictions of the model could be compared directly to the measured results using the data analysis software described in section 4.1.9 and Appendix 5. Programs "MODOUT" and "MERGE" are also included at the end of Appendix 5.

The first period of operation selected for calibration purposes was

Parameter	Units		Mon	Tue	Wed	Thu	Fri	Sat	Sun	Week
Solar energy incident on collector	kWh	Measured	1007	1547	649	1408	1670	1323	1911	9515
		Predicted	1068	1584	678	1529	1715	1435	1957	9966 (+5%)
Solar energy collected	kWh	Measured	169	419	161	446	444	356	487	2483
		Predicted	178	392	161	519	433	386	449	2518 (+1%)
Solar energy input to pre-heat	kWh	Measured	126	346	125	393	369	296	393	2049
		Predicted	167	367	151	498	404	364	417	2368 (+16%)
Solar energy output from pre-heat	kWh	Measured	131	169	163	217	172	188	149	1188
		Predicted	151	222	202	268	225	238	172	1477 (+24%)
Hot water load	kWh	Measured	271	305	504	761	354	347	187	2730
		Predicted	245	275	455	688	311	310	177	2460 (-10%)
Mean solar storage temperature	°C	Measured	39.5	38.7	32.2	34.7	42.1	44.2	51.8	40.5
		Predicted	40.8	43.7	35.9	40.0	49.9	51.2	59.5	45.9 (+5.4)

Table 4.4. Results of first calibration run.

the week commencing Monday 27th June 1983. There was no particular reason for the choice of this week, other than that the system was in a normal configuration with both solar stores in circuit and no adverse experimentation taking place. The weather conditions and collector operation for this period are shown in Figure 4.15, and the measured results are summarised in figure 4.16.

Appropriate weather data and hot water load input files for the computer model were constructed from the measured data, and the program was run.

4.2.4.2 First calibration run.

The model's predictions were compared to the measured results for the following six parameters:

a) Solar energy incident

Figure 4.17 and table 4.4 show the degree of agreement between the model and the measured results for solar irradiation on the collector plane. Figure 4.17 illustrates a high degree of agreement, as one would expect, but table 4.4 indicates that the Boes correlation (see section 3.2.2) is overestimating the total solar energy incident for the week by about 5%. However, this is within the stated limits of certainty for the measurement of solar radiation stated in section 4.1.1, and the correlation cannot therefore be rejected.

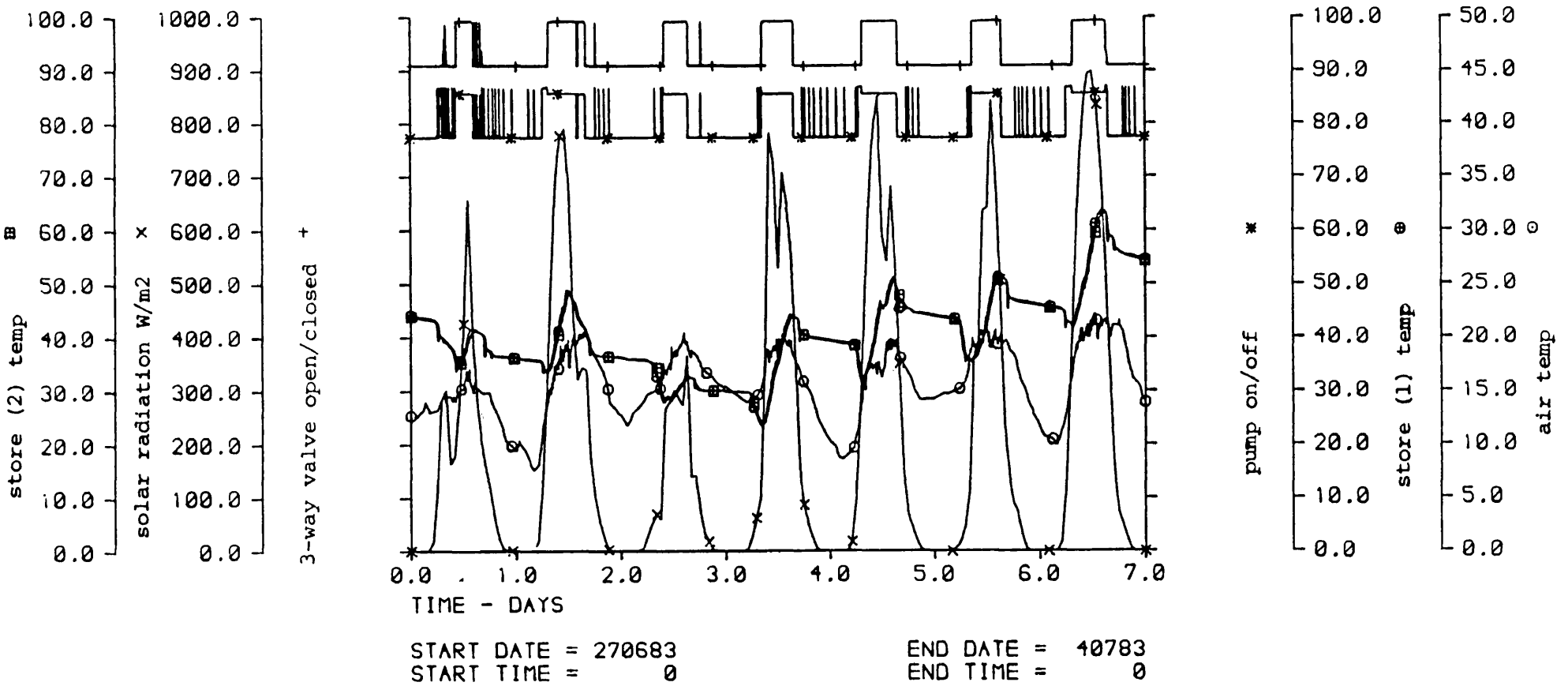

Figure 4.15. Weather conditions and collector operation week commencing: 27th June 1983.

PROJECT: Torbay Hospital

PERFORMANCE PARAMETERS FOR WEEK COMMENCING: Monday 27th June 1983

SOLAR SYSTEM PERFORMANCE

parameter		units	mon	tue	wed	thu	fri	sat	sun	week
1	Number of hours logged	hours	24	24	24	24	24	24	24	168
2	Average external air temperature	°C	13.6	15.0	16.1	15.7	14.6	17.0	16.9	15.5
3	Mains cold water inlet temperature	°C								
4	Average internal air temperature (in solar access space)	°C	23.1	23.4	22.6	22.9	22.4	23.5	24.5	23.2
5	Average solar storage temperature	°C	39.5	38.7	32.2	34.7	42.1	44.2	51.8	40.5
6	Incident solar radiation on horizontal	MJ/m^2	17.1	23.7	10.8	23.9	26.5	21.9	29.1	153.0
7	Total solar energy incident on collector	MJ	3626	5568	2338	5069	6012	4763	6878	34255
8	Solar energy collected	MJ	610	1507	578	1607	1600	1283	1754	8939
9	Solar energy input to preheat	MJ	454	1247	451	1416	1328	1064	1416	7376
10	Solar energy output from preheat	MJ	472	609	585	781	619	675	537	4278
11	Increase in heat stored	MJ	-330	2	-262	392	195	80	351	430
12	Storage efficiency	%	31.5	49.0	71.5	82.9	61.3	71.0	62.7	63.8
13	Steam energy to hot water system	MJ	873	821	2258	2235	897	447	224	7754
14	Hot water used	litres	5027	5641	9342	14117	6377	6352	3625	50481
15	Hot water load	MJ	977	1098	1816	2741	1274	1248	674	9829
16	Collector pump energy	MJ	37	54	32	43	53	42	54	315
17	Coefficient of performance	-	13	11	18	18	12	16	10	14
18	Solar fraction of total load	%	48.3	55.4	32.2	28.5	48.6	54.1	79.7	43.5
19	Overall system efficiency	%	3.9	11.0	13.8	23.1	13.6	15.9	12.9	13.7

NOTES: No status signals were available on the 3-way and other motorised valves. Collection effiency for the period was 26%. Relatively large hot water consumption noticeable on Thursday, which has been seen before.

DEFINITIONS:
(12) = (((10)+(11))/(9))*100%
(17) = (10)/(16)
(18) = (10)/(15)*100%
(19) = (((10)+(11)))/(7))*100%
1MJ = 0.278 kilowatt-hours

Figure 4.16. Performance parameters for week commencing: 27th June 1983.

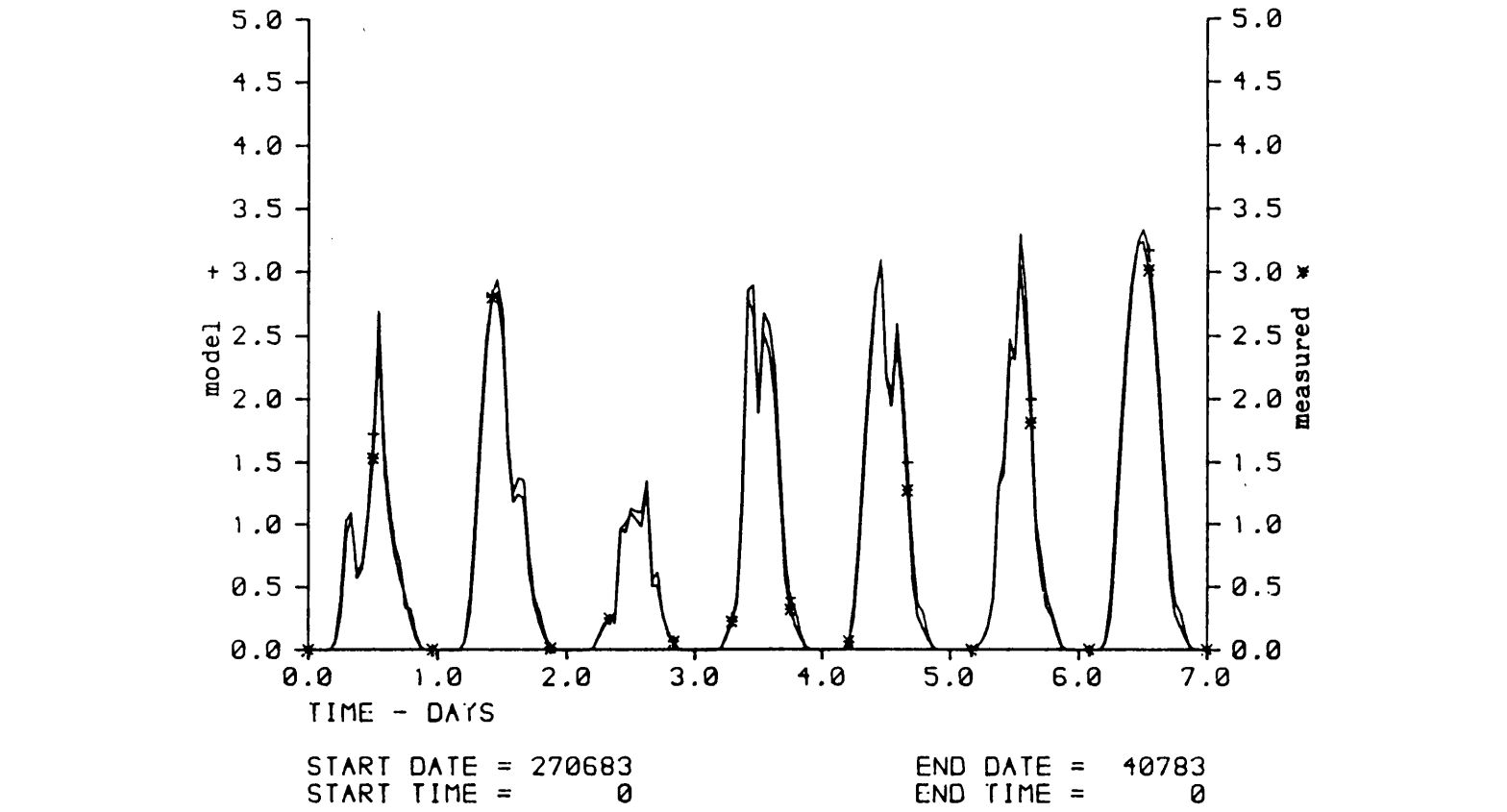

Figure 4.17. Model vs measured results (solar radiation) - Calibration run 1

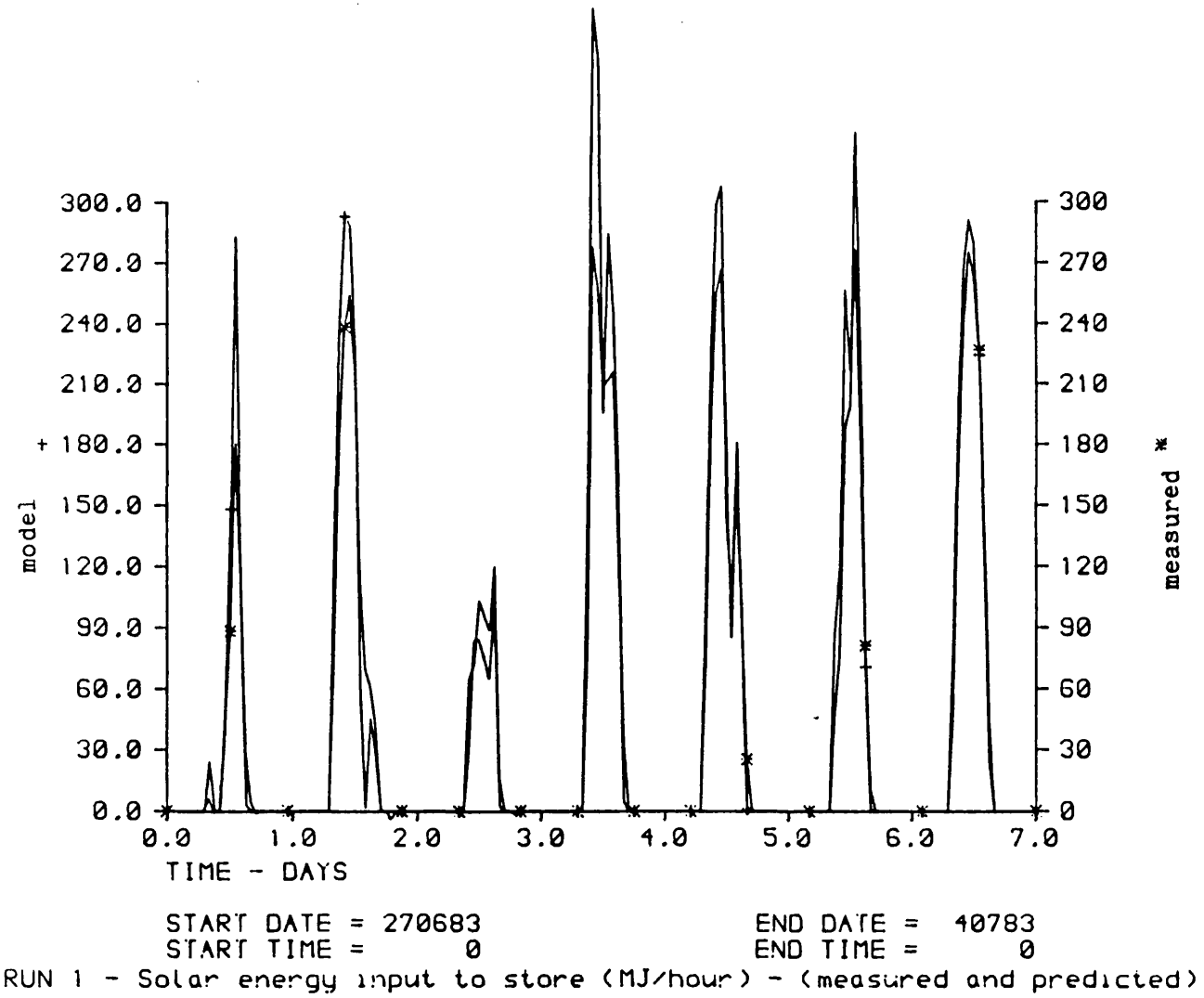

Figure 4.18. Model vs measured results (energy input to store) - Calibration run 1.

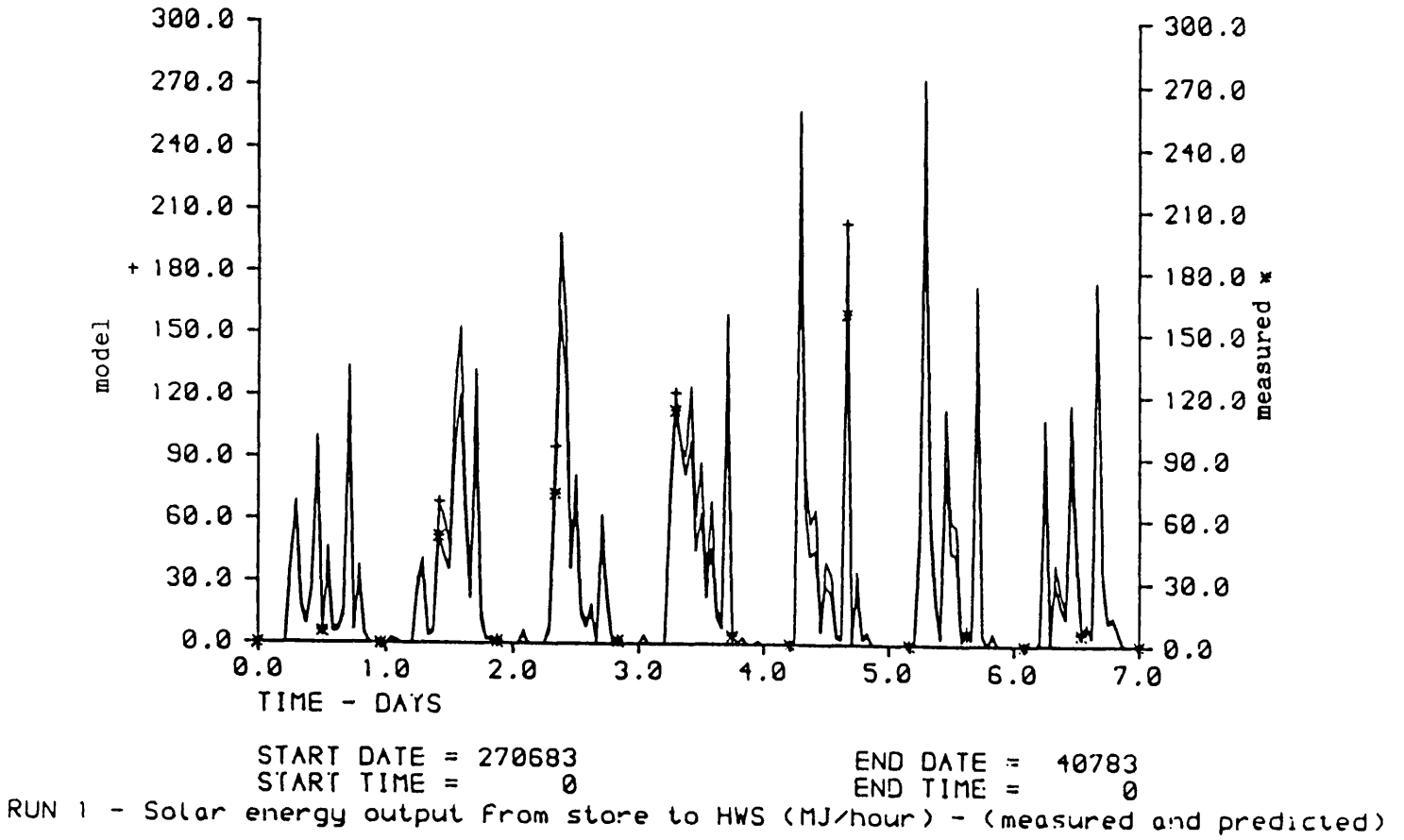

Figure 4.19. Model vs measured results (energy output from store) - Calibration run 1.

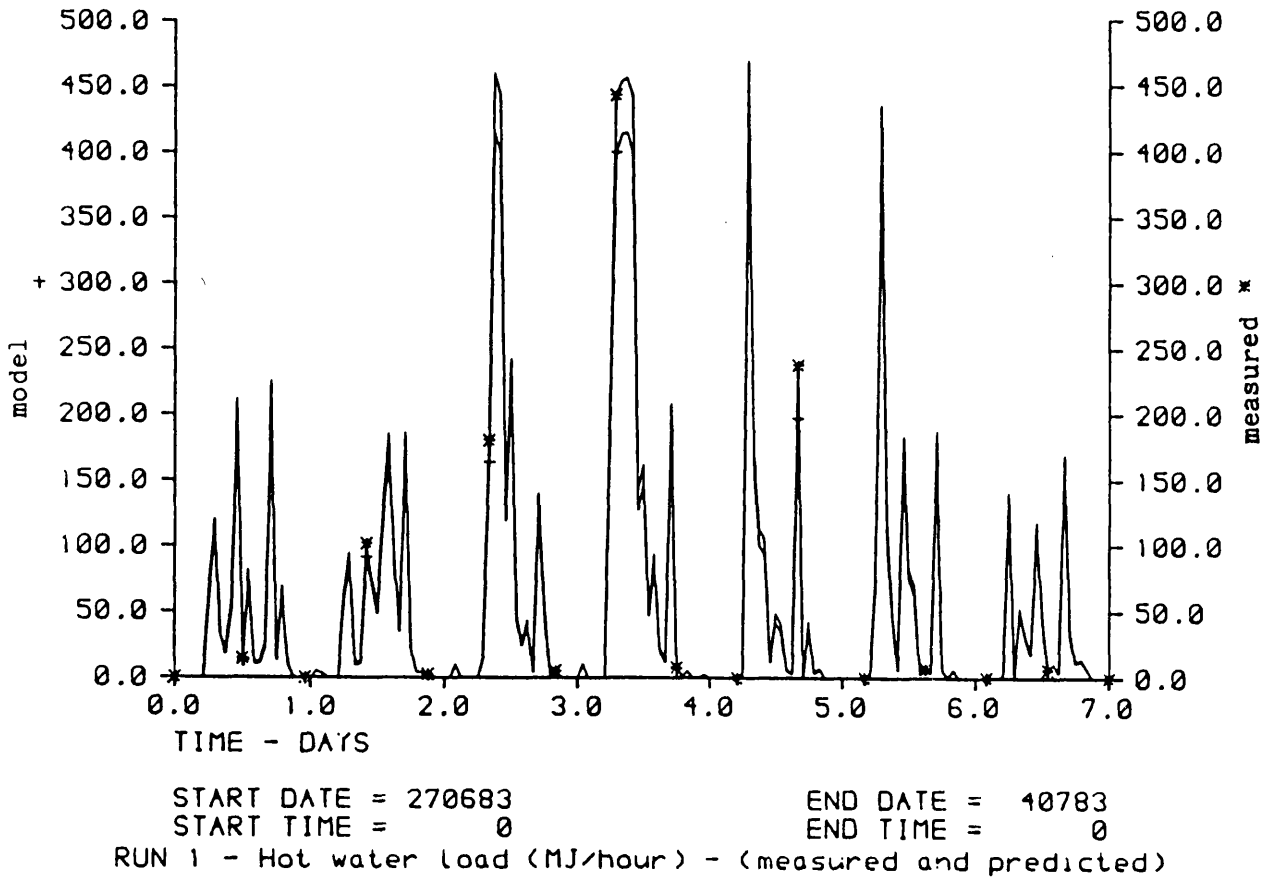

Figure 4.20. Model vs measured results (hot water load) - Calibration run 1.

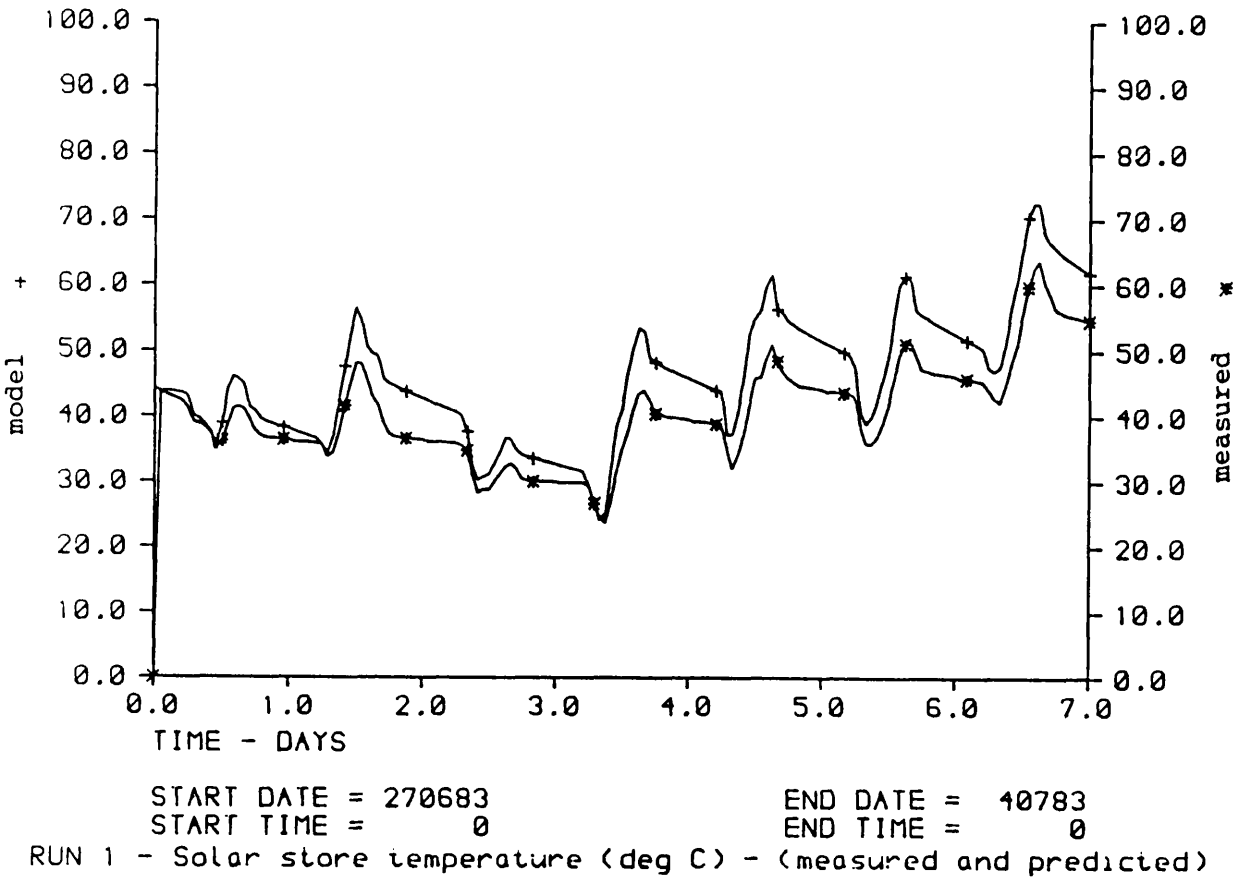

Figure 4.21. Model vs measured results (solar storage temperature) - Calibration run 1.

b) Solar energy collected

Table 4.4 indicates that the predicted value of solar energy collected is close to the measured value (+1%). This cannot be regarded as instant success for the model, however, since other factors such as store temperature affect this value.

c) Solar energy input to store

This is not the same quantity as solar energy collected, but will normally be less due to heat losses in the primary circuit pipework. Table 4.4 and figure 4.18 indicate that the model is significantly overestimating the proportion of the energy collected which reaches the store (+16%). This can be adjusted by increasing the primary pipe loss effectiveness (see section 3.2.2 "Pipe losses" for definition of pipe loss effectiveness).

d) Solar energy output from store

Figure 4.19 and table 4.4 indicate that the model is under-estimating the amount of energy lost from the solar storage tanks. This can be adjusted by increasing the store heat loss coefficient.

e) Hot water load

Table 4.4 and figure 4.20 show that the hot water load was being underestimated by 10%. This is surprising, since the hot water supply temperature has been set exactly at the measured value of 58°C, the cold water feed temperature has also been set exactly at the measured value of 16.1°C, and the volume drawn off each hour is exactly equal to the measured values. The reason for this discrepancy became clear on close inspection of the hourly results output from the model. The hot water cylinder temperature, though set at 58°C is actually only 55.5°C on average, as the temperature falls during periods of high draw-off when the auxiliary heat source is insufficient to maintain the set temperature. This was adjusted by increasing the power capacity of the auxiliary heat source from 200 to 500 kW.

f) Solar storage temperature

Figure 4.21 shows the predicted store temperature pattern against the measured values. The general form of the graphs are similar, giving confidence in the applicability of the model. However, it is clear that the performance was being over-estimated at this stage, with the predicted store temperature climbing rapidly away from the measured value during periods of high solar input.

4.2.4.3 Second calibration run.

The discrepancies from the first calibration run cannot all be corrected at a single stroke. There are complex interrelationships

between the parameters under study, which makes this impractical. A more systematic approach was called for, and it was decided to attempt to calibrate the "front end" (i.e the collector and primary circuit) of the model first. It has been shown that the primary pipe losses were being significantly under-estimated, therefore the first step was to increase the pipe loss effectiveness by a factor of 8 from 0.002 to 0.016. (There is naturally an element of "trial and error" in the choice of these figures, since the theoretical calculations based on insulation thicknesses and manufacturers' specifications for insulation performance have proved to be invalid.) The results are shown in table 4.5.

Parameter	Units		Mon	Tue	Wed	Thu	Fri	Sat	Sun	Week
Solar energy incident on collector	kWh	Measured	1007	1547	649	1408	1670	1323	1911	9515
		Predicted	1068	1584	678	1529	1715	1435	1957	9966 (+5%)
Solar energy collected	kWh	Measured	169	419	161	446	444	356	487	2483
		Predicted	194	459	184	559	500	444	543	2882 (+16%)
Solar energy input to pre-heat	kWh	Measured	126	346	125	393	369	296	393	2049
		Predicted	136	323	136	458	355	329	370	2107 (+3%)
Solar energy output from pre-heat	kWh	Measured	131	169	163	217	172	188	149	1188
		Predicted	144	200	181	244	205	214	164	1353 (+14%)
Hot water load	kWh	Measured	271	305	504	761	354	347	187	2730
		Predicted	245	275	455	688	311	310	177	2460 (-10%)
Mean solar storage temperature	°C	Measured	39.5	38.7	32.2	34.7	42.1	44.2	51.8	40.5
		Predicted	39.7	40.9	33.7	37.8	46.4	47.4	54.5	42.9 (+2.4)

Table 4.5. Results of second calibration run

a) Solar energy collected

The solar energy collected is calculated from a time-integral of collector outlet temperature minus inlet temperature, and is therefore not sensitive to heat losses in the primary circuit pipework. In fact, table 4.5 shows that the solar energy collected has actually increased significantly. This is due to the lower mean solar storage temperature which results in lower collector operating temperatures and hence increased collection efficiency.

The solar energy collected was now being over-estimated by 16%.

b) Solar energy input to preheat

Table 4.5 shows that the increase in primary pipe losses has reduced the amount of solar energy transferred to the store to within +3% of the measured value, so the indications were that the pipe loss effectiveness was now too high, and the collection efficiency was being over-estimated. This was adjusted by reducing the pipe loss effectiveness to 0.01, increasing the collector convective heat loss coefficient from 26 to 35 $W/m^2{}^\circ K$ and the back loss coefficient from 0.06 to 0.1 $W/m^2{}^\circ K$. The auxiliary heat source power rating was also increased from 200 to 500kW in order to maintain the hot water cylinder temperature at the measured value of 58°C.

4.2.4.4 Third calibration run

Table 4.6 shows the results from the third calibration run.

Parameter	Units		Mon	Tue	Wed	Thu	Fri	Sat	Sun	Week
Solar energy incident on collector	kWh	Measured	1007	1547	649	1408	1670	1323	1911	9515
		Predicted	1068	1584	678	1529	1715	1435	1957	9966 (+5%)
Solar energy collected	kWh	Measured	169	419	161	446	444	356	487	2483
		Predicted	174	420	172	530	462	412	490	2660 (+7%)
Solar energy input to pre-heat	kWh	Measured	126	346	125	393	369	296	393	2049
		Predicted	139	332	140	464	366	337	382	2160 (+5%)
Solar energy output from pre-heat	kWh	Measured	131	169	163	217	172	188	149	1188
		Predicted	145	205	185	250	210	220	174	1389 (+17%)
Hot water load	kWh	Measured	271	305	504	761	354	347	187	2730
		Predicted	268	301	499	754	340	339	194	2695 (-1%)
Mean solar storage temperature	°C	Measured	39.5	38.7	32.2	34.7	42.1	44.2	51.8	40.5
		Predicted	39.7	41.3	34.1	38.2	47.0	48.0	55.2	43.4 (+2.9)

Table 4.6 Results of third calibration run

The solar energy collected was still being over-estimated by 7% overall. This was further evidence of the inadequacy of theoretical calculations using manufacturers' specifications for predicting the heat losses through insulation when it is installed in a real environment. The collector back loss coefficient was next increased to 0.12 W/m²°K, the convective (front loss) coefficient was increased to 40 W/m²°K, and the hot water pipe

loss effectiveness was increased to 0.006.

4.2.4.5 Fourth calibration run

Table 4.7 shows the results from the fourth calibration run.

Parameter	Units		Mon	Tue	Wed	Thu	Fri	Sat	Sun	Week
Solar energy incident on collector	kWh	Measured	1007	1547	649	1408	1670	1323	1911	9515
		Predicted	1068	1584	678	1529	1715	1435	1957	9966 (+5%)
Solar energy collected	kWh	Measured	169	419	161	446	444	356	487	2483
		Predicted	171	414	171	526	456	409	482	2629 (+6%)
Solar energy input to pre-heat	kWh	Measured	126	346	125	393	369	296	393	2049
		Predicted	137	328	139	461	362	334	378	2139 (+4%)
Solar energy output from pre-heat	kWh	Measured	131	169	163	217	172	188	149	1188
		Predicted	145	203	183	248	208	218	173	1378 (+16%)
Hot water load	kWh	Measured	271	305	504	761	354	347	187	2730
		Predicted	268	301	499	754	340	339	194	2695 (-1%)
Mean solar storage temperature	°C	Measured	39.5	38.7	32.2	34.7	42.1	44.2	51.8	40.5
		Predicted	39.7	41.1	33.9	38.0	46.7	47.7	54.9	43.1 (+2.6)

Table 4.7 Results of fourth calibration run

The quite drastic increase in collector front loss coefficient had a relatively small effect on solar energy collected, indicating that the more important heat losses through the back insulation were still being under-estimated, despite the two-fold increase over theoretical levels already introduced. The proportion of

solar energy collected which is transferred to the store now agrees well with the measured results, indicating that the primary circuit pipe loss effectiveness is now correct at 0.01 (five times the theoretical figure). For the next run, therefore, the collector front loss coefficient was reset to 26 W/m²°K, and the back loss coefficient was increased further to 0.75 W/m²°K.

4.2.4.6 Fifth calibration run

Table 4.8 shows the results from the fifth calibration run.

Parameter	Units		Mon	Tue	Wed	Thu	Fri	Sat	Sun	Week
Solar energy incident on collector	kWh	Measured	1007	1547	649	1408	1670	1323	1911	9515
		Predicted	1068	1584	678	1529	1715	1435	1957	9966 (+5%)
Solar energy collected	kWh	Measured	169	419	161	446	444	356	487	2483
		Predicted	167	408	168	521	450	404	476	2594 (+4%)
Solar energy input to pre-heat	kWh	Measured	126	346	125	393	369	296	393	2049
		Predicted	133	323	137	456	357	330	374	2110 (+3%)
Solar energy output from pre-heat	kWh	Measured	131	169	163	217	172	188	149	1188
		Predicted	143	200	179	244	204	214	171	1354 (+14%)
Hot water load	kWh	Measured	271	305	504	761	354	347	187	2730
		Predicted	268	301	499	754	340	339	194	2695 (-1%)
Mean solar storage temperature	°C	Measured	39.5	38.7	32.2	34.7	42.1	44.2	51.8	40.5
		Predicted	39.5	40.8	33.6	37.7	46.3	47.3	54.4	42.8 (+2.3)

Table 4.8 Results of fifth calibration run

The solar energy collected is now within 4% of the measured value. However, this implies that the collector heat losses are still considerably too low, because there is a negative feedback effect which will increase the solar energy collected when the store temperature is reduced. For the next run, therefore, the collector back heat loss coefficient was increased to 1.5 W/m²°K and the store heat loss coefficient was increased to 7.0 W/m²°K.

4.2.4.7 Sixth calibration run

Table 4.9 shows the results from the sixth calibration run.

Parameter	Units		Mon	Tue	Wed	Thu	Fri	Sat	Sun	Week
Solar energy incident on collector	kWh	Measured	1007	1547	649	1408	1670	1323	1911	9515
		Predicted	1068	1584	678	1529	1715	1435	1957	9966 (+5%)
Solar energy collected	kWh	Measured	169	419	161	446	444	356	487	2483
		Predicted	158	402	169	507	442	402	475	2554 (+3%)
Solar energy input to pre-heat	kWh	Measured	126	346	125	393	369	296	393	2049
		Predicted	127	323	140	446	355	334	380	2105 (+3%)
Solar energy output from pre-heat	kWh	Measured	131	169	163	217	172	188	149	1188
		Predicted	136	185	158	224	187	193	159	1243 (+5%)
Hot water load	kWh	Measured	271	305	504	761	354	347	187	2730
		Predicted	268	301	499	754	340	339	194	2695 (-1%)
Mean solar storage temperature	°C	Measured	39.5	38.7	32.2	34.7	42.1	44.2	51.8	40.5
		Predicted	38.2	38.4	31.7	36.0	43.5	44.3	50.7	40.4 (-0.1)

Table 4.9 Results of sixth calibration run

Both solar energy collected and solar energy transferred to store were now within 3% of the measured values, and the mean store temperature for the week is now within 0.1°C of the measured value. One further run was carried out with an increase in the hot water pipe loss effectiveness to 0.012. The level of insulation on these pipes is identical to that on the primary circuit, and the pipe loss effectiveness should therefore be increased pro-rata for the sake of consistency.

4.2.4.8 Seventh calibration run

Table 4.10 shows the results from the seventh calibration run.

Parameter	Units		Mon	Tue	Wed	Thu	Fri	Sat	Sun	Week
Solar energy incident on collector	kWh	Measured	1007	1547	649	1408	1670	1323	1911	9515
		Predicted	1068	1584	678	1529	1715	1435	1957	9966 (+5%)
Solar energy collected	kWh	Measured	169	419	161	446	444	356	487	2483
		Predicted	158	402	169	507	442	402	475	2554 (+3%)
Solar energy input to pre-heat	kWh	Measured	126	346	125	393	369	296	393	2049
		Predicted	127	323	140	446	355	334	380	2105 (+3%)
Solar energy output from pre-heat	kWh	Measured	131	169	163	217	172	188	149	1188
		Predicted	136	185	158	224	187	193	159	1231 (+4%)
Hot water load	kWh	Measured	271	305	504	761	354	347	187	2730
		Predicted	268	301	499	754	340	339	194	2695 (-1%)
Mean solar storage temperature	°C	Measured	39.5	38.7	32.2	34.7	42.1	44.2	51.8	40.5
		Predicted	38.2	38.4	31.7	36.0	43.5	44.3	50.7	40.4 (-0.1)

Table 4.10 Results of seventh calibration run

The predictions of the model now agree with the measured results to a high degree of accuracy. The worst error is +4% on solar energy output from preheat. Figure 4.22 shows the predicted store temperature against the measured store temperature, and when this graph is compared with figure 4.21 (the first calibration run) the improvement in the quality of the simulation is clear.

The adjustments to the model during calibration runs 1 to 7 have now produced a simulation which corresponds closely to the measured performance for the particular week of operation concerned.

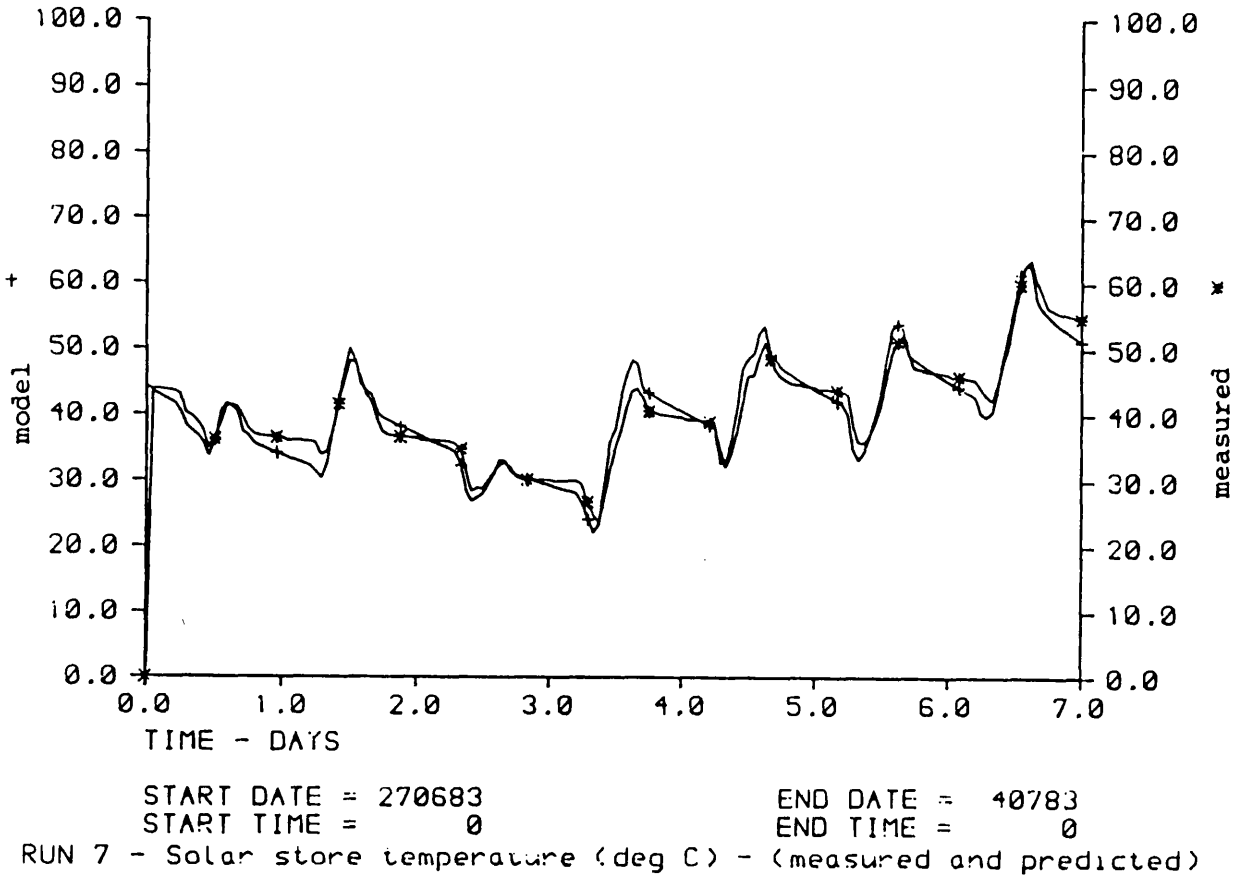

Figure 4.22. Model vs measured results (solar storage temperature) - Calibration run 7.

However, it would not have been sufficient to stop at this stage and claim that the model was providing a faithful and accurate general representation of the performance of the real system. Before such a claim can be made, the "calibrated" model must be used to simulate a second, different period of system operation without further adjustment. This provides a check on the calibration procedure, and will ensure that the agreement achieved at run 7 is not simply fortuitous.

The second period considered was the week commencing 15th August 1983. The weather conditions and collector operating characteristics for this week are shown in figure 4.23. The measured results for this week are summarised in figure 4.24.

4.2.4.9 Eighth calibration run.

Again, hourly weather data and hot water draw-off input files were prepared from the measured results, and a simulation was carried out without altering any parameters on the model. The results of the simulation are shown in table 4.11.

Parameter	Units		Mon	Tue	Wed	Thu	Fri	Sat	Sun	Week
Solar energy incident on collector	kWh	Measured	1588	1130	1591	1268	1180	463	469	7689
		Predicted	1612	1191	1567	1289	1212	484	510	7864 (+2%)
Solar energy collected	kWh	Measured	446	292	494	377	391	111	161	2272
		Predicted	400	263	442	334	388	28	110	1964 (-14%)
Solar energy input to pre-heat	kWh	Measured	325	186	379	266	283	20	75	1534
		Predicted	320	214	366	267	334	19	92	1612 (+5%)
Solar energy output from pre-heat	kWh	Measured	159	158	197	265	148	83	106	1117
		Predicted	168	160	208	260	163	77	91	1128 (+1%)
Hot water load	kWh	Measured	210	231	346	465	353	250	584	2439
		Predicted	223	245	349	467	328	237	577	2426 (-0.5%)
Mean solar storage temperature	°C	Measured	51.1	47.2	43.7	39.8	38.5	34.5	27.3	40.3
		Predicted	50.2	45.4	44.3	39.5	39.3	33.2	26.3	39.7 (-0.6)

Table 4.11 Results of eighth calibration run

Table 4.11 again shows a high degree of agreement between the predictions of the model and the measured results. There is a discrepancy of 14% in the figures for solar energy collected, but the reason for this becomes clear when figure 4.23 is re-examined. Due to a control malfunction, the collector pump was running continuously for the entire week. This does not affect the amount of solar energy transferred to the store, due to the operation of the three-way valve (see section 3.1.7), however, it does increase the amount of apparent (low grade) solar energy collected, which accounts for the 14% discrepancy. For the other parameters, the

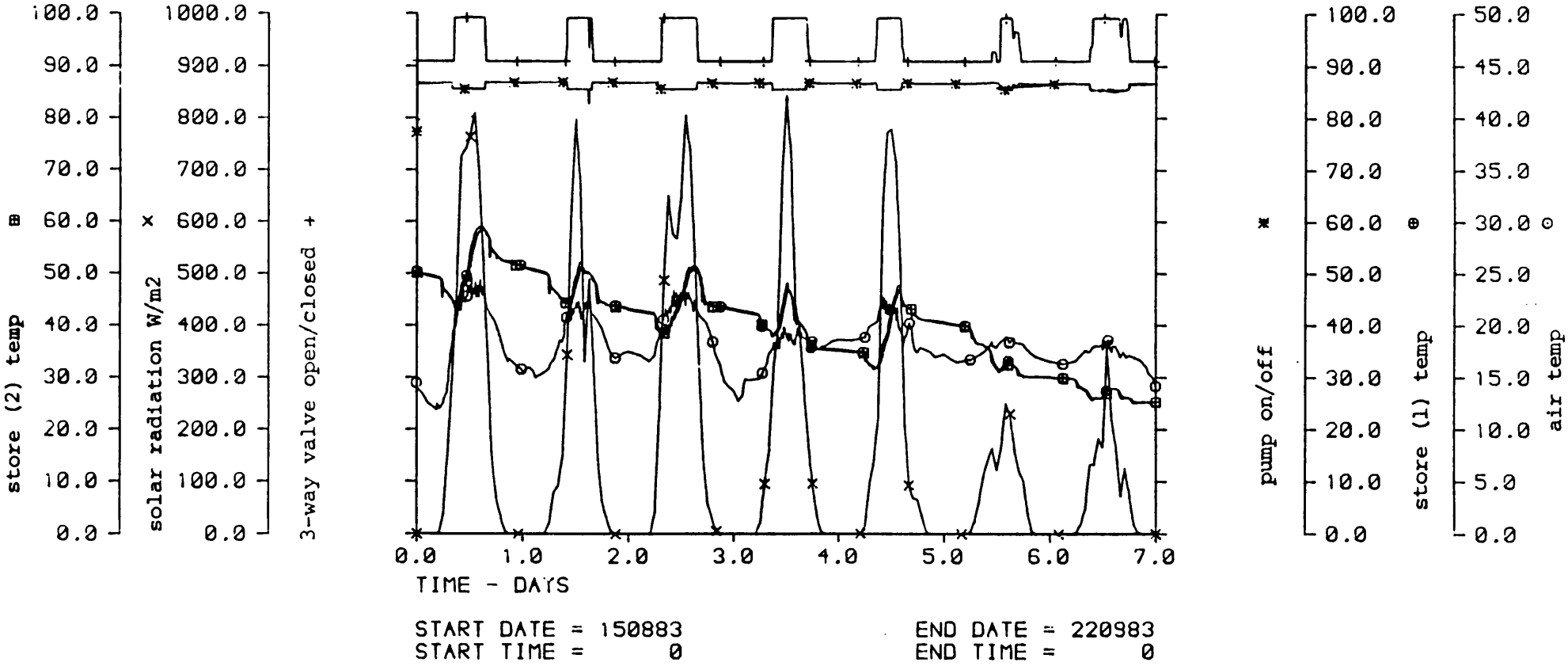

Figure 4.23. Weather conditions and collector operation week commencing: 15th August 1983.

PROJECT: Torbay Hospital

PERFORMANCE PARAMETERS FOR WEEK COMMENCING: Monday 15th August 1983

SOLAR SYSTEM PERFORMANCE

parameter		units	mon	tue	wed	thu	fri	sat	sun	week
1	Number of hours logged	hours	24	24	24	24	24	24	24	168
2	Average external air temperature	°C	17.9	18.3	19.0	17.1	19.1	17.4	17.0	18.0
3	Mains cold water inlet temperature	°C								
4	Average internal air temperature (in solar access space)	°C	26.8	26.1	26.4	24.9	25.3	23.2	22.4	25.0
5	Average solar storage temperature	°C	51.1	47.2	43.7	39.8	38.5	34.5	27.3	40.3
6	Incident solar radiation on horizontal	MJ/m^2	21.4	17.0	20.7	17.3	15.1	7.9	7.9	107.3
7	Total solar energy incident on collector	MJ	5718	4068	5727	4566	4248	1666	1687	27680
8	Solar energy collected	MJ	1606	1052	1777	1358	1407	399	579	8178
9	Solar energy input to preheat	MJ	1171	669	1364	958	1017	71	271	5521
10	Solar energy output from preheat	MJ	574	569	708	955	533	298	383	4020
11	Increase in heat stored	MJ	46	-346	-1	-325	220	-437	-202	*
12	Storage efficiency	%	52.9	33.3	51.8	65.7	74.1	*	66.8	53.9
13	Steam energy to hot water system	MJ	355	416	629	652	529	692	2395	5668
14	Hot water used	litres	4580	5040	7179	9600	6755	4874	11870	49899
15	Hot water load	MJ	757	831	1245	1675	1272	899	2101	8782
16	Collector pump energy	MJ	*	*	*	*	*	*	*	*
17	Coefficient of performance	-	*	*	*	*	*	*	*	0
18	Solar fraction of total load	%	75.8	68.5	56.8	57.0	41.9	33.1	18.2	45.8
19	Overall system efficiency	%	10.8	5.5	12.3	13.8	17.7	-8.4	10.7	10.7

NOTES: Pump still running continuously due to malfunction of TA211D controller, hence very low system COP. Otherwise operation is satisfactory. It is interesting that only a small amount of energy (apart from pumping energy) is lost from the panels when the pump is running all night. This is because the small amount of water contained in the solar primary circuit soon reaches thermal equilibrium at a very low temperature.

DEFINITIONS:
(12) = (((10)+(11))/(9))*100%
(17) = (10)/(16)
(18) = (10)/(15)*100%
(19) = (((10)+(11)))/(7))*100%
1MJ = 0.278 kilowatt-hours

Figure 4.24. Performance parameters for week commencing: 15th August 1983.

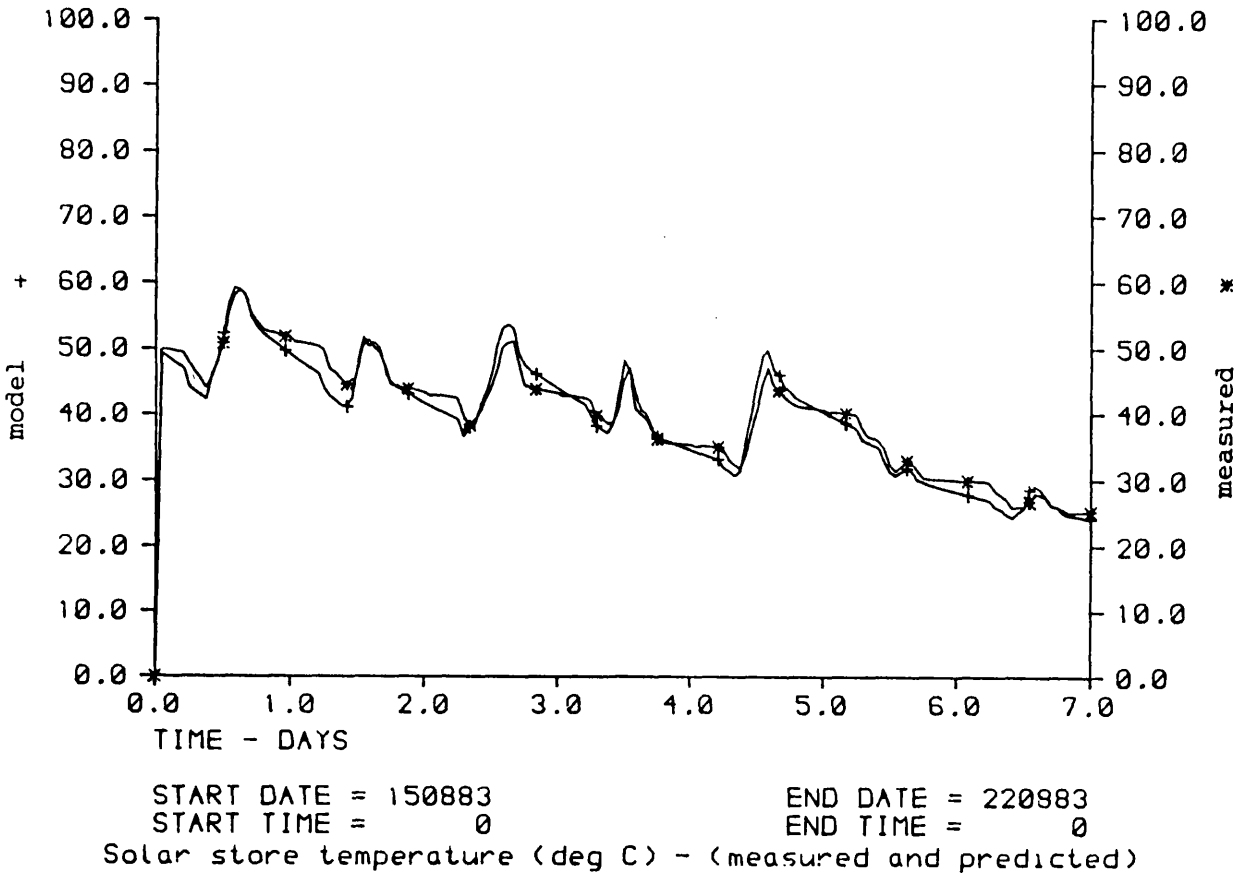

Figure 4.25. Model vs measured results (solar storage temperature) - Calibration run 8.

predictions of the model were in close agreement, the worst error being 5% on solar energy transferred to store. Figure 4.25 shows the predicted and measured store temperatures for this week, and demonstrates the excellent degree of agreement achieved.

The main purpose of this thesis, as described in Chapter Two, is to use the calibrated computer model to investigate the extent to which the long term performance of the system is affected by alterations in the pump control settings (dTon and dToff). The calibration process would not be complete, therefore, without a comparison between the actual pump switching characteristics and those of the computer model.

Table 4.12 lists the "pump on" and "pump off" times, actual and modelled, for the calibration week commencing 27.6.83.

DATE	REAL SYSTEM	MODEL
27.6.83	on at 08.00 off at 15.57	on at 10.26 off at 14.02
28.6.83	on at 07.25 off at 13.55 on at 14.00 off at 14.07 on at 14.12 off at 15.50	on at 07.02 off at 14.01 on at 15.02 off at 16.01
29.6.83	on at 09.49 off at 15.18	on at 09.09 off at 15.01
30.6.83	on at 08.24 off at 15.39	on at 08.00 off at 15.04
1.7.83	on at 07.28 off at 15.37	on at 07.04 off at 15.00
2.7.83	on at 08.38 off at 15.21	on at 08.05 off at 15.00
3.7.83	on at 07.38 off at 15.08	on at 07.05 off at 14.23

Table 4.12 Actual vs modelled pump switching characteristics

The main discrepancy arises from the fact that the model uses only hourly average values of solar radiation, and assumes constant solar radiation over the hour. This naturally leads to pump switchings occurring on or near the hour, when a step change in the level of solar radiation is input. Nevertheless, the results indicate a good agreement between modelled and actual pump switching characteristics. (Tuesday the 28th June 1983 is a particularly good example, as the pump cycled on and off three times that day.)

It may now be stated that the model is providing a faithful and

accurate representation of the performance of the real system, and can be used to make long-term performance predictions.

It is worth noting at this point one of the most important lessons learnt from the calibration process, namely the size of the discrepancy between theoretical calculations of heat losses through insulation (based on manufacturers' specifications) and actual heat losses measured. The measured heat losses have exceeded the theoretical values by a factor of five or more, though the insulation was in good condition and was properly installed. The same experience has been found on previous solar heating field trials. The most probable explanation for this discrepancy is that manufacturers' specifications are derived from tests carried out under rigorous laboratory conditions, where factors such as humidity are tightly controlled, and air leakage or insulation dampness are eliminated. The evidence suggests that such ideal conditions rarely, if ever, exist in practice. If this discrepancy is universal (and there is no reason to believe that it is restricted to solar heating systems) then it makes a mockery of conventional heat loss and cost-effectiveness calculations normally applied to insulation levels.

This topic looks worthy of further study, but has not been followed up in depth by the author as it is not directly related to the subject of this thesis.

CHAPTER FIVE

5. RESULTS AND DISCUSSION.

Chapter Four described the techniques used to collect accurate measured data from the site, and the use of these data to calibrate the computer model.

This chapter describes the measured results and the results of the long-term computer simulations carried out.

5.1 Measured results.

Results were collected and analysed for a total of 249 complete days of system operation between 15th June 1983 and 27th April 1984.

5.1.1 Performance summary

The measured results are summarised on a monthly basis in tabular form in figure 5.1. The same results are presented in the form of a Sankey diagram in figure 5.2. The measurement of steam energy supplied is suspect, as indicated in figure 5.2, due to problems associated with condensate flow metering. However, this uncertainty does not affect the accuracy of any of the solar measurements.

Figure 5.3 is a monthly bar chart which shows the solar energy incident on the collector plane, the hot water load, the solar energy used and the solar fraction for each month. High solar

	Units	Jun 83	Jul 83	Aug 83	Sep 83	Oct 83	Nov 83	Dec 83	Jan 84	Feb 84	Mar 84	Apr 84	TOTAL
1 Number of days logged	days	14	22	21	26	24	30	15	21	20	29	27	249
2 Mean external air temperature	deg C	15.2	18.9	17.3	14.0	10.2	9.0	7.1	5.5	4.5	5.4	8.1	10.3
3 Mains cold water inlet temperature	deg C	13.8	17.0	18.5	16.2	12.3	9.8	8.7	7.5	6.3	6.1	8.1	11.1
4 Mean internal air temperature	deg C	23.0	25.9	25.4	20.7	17.7	15.2	14.6	12.6	12.7	13.8	16.8	17.8
5 Mean solar storage temperature	deg C	40.8	44.3	41.7	25.6	30.8	13.9	15.8	13.0	12.8	14.4	25.5	24.6
6 Incident solar radiation on horizontal	MJ/m2	276.3	495.4	383.0	257.7	156.0	79.3	44.7	62.8	95.4	231.6	469.6	2579
7 Total solar energy incident on collector	MJ	63545	120569	104879	75885	62055	29157	25894	29003	34540	70506	136333	752366
8 Solar energy collected	MJ	15819	29083	30534	22175	20437	11789	10013	9316	9922	20153	40615	219856
9 Collection efficiency	%	24.9	24.1	29.1	29.2	32.9	40.4	38.7	32.1	28.7	28.6	29.8	29.2
10 Solar energy input to pre-heat	MJ	12978	23714	22447	13698	11696	3331	5004	4317	5020	12941	32948	148094
11 Solar energy output from pre-heat	MJ	7769	15488	14029	10579	8332	4576	4548	5668	6069	13132	24736	114926
12 Increase in heat stored	MJ	266	-130	103	-7	365	-560	-8	-437	-193	-129	810	80
13 Storage efficiency (1)	%	61.9	64.8	63.0	77.2	74.4	120.5	90.7	121.2	117.1	100.5	78.6	77.6
14 Steam energy to hot water calorifiers	MJ	12277	7628	12184	29233	24621	57509	29179	49001	34125	49452	37937	343146
15 Hot water used	litres	81488	162290	153170	271443	275374	369685	182853	287389	227943	396235	345454	2753324
16 Hot water load	MJ	16243	24614	26073	52347	55285	74818	36130	59530	47841	87498	70410	550789
17 Collector pump energy	MJ	561	951	-	-	330	120	173	149	166	379	827	3656
18 Coefficient of performance	-	13.8	16.3	-	-	25.3	38.2	26.3	38.0	36.5	34.7	29.9	24.7
19 Solar fraction of total load	%	47.8	62.9	53.8	20.2	15.1	6.1	12.6	9.5	12.7	15.0	35.3	20.9
20 Overall system efficiency	%	12.6	12.7	13.5	13.9	14.0	13.8	17.5	18.0	17.0	18.4	18.7	15.3

Notes: 1 MJ = 0.278 kWh

(1) Storage efficiencies exceeding 100% occur when air in plant room is warmer than solar storage tanks.

(13) = 100% * ((11)+(12)/(10))
(18) = (11)/(17)
(19) = 100% * ((11)/(16))
(20) = 100% * (((11)+(12))/(7)))

FIGURE 5.1

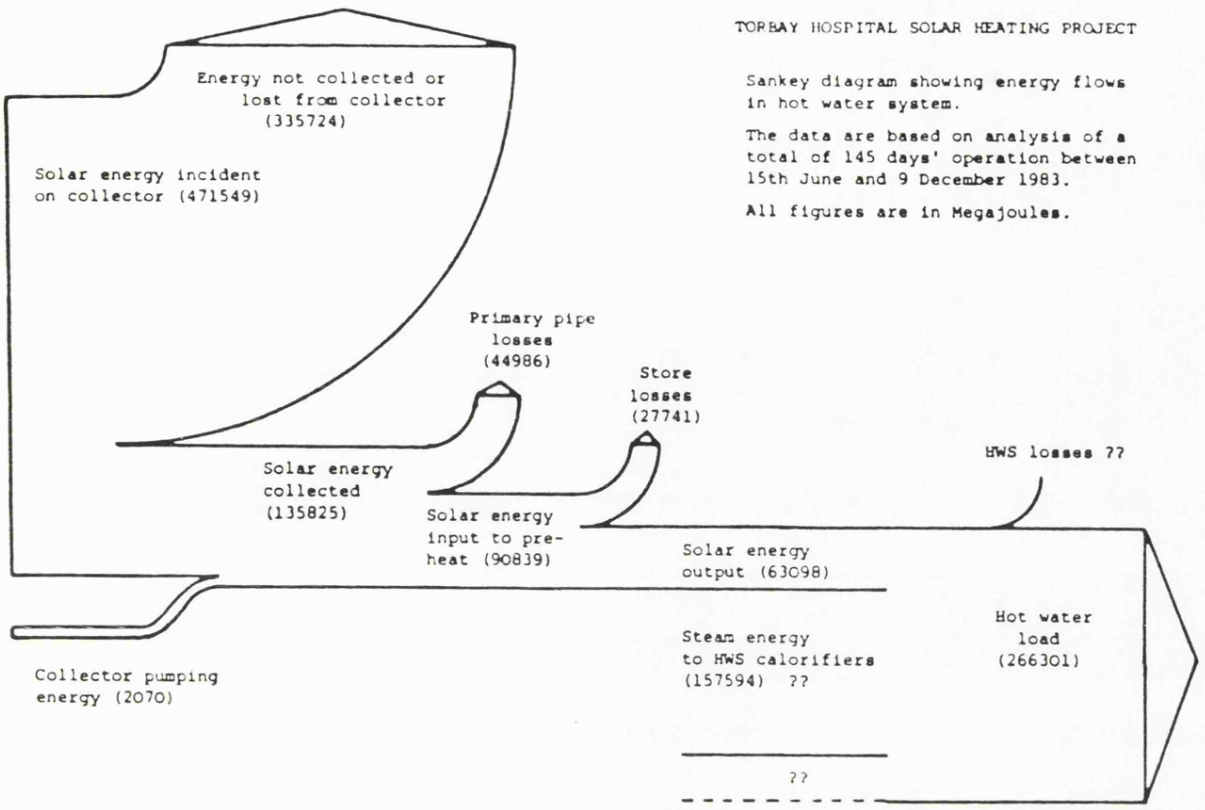

FIGURE 5.2

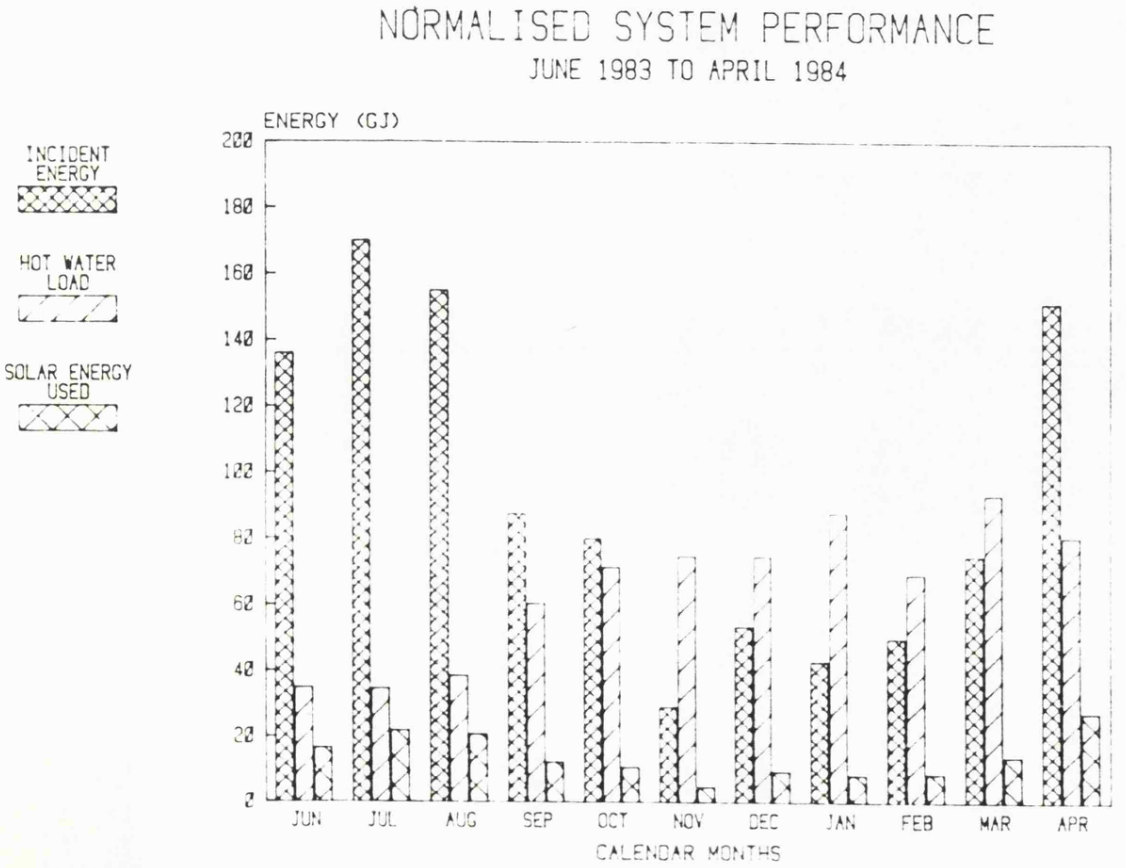

FIGURE 5.3

fractions were recorded in June, July and August when the incident solar radiation was above average and relatively little hot water was being used. The solar fractions were much lower during the winter months when the hot water load was higher and the incident solar radiation was below average levels.

(Note: Figure 5.3 shows "normalised" results, that is to say that the measured energy totals for each month have been multiplied up to compensate for missing days' data.)

5.1.2 Mains cold water inlet temperature.

The mains cold water inlet temperature will have a significant effect on the solar energy output, hence it is an important parameter which must be defined by the computer model.

The variation in measured mains cold water inlet temperature during the monitoring period is illustrated in figure 5.4. The seasonal variation may be represented by equation (5.1):

$$\text{MCW temp} = 12.3 - 6.2 \cos[(2\pi/365).(D - 25)] \qquad (5.1)$$

where: D = day of year (Jan 1st = day 1, etc)
which gives the sine wave shown in figure 5.4. This was the representation used in the computer model.

5.1.3 Hot water demand profile.

The measured hot water demand profile was that shown in figure 5.5. This was the profile used in the computer simulations. When different daily hot water loads were used, the hourly draw-off figures were changed pro-rata to maintain the same load profile.

5.2 First long-term simulations - Base system.

The calibrated model was first used to predict the energy savings per annum over a range of hot water loads. (At this stage it became clear that the number of year-long simulations would have to be limited, as each run used approximately 1.5 hours of CPU time on the University mainframe computer.) Seven runs were performed at daily hot water draw-offs of 500, 2000, 6000, 9633, 12000, 13500 and 16000 litres, in order to assess the sensitivity of the performance to this parameter. The results are shown in figure 5.6.

The curve shows that the useful solar energy output per year increases with increasing hot water consumption, as one would expect, though not in a linear fashion. The curve is asymptotic, and there will come a point where the maximum useful solar energy is being obtained, and further increases in hot water consumption have a negligible effect. The graph shows that the average solar energy used per year will be 55 MWh at a hot water consumption rate of 10 m^3 per day, and 67 MWh at a consumption rate of 16 m^3 per day. This graph forms a useful datum against which the results of

subsequent simulations may be compared.

5.3 Effect of altering the control strategy.

This is the beginning of the sensitivity analysis described in Chapter Two. (It is worth re-reading Chapter Two briefly at this point.)

5.3.1 Effect of varying switch-on setting dTon.

The next set of simulations were carried out using a constant hot water daily demand of 12 m^3 per day. The value of the pump switch-off setting (dToff) was held constant at 0.8°K, while the switch-on setting was varied from 1°K to 20°K in steps of 1°K. The results are shown in figure 5.7. The graph shows that the annual solar energy output is reduced from 59.8 to 55.4 MWh when the switch-on setting is raised to 20°K (a performance penalty of 7.3%). This is an important result. The curve is relatively flat at the bottom end of the range, where increasing dTon from 1 to 6°K causes only a 1.2% reduction in solar energy used, but the sensitivity increases rapidly with increasing dTon after this point

It is also interesting to note that the performance penalty in percentage terms is slightly higher during the winter months (8.9%) than during the summer months (6.2%)

5.3.2 Effect of varying dTon at low load

A second set of runs were performed at a lower hot water usage rate of 2m3/day, to find out whether the performance of a lightly-loaded system with higher operating temperatures is equally sensitive to the control setting dTon. The results are shown in figure 5.8. The annual solar energy output is reduced from 20.03 to 19.07 MWh when the switch-on setting is raised to 20°K. This represents a performance penalty of almost 5%, showing that the performance of a lightly loaded, oversized system is slightly less sensitive to the control setting dTon.

5.3.3 Effect of varying dTon with lower collector heat capacity

A third set of runs were performed using the original hot water load of 12m3/day and a lower collector heat capacity of 2.0kJ/m²°K. The results are shown in figure 5.9. The lower heat capacity improves the performance fractionally throughout the range of dTon, but does not affect the sensitivity. The percentage reduction in solar output when dTon is increased from 1 to 20°K is still 7.2%.

5.3.4 Effect of varying dTon with lower heat losses

A fourth set of runs were performed using the original, theoretical heat loss coefficients for solar panels, pipework, solar storage tanks and hot water tanks. The results showed a significant

decrease in the sensitivity to dTon, the percentage reduction in solar output being 5.0% (compared with 7.3% for the calibrated system) when dTon was increased from 1 to 20°K.

5.3.5 Effect of varying switch-off setting dToff

The ideal switch-off setting is a small positive value at which the energy gain is equal to the cost of pumping. The ideal value will therefore depend on the heat capacity flowrate through the collector array and the absorbed power of the pump, such that:

$$dToff(ideal) = (\text{pump power } P)/(\dot{m}.Cp) \qquad (5.2)$$

For the system under study,

$\dot{m}$ = 3.7 Kg/s, Cp = 4180 J/Kg°K, P = 1500 watts

therefore,

dToff(ideal) = 0.1°K

Such an ideal setting is difficult to achieve reliably over a wide range of absolute operating temperature using inexpensive controllers.

A sensitivity analysis was carried out to determine the effect of varying the switch-off setting dToff on long-term performance. The

next set of simulations were again performed under a constant hot water daily demand of 12m3 per day. The switch-on setting (dTon) was held constant at 6°K, while the switch-off setting was varied from 0.1°K to 5.5°K in steps of 0.5°K. The results are shown in figure 5.10. The graph shows that the annual solar energy output is reduced from 59.2 MWh to 57.6 MWh when the switch-off temperature differential is increased from 0.1°K to 5.5°K (a performance penalty of 2.7%). The graph indicates a more or less constant sensitivity over the range 0.1 <= dToff <= 5.5°K. The performance reduction is only 0.4% over the interval 0.1 to 1.0°K.

5.3.6 Effect of varying dToff at low hot water load

The next set of simulations were carried out under a hot water daily demand of 2 m3/day, while dToff was varied as above. The results are shown in figure 5.11. The annual solar energy output is reduced from 19.93 to 19.66 MWh when dToff is increased from 0.1 to 5.5°K (a performance penalty of 1.4%). These results indicate a lower sensitivity to dToff for a lightly loaded, oversized system.

5.3.7 Effect of varying dToff with lower collector heat capacity

The next set of simulations were carried out using the original hot water load of 12 m3/day and a lower collector heat capacity of 2 kJ/m²°K. The results are shown in figure 5.12. The lower heat capacity improves the performance fractionally throughout the range of dToff, but does not affect the sensitivity.

5.3.8 Effect of control strategy on stability

The steady-state theoretical analysis of Chapter Two led to the stability criterion of equation 2.8:

$$dTon/dToff >= (\dot{m}.Cp)/(Fr.Ul)$$

which, for the solar heating system under study, implies

$$dTon/dToff >= 12.7$$

It is interesting to test this steady-state analysis by using the dynamic model to assess the effect of the control settings dTon and dToff on the total number of pump switchings occurring over a full year of system operation under normal meteorological conditions. The total number of pump switchings was therefore recorded for each of the simulations described earlier, and the results are shown in figure 5.13, where the number of pump switchings is plotted against the ratio dTon/dToff.

The first point to note is that the number of pump switchings is virtually independent of load and collector heat capacity (the curve is similar for all six sets of simulations). This supports the stability criterion above, where dTon/dToff is expressed in terms of $\dot{m}$, Cp, Fr and Ul. However, the instability point predicted by the steady-state analysis (dTon/dToff = 12.7) is considerably higher than the instability point found by the dynamic

model (dTon/dToff = 8). This may be due to the variable nature of the collector overall heat loss coefficient, Ul, as discussed in Chapter Two.

It is useful to apply a curve-fit to the graph of figure 5.13. Logarithmic, exponential and power type curves were fitted to the graph, and the best correlation was obtained using the power relationship:

$$\text{no. of pump switchings/year} = 5400/[(\text{dTon/dToff})^{1.05}] \qquad (5.3)$$

Comparing figure 5.13 with figures 5.7 to 5.12, it will be observed that the simulations carried out with low values of dTon/dToff (i.e unstable operation) give rise to an excessively high number of pump on/off cycles per year, but do not necessarily show a performance penalty in terms of the annual solar energy output. For example, the use of dTon = 1.0°K, dToff = 0.8°K (i.e dTon/dToff = 1.25) produced a high value of solar energy output (59.7 MWh/year) though it caused 5000 pump switching cycles during the year. The wear and tear on pumps, switches and relays caused by such unstable operation will lead to unnecessarily high maintenance costs in the long-term, and this consideration calls for a stable control system design.

5.4 Effects of other design variable changes on performance

Much has been said in this chapter about the effect of altering the control strategy on stability and the long-term thermal performance of the solar heating system under study. It has been stated categorically that, for the system under study, a performance penalty of more than 7% will be incurred by the use of an excessively high switch-on temperature differential (dTon).

In order to put these results into a more general perspective, further simulations were carried out to investigate the effects of altering other important design variables such as collector tilt angle, storage volume, insulation levels and heat exchanger effectiveness. For the sake of interest, the effect of siting the same system at Kew and Eskdalemuir is also investigated.

Figure 5.14 illustrates the effect of reducing the collector tilt angle to 40 degrees from horizontal. Annual solar energy output is increased by 6% at a hot water load of 12 m3/day.

Figure 5.15 illustrates the effect of reducing the storage volume to just 3000 litres (11.1 litres/m^2) and the effect of increasing the storage volume to 13500 litres (50 litres/m^2 = BS 5918 recommended ratio). The drastic reduction in storage volume results in a significant performance penalty of 10% in annual solar energy output at 12 m3/day hot water consumption. The increase to 13500 litres yields an improvement of 7%.

Figure 5.16 illustrates the effect of improving the insulation of the storage tank to halve the store heat loss coefficient. An increase of 4% is obtained at 12 m^3/day hot water consumption, a surprisingly small improvement.

Figure 5.17 illustrates the effect of halving the pipe heat losses in the primary loop. A small improvement of 3.4% is obtained at 12 m^3/day hot water load.

Figure 5.18 illustrates the effect of increasing the collector/store heat exchanger effectiveness threefold. An increase in annual solar energy output of 4% is obtained at 12 m^3/day hot water consumption.

Figure 5.19 shows the predicted performance of the system at the inland sites of Kew and Eskdalemuir. The appropriate sets of weather data were retrieved from the meteorological database and assembled in the manner described in section 4.2.3. Allowance was made for the different mains cold water inlet temperatures at these sites. The annual solar energy output is reduced by 9% when the system is sited at Kew, and by 12% when sited at Eskdalemuir in Scotland (both figures refer to hot water loads of 12 m^3/day).

The above results show that the sensitivity of the system's performance to alterations in the control settings dTon and dToff is on a par with the sensitivity to other major design variable changes.

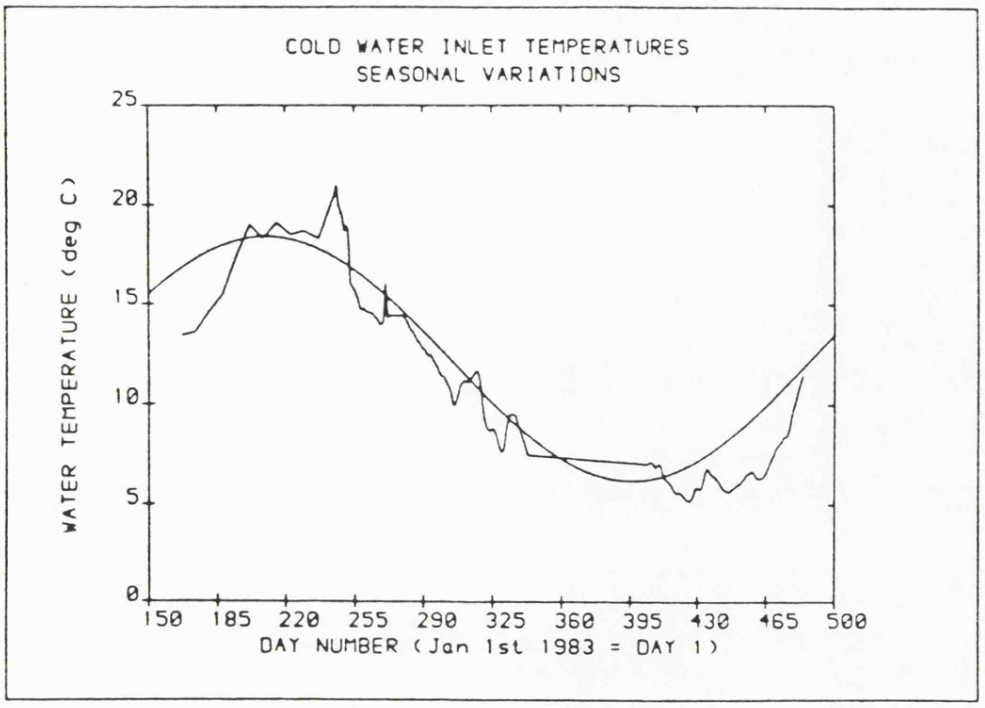

FIGURE 5.4

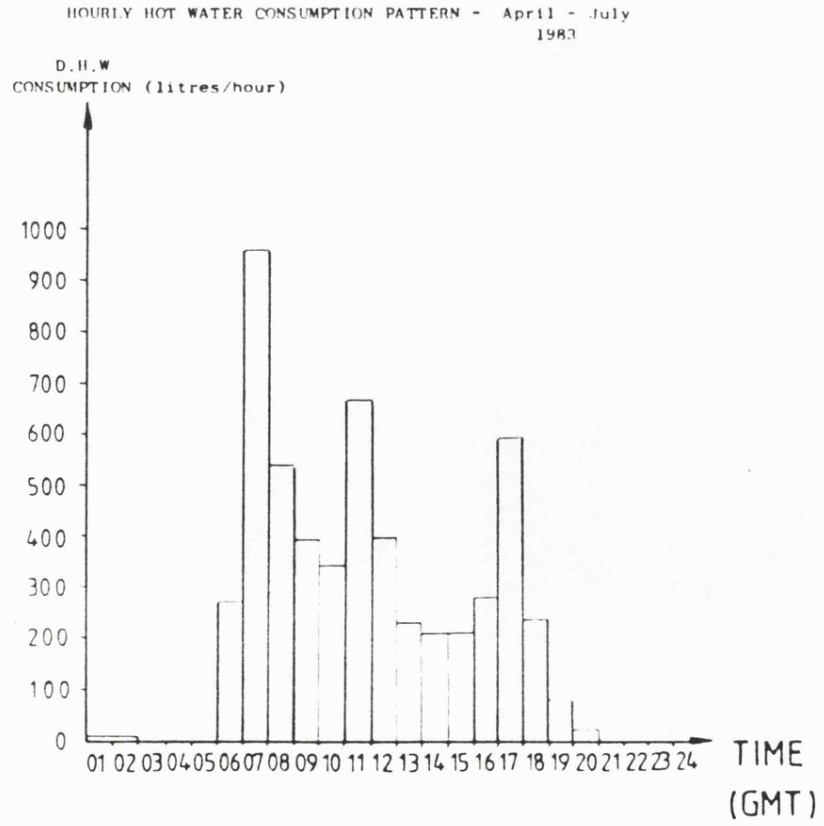

Note: This graph is based on the analysis of 28 days' data between 13th April 1983 and 10th July 1983.

Average daily hot water consumption = 5470 litres.

FIGURE 5.5

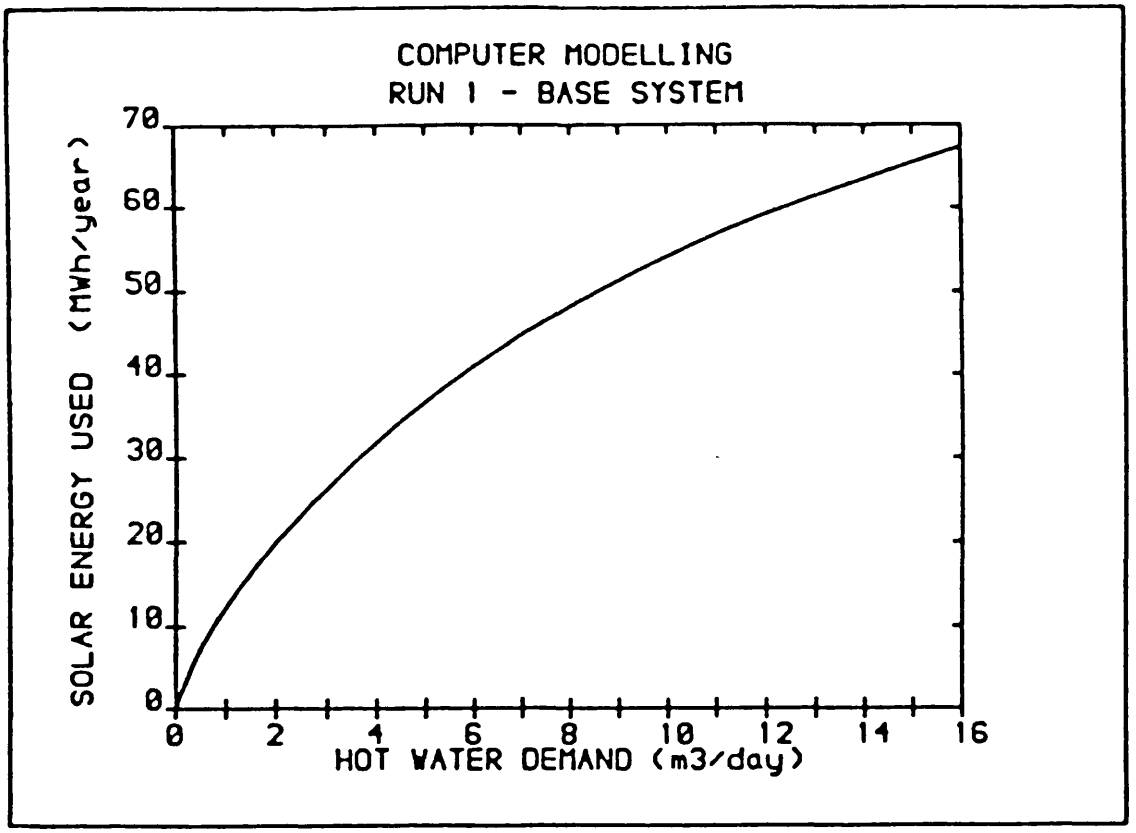

FIGURE 5.6

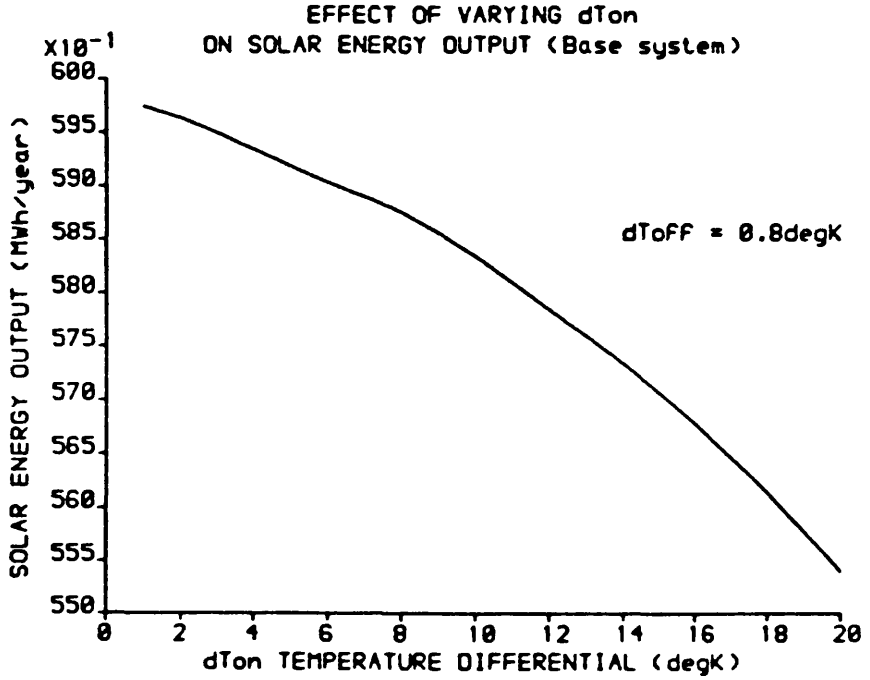

FIGURE 5.7

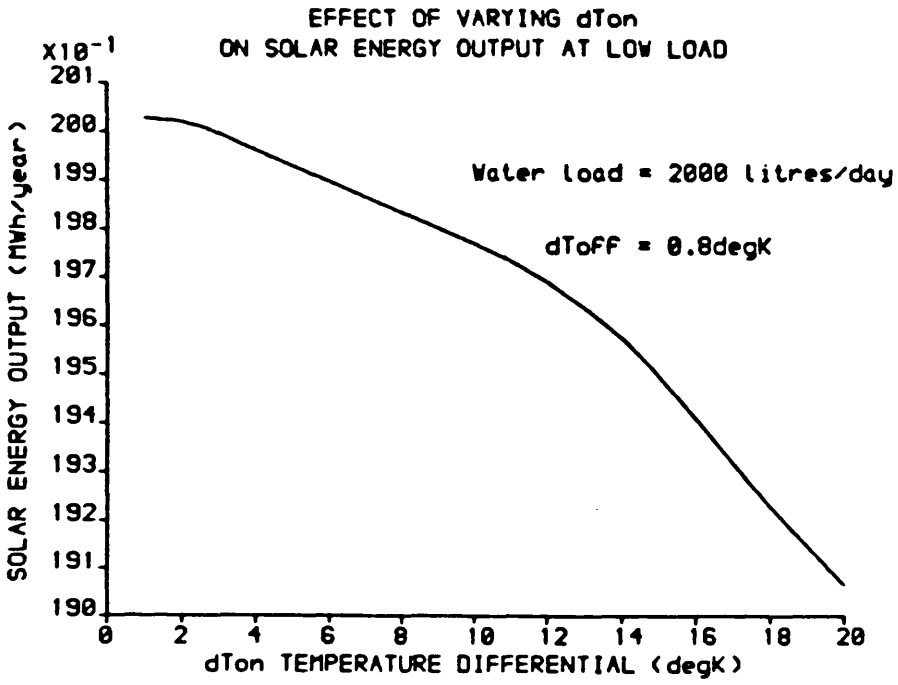

FIGURE 5.8

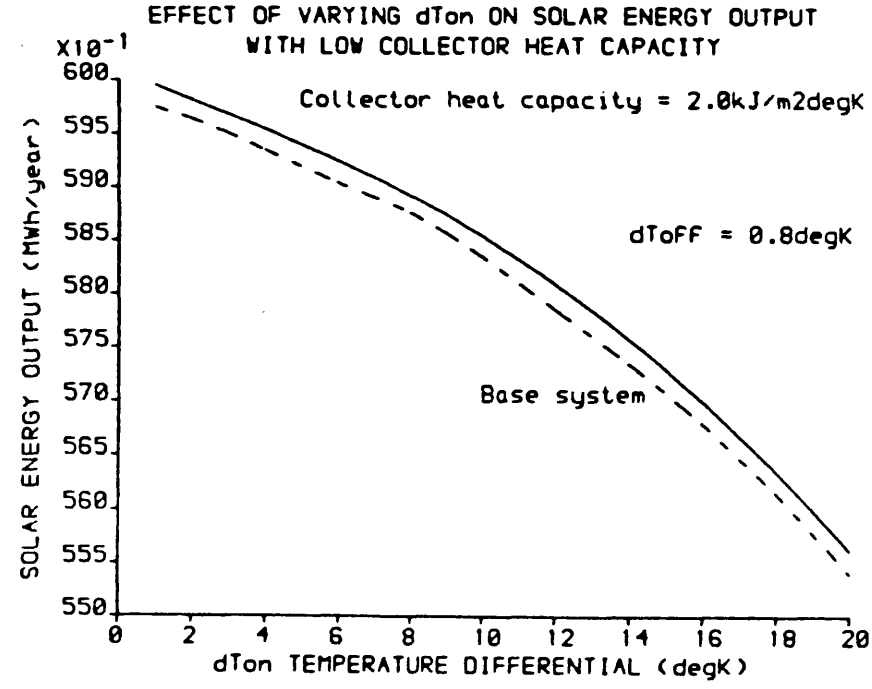

FIGURE 5.9

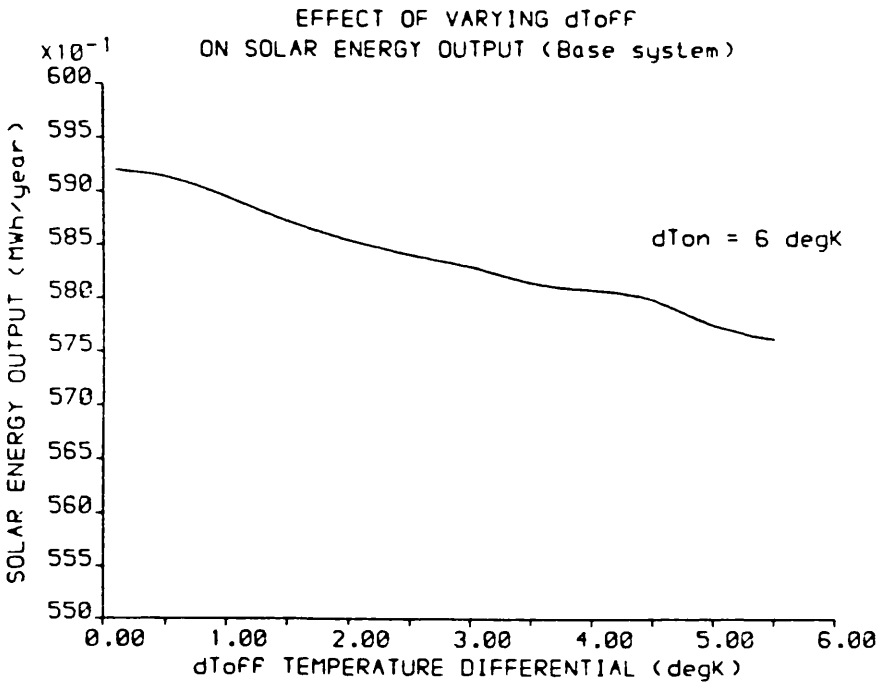

FIGURE 5.10

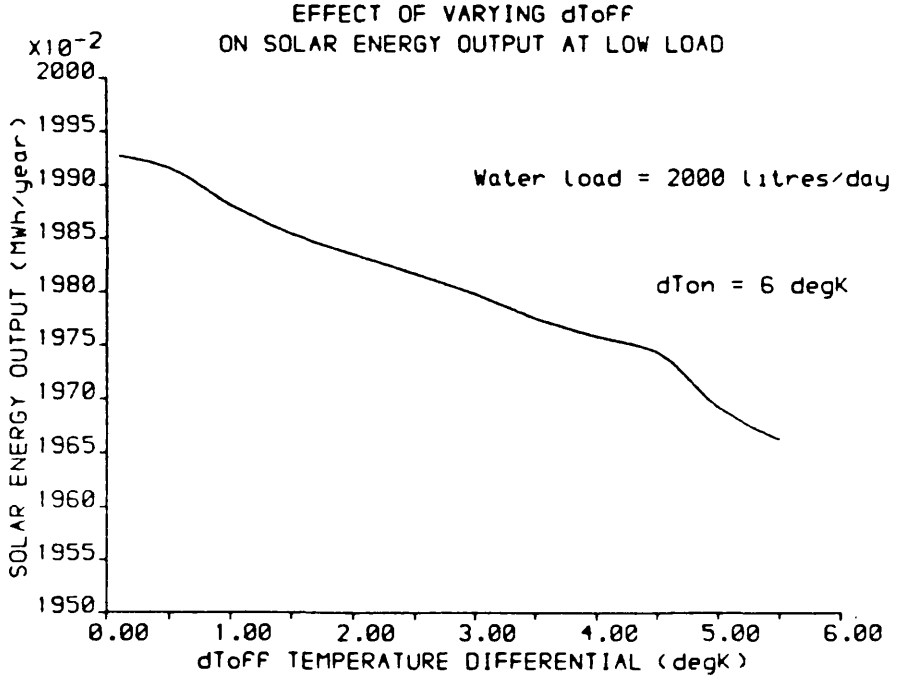

FIGURE 5.11

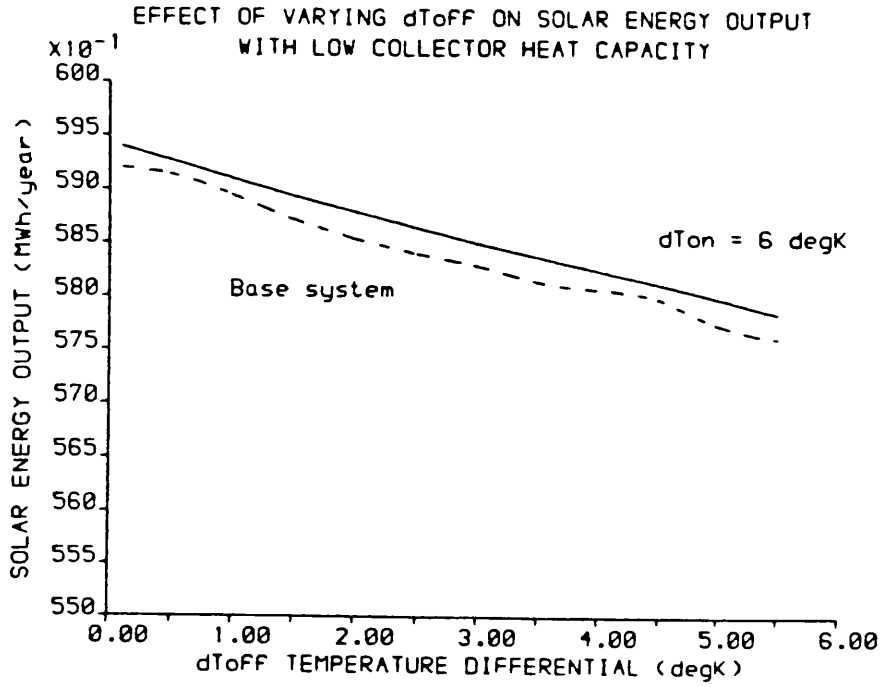

FIGURE 5.12

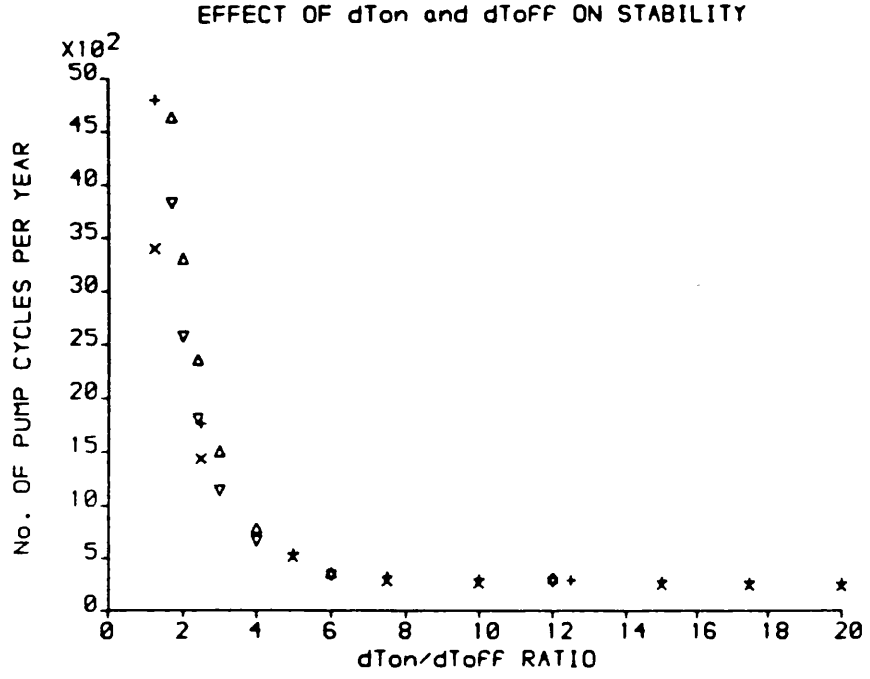

FIGURE 5.13

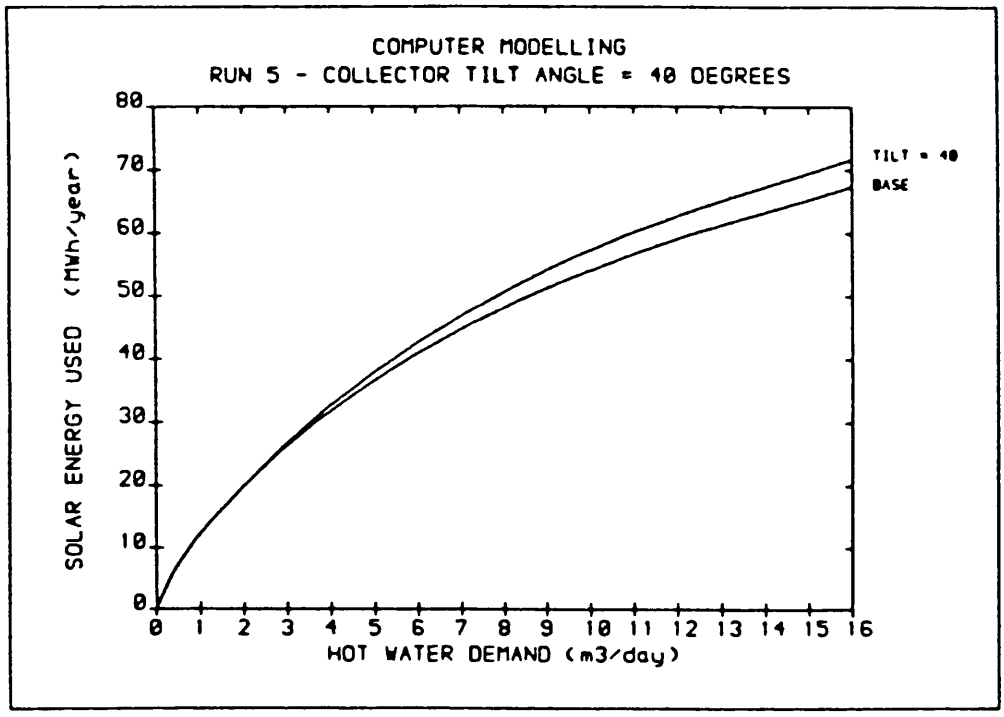

FIGURE 5.14

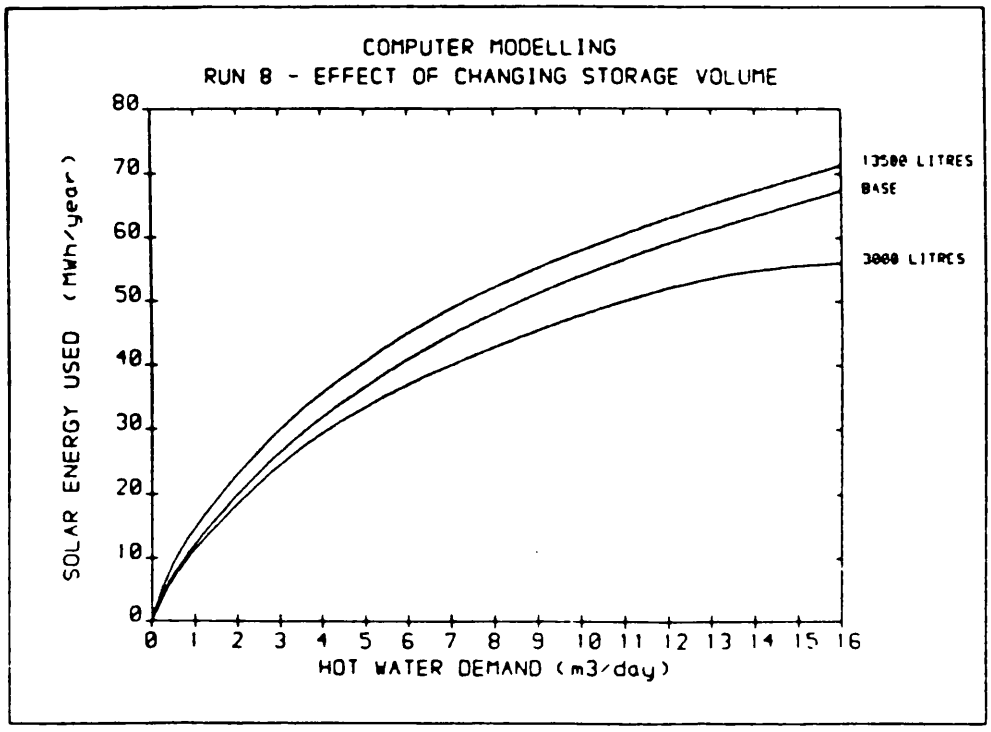

FIGURE 5.15

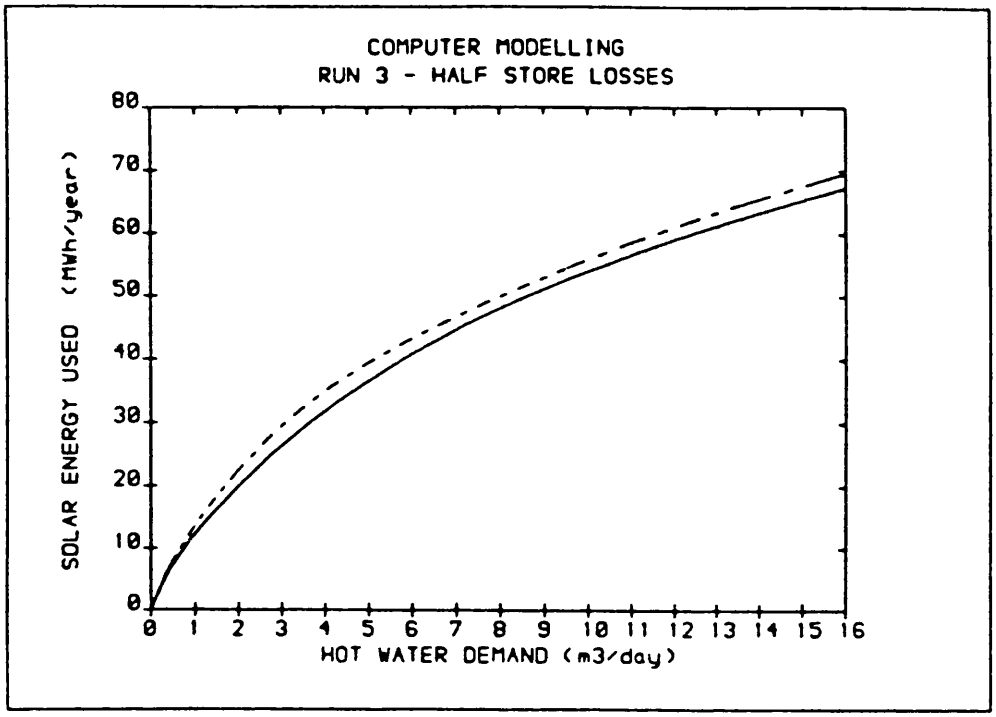

FIGURE 5.16

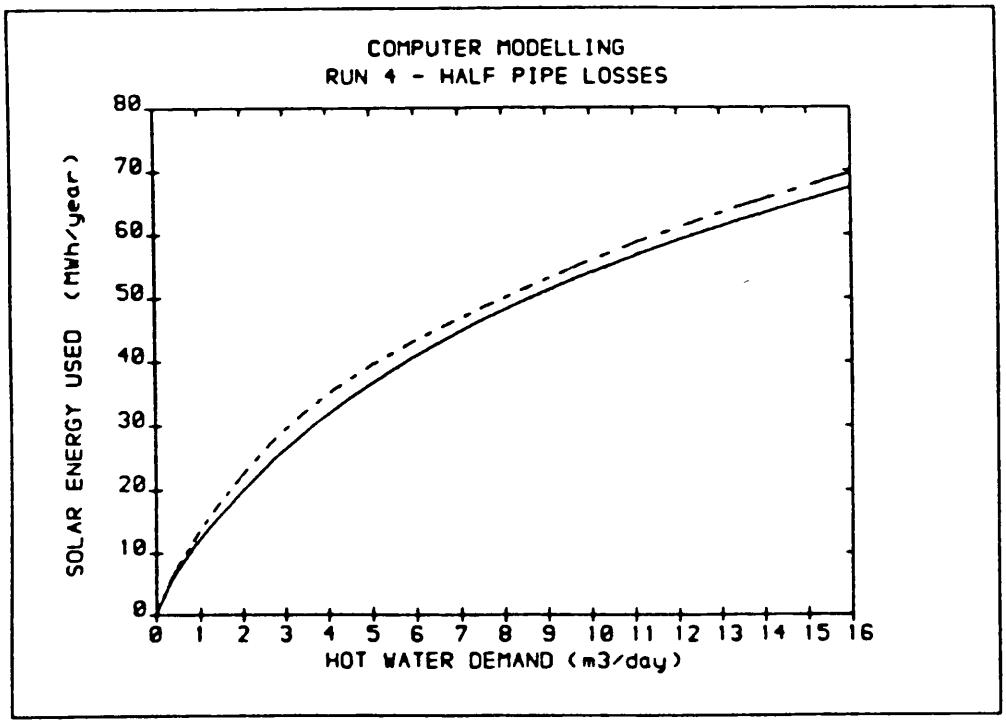

FIGURE 5.17

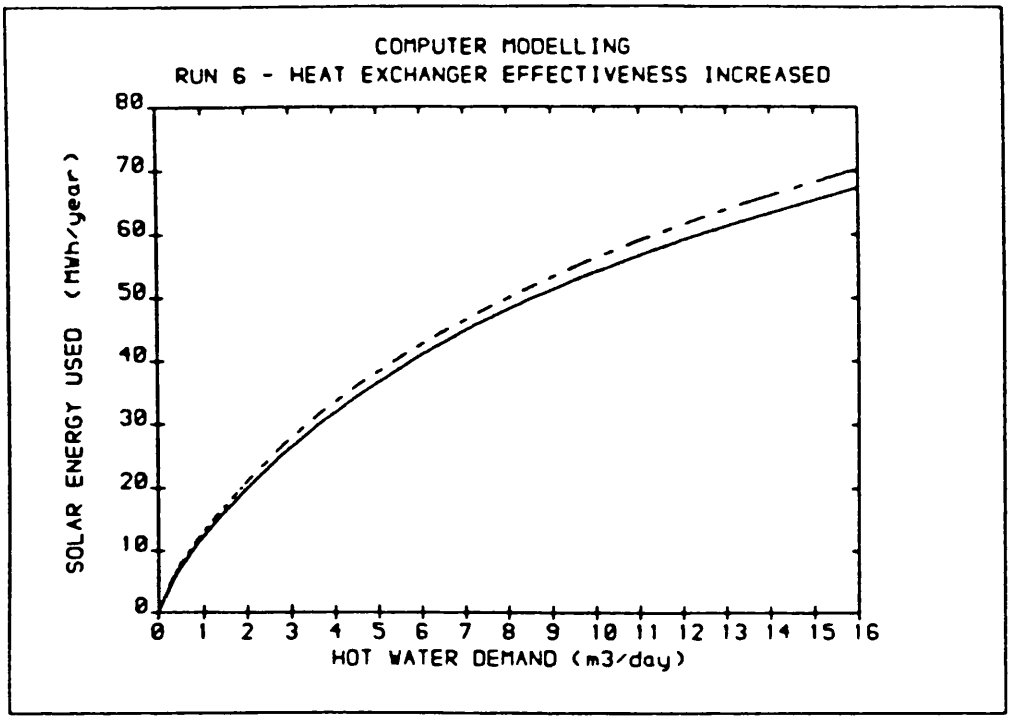

FIGURE 5.18

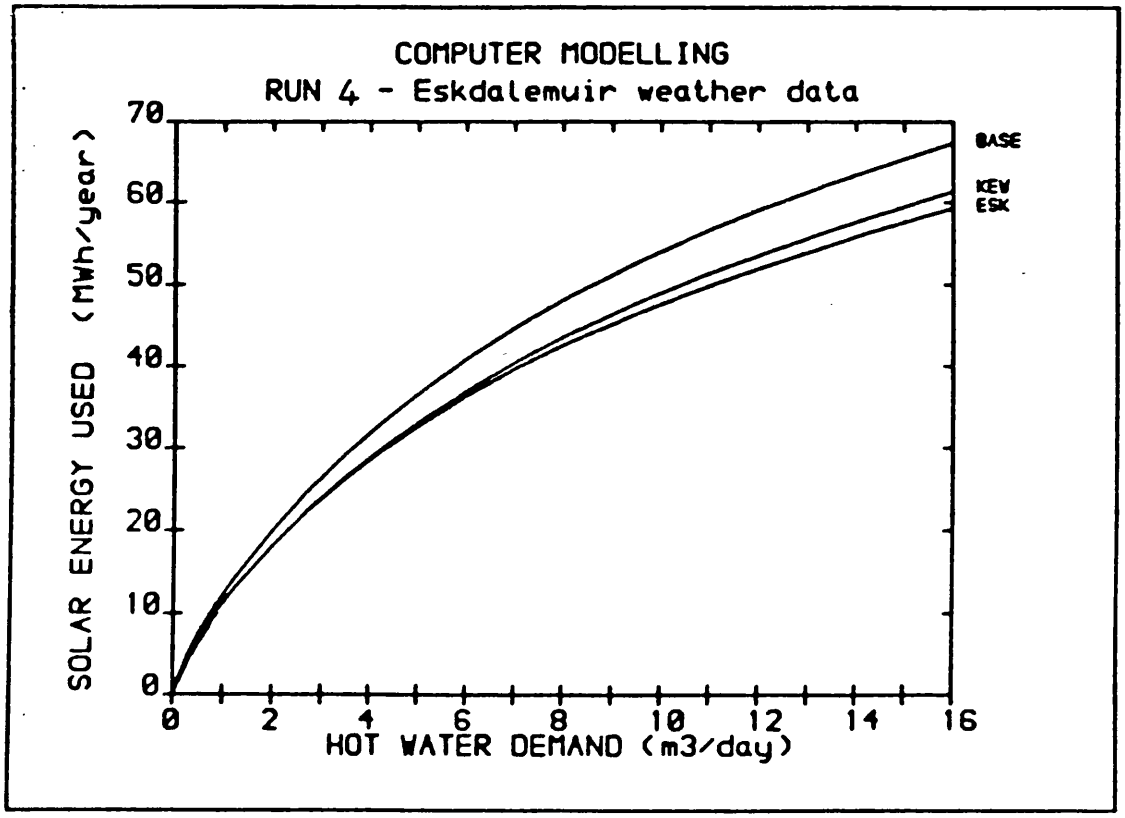

FIGURE 5.19

CHAPTER SIX

6. CONCLUSION

The generally-held assumption which has been investigated and challenged in this thesis is as follows:

> that the long-term thermal performance of solar water heating systems is not sensitive to the control temperature differential between the solar absorber plate and the solar store at which the circulating pump is switched on (dTon).

The surprising nature of the above assertion, together with the results of the theoretical analysis of Chapter Two, aroused the curiosity and suspicion of the author and prompted the current investigation. The measured results from a large-scale solar water heating field trial in the UK were carefully correlated with the predictions of a detailed computer model to produce a faithful and accurate simulation of the performance of the real system. The calibrated model was then used to investigate the above statement.

Apart from the investigation of the above assumption, further sensitivity analyses were carried out into the effect of the switch-on and switch-off temperature differentials on stability and thermal performance. The effects of other major design variable changes on the performance were also assessed, in order to put the results into a general perspective.

CHAPTER SIX

The conclusions from the above investigation are given in this chapter.

6.1 The effect of varying dTon

A statement by Duffie & Beckman (1980), and recent work by Howells (1984) have suggested that the switch-on temperature differential dTon may be raised as high as 20°K without incurring a significant long-term performance penalty. The statement by Duffie & Beckman, however, is made without evidence or reference to work by other authors. Howells' work is based on computer simulations, but was carried out without the benefit of a model specifically calibrated using measured data. It is also not clear from Howells' work what level of load the system studied was under.

The results of chapter five have shown that, for the system under study, the use of a pump switch-on temperature differential of 20°K will result in a reduction of more than 7% in the annual solar energy output, which is a significant performance penalty by any standards. A performance reduction of only 1.2% was found when dTon was increased from 1 to 6°K. Above this point, the sensitivity increased rapidly with increasing dTon.

The reason for the discrepancy between these results and those found by Howells is thought to be connected with the magnitude of the measured heat losses from the collectors, the collector loop pipework, and the solar storage tank. In practice, these heat

losses have been found to be much higher than theoretical calculations predict, despite the use of quality proprietary insulation which has been properly installed. The use of a high switch-on temperature can therefore lead to substantial amounts of collectable, medium-level solar radiation being wasted due to the absorber itself establishing a quasi-steady heat exchange equilibrium with the surrounding air without reaching a temperature sufficient to turn the pump on. The steady-state analysis of chapter two showed that up to 120 W/m^2 of collectable solar energy may be lost in this way if the overall heat loss coefficient for the collector is 6 $W/m^2{}^\circ K$. The results of chapter five support this argument, particularly in view of the following observations:

a) the performance penalty (in percentage terms) associated with a high dTon temperature was greater during winter months.

b) the sensitivity of the performance to dTon is significantly reduced when the original, theoretical heat loss coefficients are used instead of the measured values.

The other, qualitative argument presented in chapter two was to the effect that the intermittent nature of the solar radiation in the UK climate coupled with a high collector heat capacity and a high dTon value could lead to a substantial waste of collectable solar energy as the absorber heats up and cools down across a wide temperature band without causing the circulating pump to switch on. This argument has not been vindicated by the results of the

modelling, as the sensitivity was virtually unaffected when the collector heat capacity was halved. However, the chief limitation of the model in this respect is that it uses only hourly average values of solar radiation, and assumes constant radiation intensity over the hour, as discussed in chapter three. The above argument cannot therefore be considered disproved. Detailed short-term laboratory tests with the aid of a solar simulator would be required to test this theory fully.

6.2 Effect of varying dToff

The results of chapter five show that, for the system under study, a performance penalty of 2.7% will be incurred by raising the switch-off temperature differential dToff from 0.1°K to 5.5°K, and that the sensitivity is approximately constant over this interval. The optimum value of dToff is 0.1°K, at which point the energy gain equals the cost of pumping. The requirement of stable pump control also calls for as low a value of dToff as possible, as shown by figure 5.13. However, such a low value of dToff is difficult to achieve consistently over a wide range of absolute operating temperature using inexpensive controllers and temperature sensors. For example, a true differential of +0.1°K at a store temperature of, say, 25°C might be found to have drifted negative at a store temperature of 50°C. For a large installation, therefore, the extra expenditure required for a high quality controller using platinum resistance thermometers instead of standard nickel sensors can be justified.

6.3 Overall conclusions

The results of the performance sensitivity and switching stability analyses described in chapter five support the hypotheses presented in chapter two and show that, contrary to current opinion, the performance of the solar water heating system studied is sensitive to the control temperature setting dTon. This observation is linked to the large discrepancy between the theoretical and measured heat losses throughout the system, a discrepancy which emerged during the calibration of the computer model. It is demonstrated that lower heat losses lead to a lower sensitivity to dTon.

Putting these results into perspective, it is evident that the sensitivity of the long-term performance of the system to the control setting dTon is at least on a par with, and in some cases greater than, the sensitivity to changes in other major design variables such as collector tilt angle, storage volume, and insulation levels.

The results also show that a compromise is required between stable pump control and optimum thermal performance. Considerations of stable control call for a high value of dTon with a low value of dToff, while considerations of thermal performance call for low values of both dTon and dToff. Significant long-term performance penalties will result from the use of values of dTon above 6°K or

values of dToff above 1°K, while an excessive number of pump switchings per year will result from the use of a dTon/dToff ratio less than 8.

It would not be proper to generalise the above results rigidly to all solar water heating systems, as they have been obtained through a detailed study of one particular installation. The results do, nevertheless, serve to disprove the common general assumption that the long-term thermal performance of solar water heating systems is insensitive to the control setting dTon. Furthermore, the system studied is fairly typical of solar water heating systems utilising single-glazed, flat plate solar collectors, and the results have supported the mathematical hypotheses presented in chapters two and three. The results are therefore of some general value, and lead to the recommendation that a pump switch-on setting of 4-6°K with a switch-off setting of 0.1-0.5°K should be employed to achieve optimum performance of a solar water heating system utilising flat plate solar collectors in the UK.

The switch-on criterion of 4-6°K can be achieved reaasonably easily by the use of standard, inexpensive controllers and nickel-based temperature sensors. However, such controllers are not capable of consistently resolving temperature differentials to the degree required to meet the switch-off criterion of 0.1-0.5°K over the full operating temperature range. For large installations, therefore, the use of high quality controllers with calibrated platinum resistance thermometers as temperature sensors will prove cost-effective and is strongly recommended.

7. BIBLIOGRAPHY

Beckman, W.A., S.A.Klein, and J.A.Duffie, "Solar heating design by the f-chart method.", Wiley New York, 1977.

Boes, E.C. et al, "Distribution of direct and total solar radiation availabilities for the USA", Sandia Report SAND 76-0411, 1976.

Bliss,R.W., "The derivations of several 'plate efficiency factors' useful in the design of flat plate solar heat collectors", Solar Energy, 3(4), 55, 1959.

Brinkworth, B.J., and Hughes, T.D.R., "Accelerated response of thermopile pyranometers.", Solar Energy, 18, pp403-404

Campion, P.J. et al., "A code of practice for the detailed statement of accuracy.", National Physics Laboratory, HMSO, London, 1969.

Collares-Pereira, M, and A. Rabl., "The average distribution of solar radiation correlations between diffuse and hemispherical and between daily and hourly insolation values", Solar Energy 22, 155-164, 1979.

Commission of the European Communities, "Reporting format for solar heating systems.", 1980.

Dane, G.E., "Data analysis software for the Port Isaac School Solar Heating Field Trial", Technical report BU/SABE/EG9, University of Bath, 1980.

Dane, G.E., "Port Isaac School Solar Heating Field Trial. Sensors, measurement systems, calibration and practical installation.", Technical note BU/SABE/EG7, University of Bath, June 1980.

Dane, G.E., "The effects of sensor mounting on the accuracy of fluid temperature measurements in pipes." Technical note BU/SABE/EG5, University of Bath, March 1980.

Deacon, E.L. "The overestimation error of cup anemometers in fluctuating winds.", J.Sci.Instrum. London, 28, p231, 1951.

Duffie, J.A. and W.A.Beckman, "Solar Engineering of thermal processes, Wiley, New York, 1980.

Glazebrook, R., Dictionary of applied physics. Vol 3. "Meteorology, metrology and measuring apparatus.", London, 1923.

Heywood, H., "The computation of solar radiation intensities", Solar Energy, 10, 51, 1966.

Howells,P.B., "Simulation of system control strategies for solar thermal applications", PhD thesis, University College Cardiff, 1984.

Hottel,H.C. and B.B.Woertz, "The performance of flat plate solar heat collectors", Trans.ASME, 64, 91-104, 1942.

BIBLIOGRAPHY

Hottel,H.C. and A.Whillier, "Evaluation of flat plate solar collector performance", Transactions of the conference on the use of solar energy, 2, Part 1, 74, University of Arizona Press, 1958.

International Energy Agency, "Data requirements and thermal performance evaluation procedures for solar heating and cooling systems.", August 1979.

Jorgensen, O., "Investigation of the performance of solar heating and cooling systems", International Energy Agency, 1982.

Kenna, J.P., "The SEU design method for solar heating systems.", Solar Energy Unit, University College, Cardiff, Helios 15, July 1982.

Kovarik, M. and P.F.Lesse, "Optimal control of flow in low temperature solar heat collectors", Solar Energy, 18, 431, 1976.

Lewis, R.T., "The Port Isaac data logging system software manual.", University of Bath, September 1980.

Lewis, R.T., "Data logging system software (SABER 2).", Technical note BU/SABE/EG18, University of Bath, (to be issued).

Liu, B.Y.H. and R.C.Jordan, "The interrelationships and characteristic distribution of direct, diffuse and total radiation", Solar Energy 4(3), pp1-19, 1960.

Mabbs, D.G., "Methods for estimating the diffuse fraction of hourly, daily and monthly average global radiation", University of Wisconsin, 1980.

Meteorological Office, Met.O.912, "Solar radiation data for the United Kingdom 1951-1975", 1980.

Meteorological Office. Handbook of meteorological instruments, Part 1. HMSO London, 1969.

Norris, D.J., "Calibration of pyranometers in inclined and inverted positions.", Solar Energy, 16 pp53-55, 1974.

Pye,D.B. and J.L.J.Rosenfeld, "The mathematical modelling of active solar water and space heating systems", Paper submitted for ISES conference C23, Geological Society, London, October 1980.

Sheridan, N.R., K.J.Bullock, and J.A.Duffie, "Study of solar processes by analogue computer.", Solar Energy, 11,69 (1967)

Smith, C.T. and T.A.Weiss, "Design applications of the Hottel-Whillier-Bliss equation", ISES Congress, Los Angeles, Extended abstracts, Paper 34/6, July 1975.

Wendt, R.E., "Flow- its measurement and control in Science and Industry." Vol 1 Part 2, Flow metering devices, Instrument Soc. of America, edited 1977.

BIBLIOGRAPHY

Whillier, A., "Design factors influencing solar collector performance in low temperature engineering applications of solar energy." (edited by R.C.Jordan) ASHRAE pp27-40, 1967.

Whillier, A., "Prediction of performance of solar collectors", Applications of solar energy for heating and cooling of buildings, New York, ASHRAE, 1977.

Winn, C.B. and D.E.Hull, "Optimal controllers of the second kind", Proceedings of the 1978 Annual Meeting of the American Section of ISES Denver, 2(2), 493, 1978.

APPENDIX I

solarimeter **measurement of the Total Radiation of sun and sky**

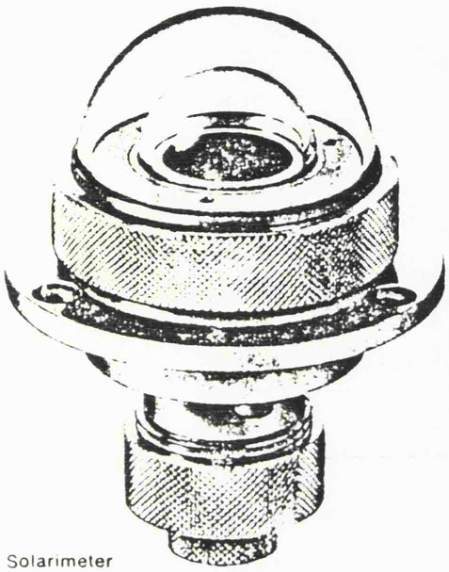

Solarimeter

In the Kipp solarimeter a Moll thermopile is used. For protection against atmospheric influences this thermopile is mounted under glass domes.
Gorczynski has indicated that a solarimeter only satisfies the cosine law if accurately ground hemispheres with a diameter of 50 mms or more are used.
Therefore a glass hemisphere to this specification is used, with an effective transmission range of 300 nm to 2.5 μm.
In order to achieve perfect stability regardless of temperature changes of the outer dome a second glass hemisphere, also accurately ground, is incorporated within the outer dome. This second hemisphere blocks the radiation exchange between the thermopile and the outer dome, whereby a marked increase in stability is achieved.
A white lacquered screen prevents the mounting from being heated by radiation. An easily removable drying cartridge is incorporated in the cylindrical housing in order to keep the air under the glass domes free from moisture. The base of the instrument is provided with a spirit level for placing the solarimeter exactly horizontally.
All solarimeters are individually calibrated. A calibration certificate stating both the calibration constant and the internal resistance is supplied with each instrument.

specification:
wavelength range 300 nm to 2.5 μm.
sensitivity approx. 8mV per gcal. $cm.^{-2}$ min^{-1}
115mV per Wcm^{-2}
internal resistance approx. 10 ohms
accuracy within 1%
linearity better than 1% over the whole range
With increasing ambient temperature there is a small decrease in sensitivity of the solarimeter. The temperature coefficient is approx. 0.15% per degree centigrade as compared with the calibration temperature = 22° C.
response time: 99% of final deflection in 30 sec.
70% of final deflection in 3 sec.
diameter screen 30 cms – height 11 cms –
weight 3.7 kg incl. base and screen
weight solarimeter only: 0.8 kg

SOLARIMETER
FOR OUTDOOR INSTALLATION

CM 5 - CM 6

The solarimeter base is provided with a spirit level. It should be placed in a horizontal position by means of the two levelling screws.

The solarimeter CM 5 is screwed onto the base by means of the three screws provided.
The screen is fixed by pushing the three studs into the three supports on top of the base and tightening the srews.

The instrument should be positioned in such a way that the **output cable** is pointing NORTH.

In order to avoid condensation on the inside of the glass domes the interior of the solarimeter is kept dry by means of a built-in drying cartridge.
This drying cartridge (1) can be withdrawn from the mounting after removal of the retaining screw-ring (2) as indicated in fig. 1. Upon pulling the two parts of the cartridge apart, the perforated tube can be filled with new silicagel or other suitable drying agent.

For cleaning, the outer glass dome can be taken off as indicated in fig. 1. Upon unscrewing the retaining screw-ring (3) the glass dome (4) can simply be lifted off. In re-assembling care should be taken that the ring is screwed home very tightly.

Connection to measuring equipment

The solarimeter is provided with a two-core output cable. Black is the negative terminal and blue the positive.

If long cables are used between the solarimeter and the measuring equipment, the possible influence of the resistance of these cables should be taken into account.
In the case of measuring equipment with a high input resistance (such as the integrator CC 1) the resistance of the connecting cable can usually be neglected.

When recording meters with a low internal resistance are used, the risistance of the cables may have a considerable influence. A correction is therefore required in order to avoid faulty measuring results.

For the calibration in conjunction with the solarimeter of an indicating instrument not supplied by us, two methods can be applied as shown in figures 2 and 3 page 4.
These schemes also enable the operator to determine the eventual influence of the resistance of the connecting cables.

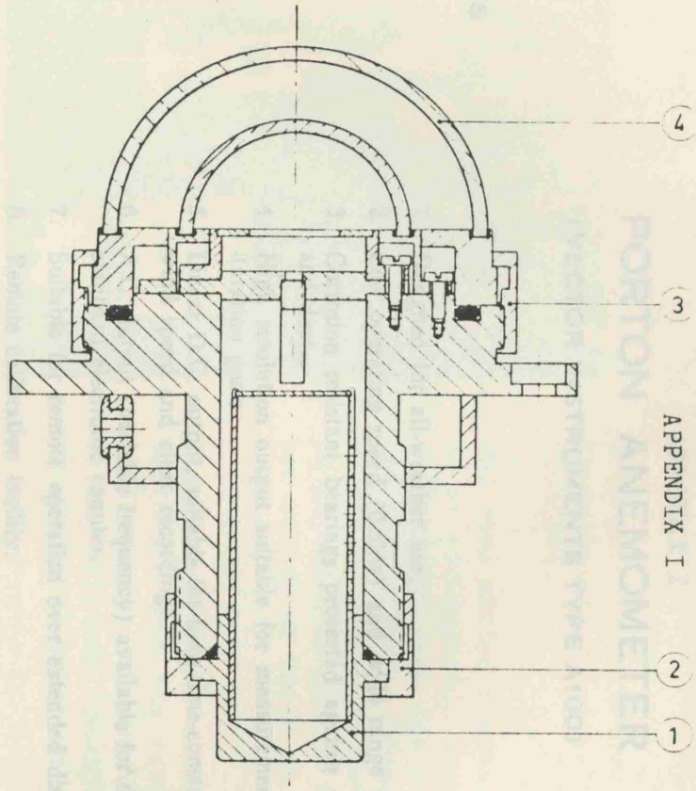

FIG 1

APPENDIX I

APPENDIX I

PORTON ANEMOMETER

(VECTOR INSTRUMENTS TYPE A100)

FEATURES

1. Designed for all-weather use.
2. Low operating speed (0.5kts) and wide range (100kts).
3. Corrosion resistant bearings protected against entry of moisture droplets and dust.
4. High resolution output suitable for measurement of turbulence and short duration gusts.
5. Linear D.C. output, suitable for long time-constant filtering to obtain mean wind speed and clear recordings.
6. A.C. output (variable frequency) available for direct reading in kts on any standard electronic counter.
7. Suitable for remote operation over extended distances.
8. Remote calibration facility.
9. Rotor attached by patented gravity sensitive fastener for rapid fitting and release in portable applications.
10. Small size and light weight.

SPECIFICATION

Physical Dimensions—	Height	235mm.
	Rotor diameter	152mm.
	Body diameter	55mm.
	Number of cups	3.
	Cable length	3m.
Materials—	Anodized aluminium alloy and A.B.S. for exposed parts.	
Weight—	Total	310gm.
	Rotor	30gm.
Performance—	Threshold speed	0.5kts.
	Maximum speed	Over 100kts.
	Accuracy	Within 2% plus 0.2kts. (rotor & AC o/p).
	Linearity	Within 2% plus 0.2kts. (rotor & AC o/p).
Electrical Characteristics—	Supply voltage	10v. to 16v.
	Supply current	30mA nom. at 12v.
	Output voltage—DC	0 to 11v. with 12v. supply.
	AC	10hz per kt., 7.5v. peak to peak.
	Output resistance	Less than 500ohms. (DC o/p). Less than 2k. ohms. (AC o/p).
	Ratemeter linearity	½% of full output.
	Ratemeter sensitivity	10v. DC o/p for 1KHz i/p (100kts). Provision for adjustment to 10v. DC o/p for 250Hz. (25kts).
	Temperature stability	Output change within 2% from −25°c to +55°c.
	Output ripple	30mV max.
	Ratemeter lag	0.15 sec. max. time-constant.
	Life	Lamp in photo-electric circuit rated 10 years min. at 16v.
	Calibration signal	2v. RMS sine minimum.
	Connections	5-wire system. 4- or 3-wire system may be used for local operation or without remote calibration facility.
Fixing—	Standard ⅜" Whitworth (camera tripod) and 6° taper fittings both available.	

SWITCHING ANEMOMETERS

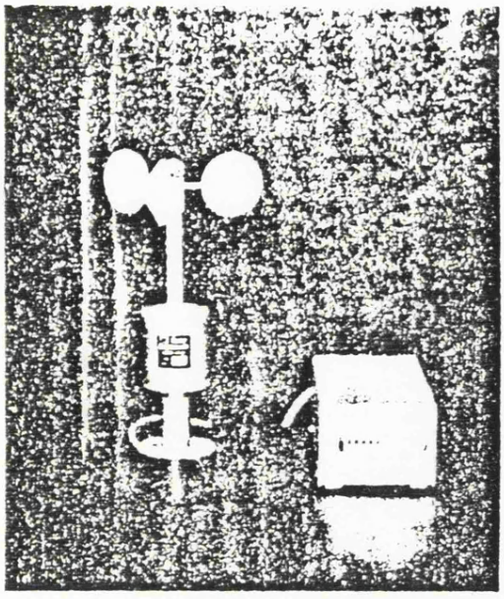

A range of anemometers for run of wind measurements or operation with electronic counters.

The reed switch anemometer will operate an electromagnetic counter directly without the need for an amplifier whereas the photoelectric anemometers can provide multiple pulses per revolution of the rotor and give direct reading in metres per second or knots on an electronic counter.

The photoelectric anemometer has a lower threshold than the reed switch type, and will operate at lower temperatures and in any attitude (though both are intended for vertical mounting).

Type A100R Switching Anemometer

A reed switch anemometer in which a magnet turns with the rotor spindle and the resulting varying field causes a mercury-wetted reed switch to make and break contact once per revolution of the rotor.

Specifications

Size	-	Height 200mm, case diameter 55mm, attached cable 3m.	
Rotor	-	Standard 3-cup 150mm diameter.	
Weight	-	Total 350g (including cable).	
Fixing	-	Rotor	Patented gravity sensitive fastener for rapid attachment and release.
	-	Anemometer	Standard tripod thread ($\frac{1}{4}$" BSW). Taper adaptor also available. Note: Mounting must be within 15° of vertical.
Materials	-	Anodized aluminium alloy and rigid ABS plastics for exposed parts.	
Performance	-	Threshold 0.3m/s, maximum over 50m/s, linearity 2%, accuracy 2% ± 0.1m/s, distance constant 5m.	
Calibration	-	0.80 revolutions per metre (1 pulse per $1\frac{1}{4}$ metres).	
Temp. range	-	-30 to +55°C.	
Electrical	-	Switching voltage	100 Volts d.c.
		Switching current	0.5 Amps max.
		Switch rating	28 Watts max. (d.c. resistive).
		Duty cycle	50% ±5%.
		Contact resistance	0.05 Ohms.
		Actuating time	1.5mS.
		Switch bounce	Nil.
		Min. current	Nil (life not reduced by use in dry circuits).
		Switch life	25×10^9 operations minimum.

Counter Unit Type EMC1

A six-digit electromagnetic counter with manual reset and on/off switch mounted in a metal box with sockets to accept A100R anemometer and 12V dc input power. Includes pulse suppression circuit.

APPENDIX I

Matthey

Thermafilm

platinum resistance temperature detectors

FEATURES

● Stable in sealed steel tubes ● to maximum rated temperature

- Thick film design/fast response
- 100 ohm calibration: 38.5 ohm F.I.
- High stability
- Three R_u tolerance grades ±0.075%, ±0.1%, ±0.25%
- Meets BS 1904 and DIN 43760
- Excellent vibration and shock resistance
- Direct replacements for 3 mm dia. wire wound devices. (Type 100P30)

Because of their high accuracy and reliability, Platinum Resistance Thermometers are becoming more and more the preferred method of temperature measurement over the range −70°C to +600°C.

Matthey Thermafilm Detectors are thick film PRTD's (Platinum Resistance Temperature Detectors) precisely manufactured in an automated production line to new standards of accuracy, stability and reproducibility. Thermafilm offers not only low cost replacements for conventional wire wound PRTD's but high accuracy, high sensitivity alternatives to thermocouples and technically superior replacements for thermistors.

Thermafilm is available in three grades of tolerance. Grades 1 and 2 detectors meet the requirements of BS 1904 and DIN 43760 in all respects. Grade 3 detectors (at lower cost) are identical in performance to Grade 2 but have a wider tolerance (±0.25%) on ice point resistance, R_u. In addition, Thermafilm has operational advantages such as superior thermal response, much better resistance to vibration and shock, and the ability to remain stable at 600°C.

Thermafilm Detectors are available now in three different configurations covering a wide range of possible uses. Types 100S25 and 100W47 are produced on flat substrates and are ideal for applications when air, gas, or surface temperature measurements are to be made. Type 100P30 is rod shaped and designed to be a direct size replacement for conventional wire wound elements, but with all the advantages of faster response, excellent stability, and better resistance to vibration and shock. Other shapes and sizes can be considered to suit special applications.

Operational Stability in sealed probes

Matthey Thermafilm detectors have been thoroughly tested in air for long periods at temperatures up to 600°C. The results show excellent stability. However, many applications require PRTD's to be sealed into metal probes. Matthey have therefore tested Thermafilm 100P30 sealed into probes made from stainless steel to AISI 316 = En 58 J (BS 907). The results after 250 hours at 600°C show that the drift in R_u remains within ±0.05%.

●●● Calibration Certificates can be supplied to order ●●●

100P30

A 3 mm diameter cylindrical device which is a direct replacement for conventional PRTD's made from high purity platinum wire.

It consists of a high stability platinum track deposited onto a rigid rod shaped substrate covered with a protective coating of ceramic glaze.

This construction ensures not only high stability and exceptional resistance to vibration and shock, but gives a thermal response faster than comparable wire devices.

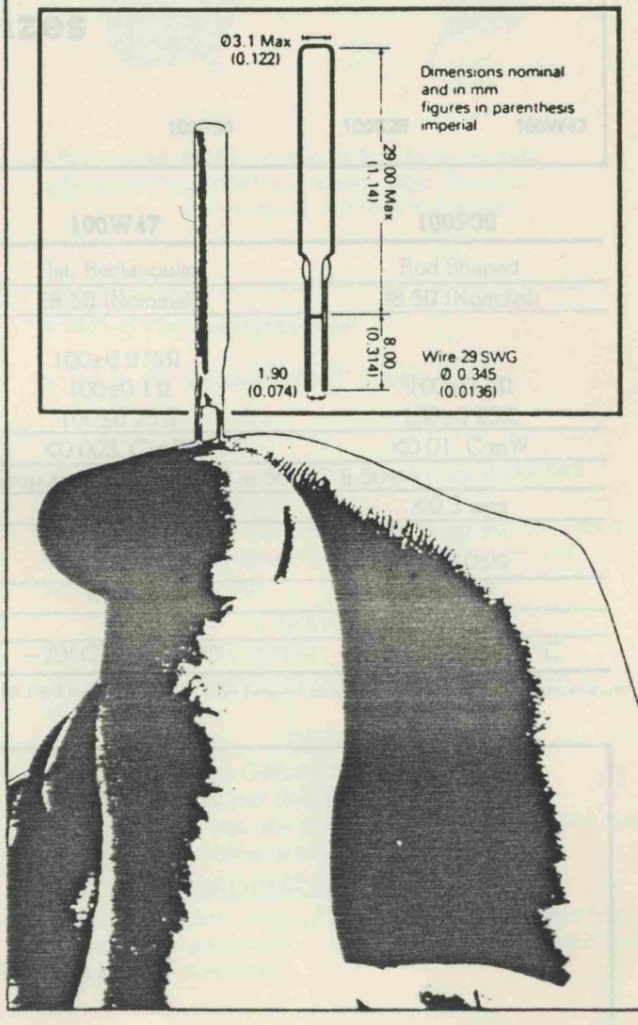

APPENDIX I

100S25

A 25 mm square flat printed device ideal for applications where conventional detectors might not be practical. The large sensing area is of particular advantage for radiated heat and surface temperature measurements. Other applications include laser focussing, medical electronics and cold junction compensation for thermocouples.

Thermafilm 100S25 consists of a high stability platinum track printed on to a rigid alumina substrate whose high thermal conductivity ensures a fast thermal response. A protective ceramic glaze coating covers the detector body and ensures good insulation resistance.

One face of the device is flat and completely insulated. It can, therefore, be placed in intimate thermal contact with flat surfaces.

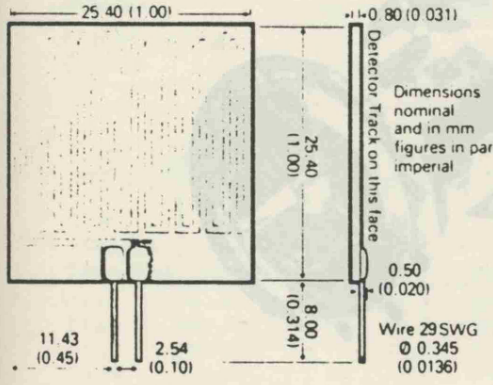

100W47

Type 100W47 is a 4.7 mm wide flat device which is very suitable for surface temperature measurements (e.g. busbars, pipework etc). It is also designed to fit inside 6 mm (¼") O.D. tubes or probes where it becomes self locating across the diameter.

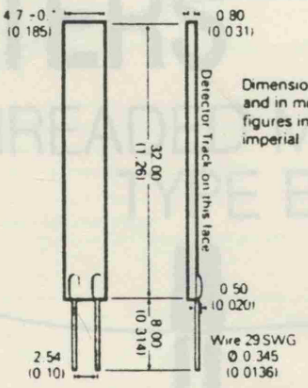

Actual Sizes

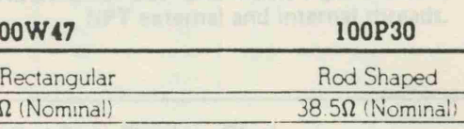

Technical Data	100S25	100W47	100P30
Configuration	Flat, Square	Flat, Rectangular	Rod Shaped
Fundamental Interval	38.5Ω (Nominal)	38.5Ω (Nominal)	38.5Ω (Nominal)
Zero Point Resistance R_0			
Grade I	100±0.075Ω	100±0.075Ω	–
Grade II	100±0.1Ω	100±0.1Ω	100±0.1Ω
Grade III	100±0.25Ω	100±0.25Ω	100±0.25Ω
Self Heating*	<0.005°C/mW	<0.005°C/mW	<0.01°C/mW
Surface Insulation	10 MΩ at room temp and 240V or 1 MΩ at 500°C & 50v		
Thermal Response**	<0.25 secs	<0.15 secs	<0.3 secs
Stability after temperature cycling***	<±0.05%	<±0.05%	<±0.05%
Capacitance (at 1KHz)	<25pF	<15pF	<10pF
Inductance	–	–	<1μH
Temperature Range	−70°C to +600°C	−70°C to +600°C	−70°C to +600°C

*Immersed in well stirred water at the ice point ** Time to reach 63% of ultimate temperature (as BS 1904 test) *** After 10 cycles between minimum and maximum rated temperatures

Matthey Printed Products Limited

Johnson Matthey Company

Alma Clowes Street : Burslem : Stoke-on-Trent ST6 3AT : England

Telex: 36141 MPPBUR G. Telegrams: Cables - Matthey Burslem Telephone Stoke-on-Trent (0782) 85631

AOT Systems

HYDRIL

INLINE TURBINE FLOWMETERS

FLANGED METERS TYPE F

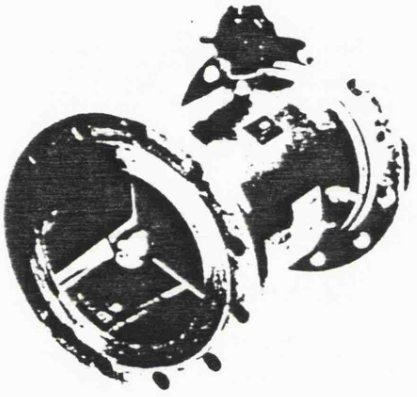

SIZES (NOM. BORE): 1/4 in to 20 in (6 to 500 mm)
CONNECTIONS: ASA 150, 300 and 600 or British Standard and DIN equivalents supplied as standard. Higher Ratings ASA 900, 1500 & 2500 available to special order.

THREADED METERS TYPE B

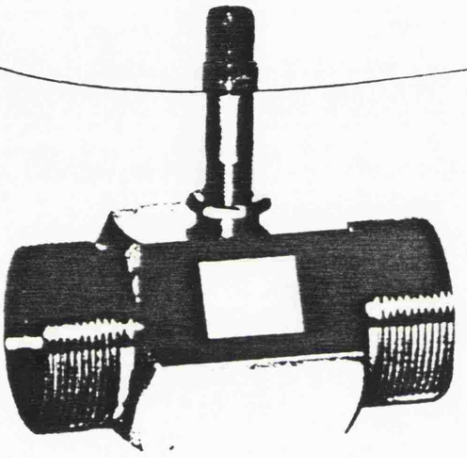

SIZES (NOM. BORE): 1/4 in to 2 in (6 to 50 mm)
CONNECTIONS: BSP and Metric Pipe Threads, NPT external and internal threads.

- Proven Reliability
- High Accuracy
- Liquid or Gas Use
- Wetted Parts Stainless Steel
- 1/4" to 20" Nominal Bore (F Type)

AOT flowmeters are precision designed to provide high orders of performance, accuracy, and reliability under the severest conditions encountered in the Oil, Gas, Petrochemical, Chemical and other Industries.

CALIBRATION

All AOT flowmeters are individually calibrated under stringent laboratory control.

Where flowmeters are intended for use in fiscal or custody transfer applications, AOT will be pleased to co-operate in arranging for independent certification tests in accordance with the regulatory requirements of the Government or Authority concerned. In addition AOT can offer calibration tests certified in accordance with the initial calibration service on water over a flow range of 20-3000 m^3/hr.

HAZARDOUS AREA USE

Intrinsically safe (I.S.) operation is covered by BASEEFA Certificate No. EX78187.

Flameproof (FLP) operation is covered by BASEEFA Certificate No. EX79125.
Enclosures to NEC 500 can also be supplied (UL Listed). (Consult factory to determine which flowmeters and pick-ups have cover).

MATERIALS

Stainless Steel throughout.
Type F alternatively fitted with carbon steel flanges and bodies.

BEARINGS

Liquids—Tungsten Carbide/Stellite sleeve
Gases—Shielded ball Stainless Steel
Alternative bearings are fitted for special applications such as cryogenics, contaminated gases etc.

ASSOCIATED ELECTRONICS

A comprehensive range of electronic signal conditioning and read-out equipment is available for use in conjunction with all AOT flowmeters.

(See rear of Catalogue for Ordering Data)

Publication P61/01

GENERAL SPECIFICATIONS

LIQUIDS

ACCURACY	Linearity (10% to 100% flow range) meters sized 3" and above. ±0.25% for low viscosity hydrocarbons (less than 5 centistokes) and water based liquids ±0.15% under specified conditions. Linearity (10% to 100% flow range) meters sized 2" and below: ±0.5% for low viscosity hydrocarbons (less than 5 centistokes) and water ±0 25% under specified conditions. Note: For linearity performance at higher fluid viscosities consult factory. Generally, for a given linearity specification rangeability is reduced with increasing viscosity. Repeatability: based on a 95% confidence limit and under conditions of steady flow. Meters sized 3" and above: ±0.02% or better. Meters sized 2" and below: ±0.05% or better.
MAXIMUM PRESSURE	Threaded Meters – 4000 lbf/in (250 kg/cm²) Flanged Meters – according to flange specification
PRESSURE DROP (Approx)	4 lbf/in (0.25 kg/cm²) at 100% flow range (SG1, 1 centistoke viscosity)
TEMPERATURE RANGE	Tungsten Carbide Pinions/Stellite Sleeves – 50°C to +400°C Open Ball Bearings: 50°C to ±250°C (clean liquids only)
ELECTRICAL CONNECTIONS	Either Cannon Connector Type MS-3101-A10SL-4P (supplied with mating connector) MS-3106-A10SL-4S(c) or a 3/4 in. conduit box with terminal block connections.

GASES

ACCURACY	±1% over 10% to 100% flow range (inclusive of linearity and repeatability)
MAXIMUM PRESSURE	Threaded Meters – 4000 lbf/in (250 kg/cm²) Flanged Meters – according to flange specification
PRESSURE DROP (Approx.)	Less that 1 in w.g. at 100% flow (gas density 1,29 mg/cm)
TEMPERATURE RANGE	Shielded Ball Bearings: ±50 C to +150 C

LIQUID FLOW RANGES

Type No. F Flanged Connections	Type No. B Threaded Connections	Nominal Bore in	Nominal Bore mm	Normal Operating Range imp g/min	Normal Operating Range m³/h	Maximum Operating Repeatable Range imp g/min	Maximum Operating Repeatable Range m³/h
F 1 4/1	B 1 4 1	1 4	6	0.1 — 1	0.028 — 0.275	0.06 — 1.5	0.0168 — 0.412
F 1 4 2	B 1 4 2	1 4	6	0.2 — 2	0.055 — 0 55	0.12 — 3	0.033 — 0.82
F 1 2 4	B 1 2 4	1 2	12	0.4 — 4	0.11 — 1.1	0.24 — 6	0.066 — 1.165
F 5 8 8	B 5 8 8	5 8	15	0.8 — 8	0.22 — 2.2	0.48 — 12	0.132 — 3.3
F 5 8 15	B 5 8 15	5 8	15	1.5 — 15	0.4 — 4	0.9 — 27	0.24 — 6
F 3 4 30	B 3 4 30	3 4	18	3 — 30	0.8 — 8	1.8 — 45	0.48 — 12
F 1 60	B 1 60	1	25	6 — 60	1.6 — 16	3.6 — 90	0.98 — 22
F 1-1 2 125	B 1-1 2 125	1-1 2	37	12 5 — 125	3.4 — 34	7 5 — 187	2.04 — 51
F 2 250	B 2 250	2	50	25 — 250	6.8 — 68	15 — 375	4.08 — 102
F 3 500	—	2½	75	50 — 500	13 5 — 135	30 — 750	8.1 — 202
F 4 1000	—	4	100	100 — 1000	27 — 270	60 — 1500	16.2 — 404
F 6 2000	—	6	150	200 — 2000	55 — 550	120 — 3000	33 — 825
F 8 4000	—	8	200	400 — 4000	110 — 1100	240 — 6000	66 — 1165
F 10 7000	—	10	250	700 — 7000	190 — 1900	420 — 10000	114 — 2550
F 12 10000	—	12	300	1000 — 10000	270 — 2700	600 — 15000	162 — 4050
F 16 15000	—	16	400	1500 — 15000	400 — 4000	840 — 21000	240 — 6000
F 20 25000	—	20	500	2500 — 25000	700 — 7000	1500 — 37500	420 — 10500

NOTES. 1. If ball bearings are used, minimum flow range can be reduced by a factor of 2 at low viscosities.
2. For low viscosity, non-lubricating liquids the normal and maximum flow rates should be reduced by 25%.
3. Where the operating viscosity is greater than 5 centistokes the operating ranges shown in Table 1 are applicable, but the linear range is reduced, repeatability is not affected by viscosity Specific data is available on request.
4. To convert to U S gallons conversion factor is 1 20094 multiply.

GAS FLOW RANGES — TABLE 2

Type No. F Flanged Connections	Type No. B Threaded Connections	Nominal Bore in	Nominal Bore mm	Normal Operating Range ft³/min	Normal Operating Range m³/h	Maximum Operating Repeatable Range ft³/min	Maximum Operating Repeatable Range m³/h
F 5 8 8	B 5 8 8	5 8	15	0 5 — 3 75	0 88 — 6 6	0 375 — 4 5	0 66 — 7 92
F 5 8 15	B 5 8 15	5 8	15	1 — 7 5	1 6 — 12	0 75 — 9	1 2 — 14.4
F 3 4/30	B 3 4 30	3 4	18	2 — 15	3 2 — 24	1 5 — 18	2.4 — 29.0
F 1 60	B 1 60	1	25	5 — 30	6 4 — 48	3 — 36	4 8 — 58.0
F 1-1 2 125	B 1-1 2 125	1-1 2	37	6 — 60	10 — 100	3 — 72	5 — 120
F 2 250	B 2 250	2	50	12 — 120	20 — 200	6 — 144	10 — 240
F 3 500	—	2½	75	24 — 240	40 — 400	12 — 288	20 — 480
F 4 1000	—	4	100	48 — 480	80 — 800	24 — 576	40 — 980
F 6 2000	—	6	150	100 — 1000	160 — 1600	50 — 1200	85 — 2000
F 8 4000	—	8	200	200 — 2000	320 — 3200	100 — 2400	170 — 4000
F 10 7000	—	10	250	300 — 3000	500 — 5000	150 — 3600	250 — 6000
F 12 10000	—	12	300	450 — 4500	800 — 8000	200 — 5400	340 — 9000
F 16 15000	—	16	400	675 — 6750	1200 — 12000	350 — 8100	600 — 14000
F 20 25000	—	20	500	1000 — 10000	1700 — 17000	500 — 12000	850 — 20400

NOTES 1 The above flow ranges are only applicable to the linearity specification for pressures in excess of 10 Kg/cm² for sizes up to 3 At lower pressures the rangeability reduced Details available on request
2 In many cases the stated operating flow ranges can be extended to a lower range where gas density (pressure) is sufficiently high Specific data is available on request

MATERIALS SPECIFICATIONS

	APPENDIX I
BODY (ALL SIZES)	Stainless Steel (or Carbon Steel to order)
FLANGES	Carbon Steel (or Stainless to order)
ROTOR (1/4 IN TO 3 IN)	Firth Vickers 520B or ANSI 431
ROTOR (4 IN TO 20 IN) LIQUID APPLICATIONS	Stainless Steel ANSI 321 or ANSI 431
ROTOR (4 IN TO 20 IN) GAS APPLICATIONS	Stainless Steel ANSI 321 or ANSI 431
PHONIC WHEEL WHERE FITTED	Firth Vickers 520B or ANSI 431
BEARING SUPPORTS	Stainless Steel ANSI 316 or 321
CIRCLIPS	Stainless Steel ANSI 321 or 304
BEARINGS — LIQUID APPLICATIONS	Tungsten Carbide Pinions/Stellite Sleeves
BEARINGS — GAS APPLICATIONS	Ball Bearings, Stainless Steel ANSI 440C

NOTE: Detailed materials specifications supplied upon request.

PHYSICAL DIMENSIONS

THREADED METERS

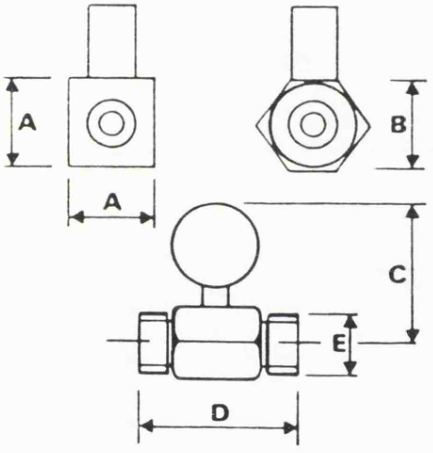

Size	A	B	C	D	E
1/4	1 (25.4)	—	5 (127)	2 (51)	3/8 B.S.P.
1/2	1 (25.4)	—	5 (127)	2-1/2 (64)	1/2 B.S.P.
5/8	1 (25.4)	—	5 (127)	2-1/2 (64)	5/8 B.S.P.
3/4	—	1.250 (32)	5-1/4 (133)	3-1/4 (83)	3/4 B.S.P.
1	—	1.625 (41)	5-1/2 (140)	3-1/2 (88)	1 B.S.P.
1-1/2	—	2.125 (54)	6 (152)	4-1/2 (114)	1-1/2 B.S.P.
2	—	2.750 (70)	6-1/2 (165)	5-1/4 (132)	2 B.S.P.

FLANGED METERS

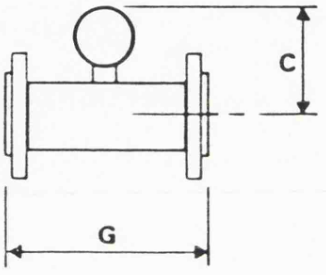

Size	C	G
1/4	5 (127)	4-1/2 (114)
1/2	5 (127)	5 (127)
5/8	5-1/4 (133)	5 (127)
3/4	5-1/2 (140)	5-1/2 (140)
1	5-3/4 (146)	6 (152)
1-1/2	6 (152)	7 (178)
2	6-1/2 (165)	7-3/4 (197)
3	7 (178)	10 (254)
4	10 (254)	14 (356)
6	11 (279)	14-1/2 (368)
8	12-1/4 (311)	18 (457)
10	13-1/4 (336)	18 (457)
12	14-1/4 (362)	18 (457)
16	16-1/2 (419)	24 (610)
20	18-1/2 (470)	24 (610)

NOTE: Face to Face dimensions (G) are constant irrespective of the flange rating.

BEARINGS SELECTION TABLE — TABLE 3

Type	Meter Sizes	Temperature Range	Typical Applications	Remarks
LIQUIDS Tungsten Carbide	1/4" to 20" (6mm to 500mm)	- 50 C to + 400 C	Oil, Water etc.	No filter required. Not suitable below 10% range on sizes below 1/2" and 5% on 3/4"
LIQUEFIED GASES	1/4" to 20" (6mm to 500mm)	200 C	Cryogenic	Filtration recommended
GASES Shielded Ball	1/4" to 12" (6mm to 300mm)	50 C to + 150 C	General Cases	Low flow applications (Clean gases only)
Sealed Ball	4" to 20" (102mm to 500mm)	50 C to + 150 C	Contaminated Gases	For gases containing solid particles in suspension
CLEAN LIQUIDS Open Ball	1/4" to 3" (6mm to 75mm)	50 C to + 250 C	Liquids with lubricating properties e.g. Hydraulic Oil	Filtration recommended

VISCOSITY EFFECTS

AOT flowmeters can be used over a wide range of viscosities. The smaller meters, from 1/4in to 1-1/2in (6 to 38mm) nominal bore, are limited to 200 centistokes. The larger meters from 2in (50mm) nominal bore and above can be used with viscosities up to 500 centistokes. Since flowmeters measure volumetrically they are unaffected by changes in specific gravity, however the calibration is affected by viscosity change. As viscosity increases for any given size of meter, the lower limit of the linear range is increased. Additionally the number of output pulses per unit volume changes slightly on the linear part of the range. These effects are directly related to the Reynolds Number. Under these conditions better linearity is attained by selecting a meter to operate at the higher end of its flow range and if necessary into over-range.

CUSTOM FLOW RANGES

In particular markets, where units of flow or nominal ranges differ from our standard, or where a large quantity of meters with particular ranges are required, Hydril AOT's manufacturing procedures are designed to permit the range of optimization needed.
This permits almost every user to get the maximum performance from Hydril AOT Meters by ensuring the maximum flow rate, and turndown rangeability of the meters are as close to the actual working ranges required as possible.

The manufacturing procedure used:

- *Is part of the regular manufacturing process
- *Is correlated against the meter serial number
- *Is highly repeatable, eg for spares and extensions, and
- *Provides the full performance specified above.

CALIBRATION & CERTIFICATION

AOT Systems liquid calibration facilities include a BCS certified 3000 m^3/hr 30" meter prover, a 4" meter prover and dynamic gravimetric oil and water calibration rigs.

Gas calibration facilities include secondary-standard calibrated meters certified by the Gas Standards Institute.

Where flowmeters are intended for use in fiscal or custody transfer applications, AOT Systems will be pleased to co-operate in arranging for independent certification tests in accordance with the regulatory requirements of the Government or Authority concerned.

Typical certification test results for AOT flowmeters are illustrated below.

F/16/15000 Viscosity Compensated Meter Calibration tested by Arab Petroleum Pipelines (SUMED)

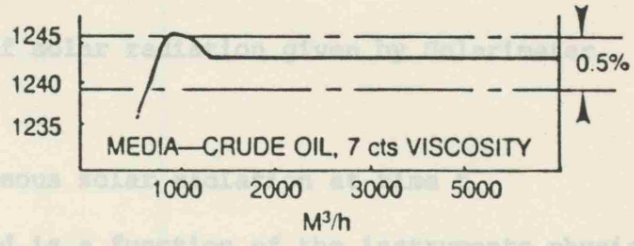

F/6/2000 Meter Calibration – for high accuracy Custody Transfer, National Iranian Oil Company tested at AOT Systems

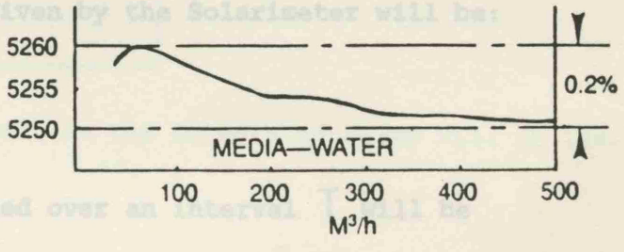

HIGH ACCURACY METERS

In addition to the flowmeters described in this data sheet, a series of high accuracy flowmeters are available for applications requiring linearity of better than ±0.15%. Please ask for separate data sheet on "CT" series flowmeters.

Development dictates that from time to time the data shown above is subject to change without notice. Please obtain a quotation.

HYDRIL®
Automatic Oil Tools Systems
Central Way, Walworth Industrial Estate
Andover, Hants SP10 5BW England
Telephone: (0264) 65961
Telex: 47107

HYDRIL®
Production Technology Division
P.O. Box 721560
Houston TX-77272,
United States of America
Telephone: (713) 777-5361
Telex: 79-0234

APPENDIX II

Response of Solarimeters to fluctuations in solar radiation

Step inputs

The output of a Solarimeter when measuring a step input of solar radiation is illustrated in figure 1 and can be described by the equation

$$\frac{dI_s}{dt} = k(I - I_s) \qquad \text{——————} \ (1)$$

Where I_s is the reading of solar radiation given by Solarimeter at time t

I is the instantaneous solar radiation at time t

k is a constant and is a function of the instruments physical properties.

For a step input, the reading given by the Solarimeter will be:

$$I_s = I_0(1 - e^{-kt})$$

Thus the total radiation measured over an interval T will be

$$\int_0^T I_s \, dt$$

$$= \int_0^T I_0\left(1 - e^{-kt}\right) dt$$

$$= I_0\left[t + \frac{e^{-kt}}{k}\right]_0^T$$

$$= I_0\left[T - \frac{1}{k}\left(1 - e^{-kt}\right)\right]$$

APPENDIX II

Since the actual solar radiation over this time interval is $I_0.t$, the error in the reading is:

$$-\frac{1}{kt}\left(1-e^{-kt}\right)$$

Thus for various values of kt, the error in reading are as follows:

kt	Error %
0.3	86
1.0	63
3.0	32
10.0	10
30.0	3.3
100	1
300	0.3

Thus providing $kt \gg 100$ the error in the integrated value will be less than 1%.

For a step input of radiation which ceases at time T_1, the response of the Solarimeter will be as shown in fig. 2

After the radiation ceases, the response of the solarimeter will be

$$I_s = I_m . e^{-k(t-T_1)}$$

Where I_m is reading of the solarimeter at time T_1.

Thus the total radiation measured over an interval T_2 will be

$$\int_0^{T_2} I_s \, dt$$

$$= \int_0^{T_1} I_0\left(1-e^{-kt}\right).dt + \int_{T_1}^{T_2} I_m e^{-k(t-T_1)}.dt$$

$$= I_0\left[t + \frac{e^{-kt}}{k}\right]_0^{T} + I_m.\left[-\frac{e}{k}^{-k(t-T_1)}\right]_{T_1}^{T_2}$$

$$= I_0\left[T_1 - \frac{1}{k}\left(1-e^{-kT_1}\right)\right] + I_m.\left[-\frac{e}{k}^{-k(T_2-T_1)} + \frac{1}{k}\right]$$

But $$I_m = I_0\left(1-e^{-kT_1}\right)$$

Hence $$\int I_s \cdot dt = I_0\left[T_1 - \frac{\left(1-e^{-kT_1}\right).e^{-k(T_2-T_1)}}{k}\right]$$

Note that if the period of measuring is long enough i.e. $T_2 \to \infty$

Then $$\int I_s \cdot dt \to I_0 t$$

i.e. there is no inaccuracy introduced by the response of the solarimeter.

However if the integration takes place over a finite interval, say $3T_1$, then the errors introduced are as follow:

kT_1	Error %
0.3	47
1.0	8.5
3.0	0.8
10.0	-
30.0	-
100.0	-
300.0	-

Thus provided $kT_1 \geq 3$ the error in the integrated value will be $\leq 1\%$.

Cyclic inputs

The output of a Solarimeter when measuring a step input of solar radiation

is illustrated in figure 3.

Assume that the solar radiation at time t is given by

$$I = \frac{I_m}{2}(1 - \cos \omega t)$$

And that the response of the solarimeter to this radiation is given by

$$\frac{dI_s}{dt} = k(I - I_s)$$

From (2) and (3)

$$\frac{dI_s}{dt} = \frac{I_m}{2} \cdot k(1 - \cos \omega t) - kI_s$$

$$I_s' + k.I_s = A(1 - \cos \omega t) \qquad \text{where } A = \frac{I_m k}{2}$$

By method of integrating factors $\quad f = k$

$$r = A(1 - \cos \omega t)$$

$$h = \int k\,dt = kt$$

$$I_s = e^{-h}$$

$$= e^{-kt}\left[\int e^{kt} \cdot A(1 - \cos \omega t)\,dt + C\right]$$

$$= A.e^{-kt}\left[\frac{e^{kt}}{k} - \frac{\omega}{\omega^2 + k^2} e^{kt}\left(\sin \omega t + \frac{k}{\omega} \cos \omega t\right) + C\right]$$

Now if $t = 0$, $I_s = 0$

$$0 = \frac{1}{k} - \frac{\omega}{\omega^2 + k^2} \cdot \frac{k}{\omega} + C$$

$$0 = 1 - k^2/\omega^2 + k^2 + Ck$$

$$C = \frac{-\omega^2}{k(\omega^2 + k^2)}$$

APPENDIX II

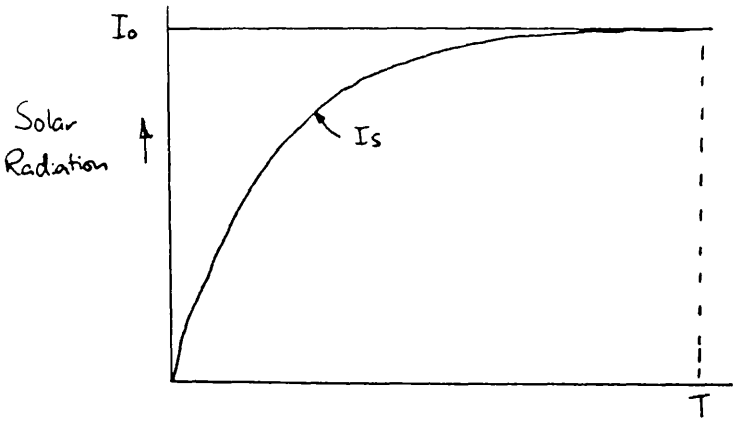

Fig. 1 Response of solarimeter to step input to solar radiation.

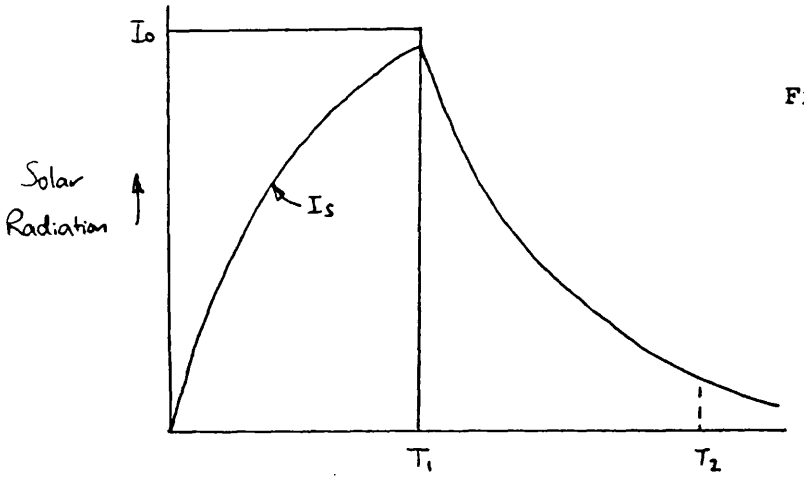

Fig. 2 Response of solarimeter to step input which ceases at time T_1

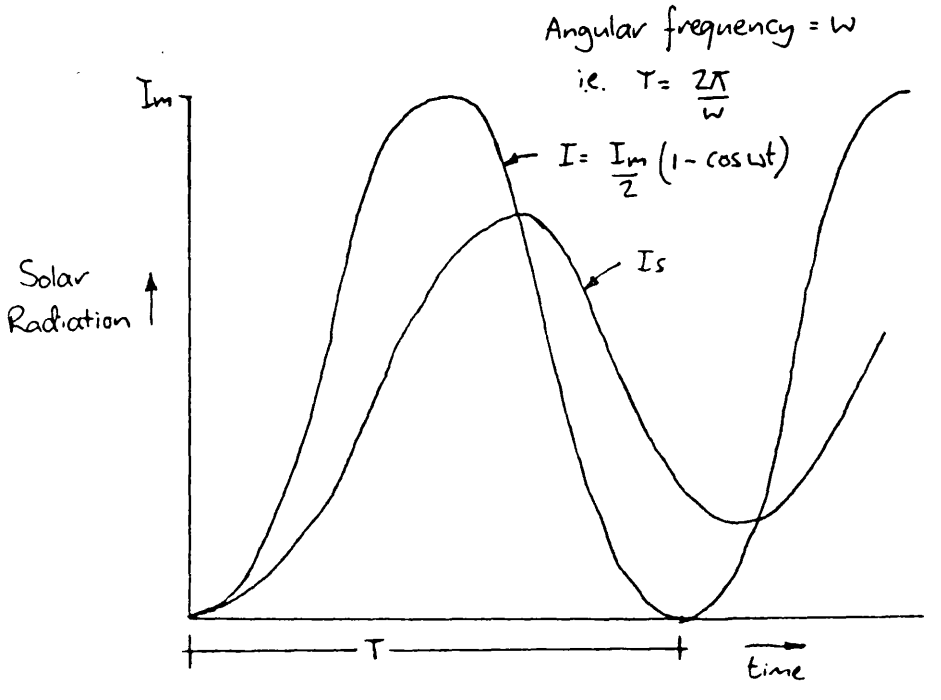

Fig. 3 Response to solarimeter to cyclic radiation input

$$\therefore \quad I_s = \frac{A}{k} - \frac{Aw}{w^2+k^2}\left(\sin wt + \frac{k}{w}\cos wt\right) - \frac{Aw^2 e^{-kt}}{k(w^2+k^2)}$$

$$I_s = \frac{I_m}{2}\left(1 - \frac{kw}{w^2+k^2}\left(\sin wt + \frac{k}{w}\cos wt\right) - \frac{w^2}{w^2+k^2}\, e^{-kt}\right)$$

or $$I_s = \frac{I_m}{2}\left(1 - \frac{k}{\sqrt{w^2+k^2}}\cdot\cos(wt-\theta) - \frac{w^2}{w^2+k^2}\cdot e^{-kt}\right)$$

i.e. this is a cosine function oscillating about a mid point which is tending to $\frac{I_m}{2}$ exponentially.

The cosine function has an amplitude of $\frac{k}{\sqrt{w^2+k^2}}$

with a lag angle of $\sin^{-1}\left(w/\sqrt{w^2+k^2}\right)$

If the output of the solarimeter is being integrated over n periods then the error inherent in the system will be

$$\frac{\int_0^{2\pi n/w} I_s\, dt - \int_0^{2\pi n/w} I\, dt}{\int_0^{2\pi n/w} I\, dt} \times 100 \quad \%$$

Now $$\int_0^{2\pi n/w} I\, dt = \int_0^{\frac{2\pi}{w}} \frac{I_m}{2}(1-\cos wt)\, dt$$

$$= \frac{I_m}{2}\left[t + \frac{\sin wt}{w}\right]_0^{\frac{2\pi n}{w}}$$

$$= \frac{I_m}{2}\cdot\frac{2\pi n}{w}$$

$$= \frac{I_m \cdot \pi n}{w}$$

And $$\int_0^{\frac{2\pi n}{w}} I_s\, dt = \int_0^{\frac{2\pi n}{w}} \frac{I_m}{2}\left(1 - \frac{kw}{w^2+k^2}\left(\sin wt + \frac{k}{w}\cos wt\right) - \frac{w^2}{w^2+k^2}\, e^{-kt}\right) dt$$

$$= \frac{I_m}{2}\left[t - \frac{k}{w^2+k^2}\left(\cos wt - \frac{k}{w}\sin wt\right) + \frac{w^2}{k(w^2+k^2)}\cdot e^{-kt}\right]_0^{\frac{2\pi n}{w}}$$

$$= \frac{I_m}{2}\left[\frac{2\pi n}{w} - \frac{k}{w^2+k^2} + \frac{w^2}{k(w^2+k^2)}\cdot e^{-\frac{2\pi k n}{w}} + \frac{k}{w^2+k^2} - \frac{w^2}{k(w^2+k^2)}\right]$$

$$= \frac{Im}{2}\left[\frac{2\pi n}{w} - \left(1 - e^{-\frac{2K\pi n}{w}}\right).\frac{w^2}{k(w^2+k^2)}\right]$$

$$\therefore \text{Error} = -\frac{\left(1 - e^{-\frac{2Kn\pi}{w}}\right).w^2}{2n\pi/w \;.\; k(w^2+k^2)} \times 100 \quad \%$$

$$= -\frac{\left(1 - e^{-nkT}\right)}{nkT\left(1 + \frac{k^2T^2}{4\pi^2}\right)}$$

Where $T = 2\pi/w$

ie. the period of oscillation of Solar radiation intensity

Errors inherent in this system of measurement for various values of kt & n are therefore:

KT	Error for given n %						
	1	3	10	30	100	300	1000
0.3	86	66	31	11	3.1	1.1	0.3
1.0	62	31	10	3.3	1.0	0.3	0.1
3.0	26	9	2.7	0.9	0.3	0.1	-
10.0	2.8	0.9	0.4	-	-	-	-
30.0	0.1	-	-	-	-	-	-
100	-	-	-	-	-	-	-

Thus it can be see that provided $nkT > 100$, the error in the integrated output of the solarimeter will be $\leqslant 1\%$.

For a typical Kipp & Zonen Solarimeter the time taken to reach 70% of its final deflection is 3 seconds. i.e. $I = I_0\left(1 - e^{-kt}\right)$

$$0.7 = 1 - e^{-3K}$$

$$k = 0.4 \text{ sec}^{-1}$$

APPENDIX III

KEY TO PARAMETERS MONITORED

P-channels : Fluid flow rates

Channel no.	Description	Units
P 1	Total DHW draw-off	litres/sec
P 2	Flow rate through heat exchanger batteries in solar calorifier	litres/sec
P 3	Total flow rate through solar panels	litres/sec
P 4	DHW re-circulation rate	litres/sec
P 5	Flow rate of condensate from HWS calorifiers	litres/sec
P 6	Wind speed (averaged over 1 hr)	metres/sec
P 7	Wind speed (averaged over 24 hrs)	metres/sec
P 8	Total DHW draw-off (1 hour)	litres
P 9	Total DHW draw-off (24 hours)	litres
P10	Total steam energy to HWS calorifiers (1 hour)	MJ
P11	Total steam energy to HWS calorifiers (24 hours)	MJ

Q-channels : Temperatures, pressures, and solarimeter readings.

Channel no.	Description	Units
Q 1	Outside ambient dry-bulb air temp	deg C
Q 2	Ambient air temp in solarimeter housing	deg C
Q 3	Incident solar radiation on horizontal plane	W/m2
Q 4	Incident solar radiation on plane of collectors	W/m2
Q 5	Mains cold water inlet temp	deg C
Q 6	Collector inlet temperature	deg C
Q 7	Collector outlet temperature	deg C
Q 8	Outlet temp from panel bank 1 (East end)	deg C
Q 9	Outlet temp from panel bank 2	deg C
Q10	Outlet temp from panel bank 3	deg C
Q11	Outlet temp from panel bank 4	deg C
Q12	Outlet temp from panel bank 5	deg C
Q13	Outlet temp from panel bank 6	deg C
Q14	Outlet temp from panel bank 7 (West end)	deg C
Q15	Inlet temp to panel bank 2	deg C
Q16	Inlet temp to panel bank 4	deg C
Q17	Inlet temp to panel bank 7	deg C
Q18	Panel bank 2 (bottom)	deg C
Q19	Panel bank 2 (centre)	deg C
Q20	Panel bank 2 (top)	deg C
Q21	Panel bank 4 (bottom)	deg C
Q22	Panel bank 4 (top)	deg C
Q23	Panel bank 7 (centre)	deg C
Q24	Temp in 3000 litre solar calorifier	deg C
Q25	Solar calorifier to accumulator interconnection	deg C

APPENDIX III

Channel no.	Description	Units
Q26	Temp in 7000 litre solar accumulator	deg C
Q27	Draw-off at top of solar accumulator	deg C
Q28	Combined draw-off from solar preheat	deg C
Q29	Flow to heat exchangers in calorifier	deg C
Q30	Return from heat exchangers in calorifier	deg C
Q31	DHW supply temp	deg C
Q32	DHW re-circulation temp	deg C
Q33	Steam supply to HWS calorifier 1	deg C
Q34	Steam supply to HWS calorifier 2	deg C
Q35	Condensate from HWS calorifiers	deg C
Q36	Inlet to calorifier from cold water tank	deg C
Q37	Internal air temp in solar access space	deg C
Q38	Steam pressure to HWS calorifier 1	bar
Q39	Steam pressure to HWS calorifier 2	bar
Q40	Condensate pressure from HWS calorifiers	bar
Q41	Minimum mains cold water inlet temperature (24 hours)	deg C
Q42	Minimum cold water inlet temperature to solar calorifier	deg C

R-channels: Daily energy totals and average temperatures.

Channel no.	Description	Units
R 1	Total data logging time in 24 hrs	hours
R 2	Total solar energy incident on horizontal plane	MJ/m2
R 3	Total solar energy incident on collectors	MJ/m2
R 4	Solar energy on collector plane during collection	MJ/m2
R 5	Average ambient dry-bulb air temperature	deg C
R 6	Solar energy collected	MJ
R 7	Solar energy input to solar calorifier	MJ
R 8	Increase in heat stored in solar calorifier	MJ
R 9	Increase in heat stored in solar accumulator	MJ
R10	Total solar energy output from preheat	MJ
R11	Mean storage temp in solar calorifier	deg C
R12	Mean storage temp in solar accumulator	deg C
R13	Electrical energy used by collector pump 1	MJ
R14	Electrical energy used by collector pump 2	MJ
R15	Time collector pump 1 on	hours
R16	Time collector pump 2 on	hours
R17	Time either pump on and heat X's in circuit	hours
R18	Not used.	
R19	Incidental heat gained in cold water tank	MJ

APPENDIX III

Channel no.	Description	Units
R20	Not used.	
R21	Steam energy to HWS by condensate cooling	MJ
R22	Total hot water load	MJ
R23	Average air temp in solar access space	deg C
R24	Degree-days (in front of panels. Base:18 deg C)	degCdays
R25	Degree-days (in solarimeter box. Base:18 deg C)	degCdays
R26	Degree-days (in front of panels. Base:15.5 deg C)	degCday
R27	Average mains cold water feed temp	deg C
R28	DHW re-circulation heating load	MJ

S-channls: Plant status signals: direct

Channel no.	Description
S 1	CHANGE TAPE
S 2	TERMINATE LOGGING
S 3	Collector circulating pump 1 on
S 4	Collector circulating pump 2 on
S 5	Not used.
S 6	3-way valve by-passing store heat exchangers
S 7	Store heat exchanger 1 open
S 8	Store heat exchanger 2 open
S 9	Store heat exchanger 3 open
S10	Store heat exchanger 4 open
S11	Dump valve on solar store open
S12	Solar preheat system cold feed bypass valve open
S13	Solar calorifier cold feed inlet valve open
S14	Solar calorifier to solar accumulator valve open

Plant status signals: computer generated

Channel no.	Description	Units
S15	Either collector pump 1 or 2 on	
S16	Either collector pump on AND solar calorifier in circuit	

APPENDIX III

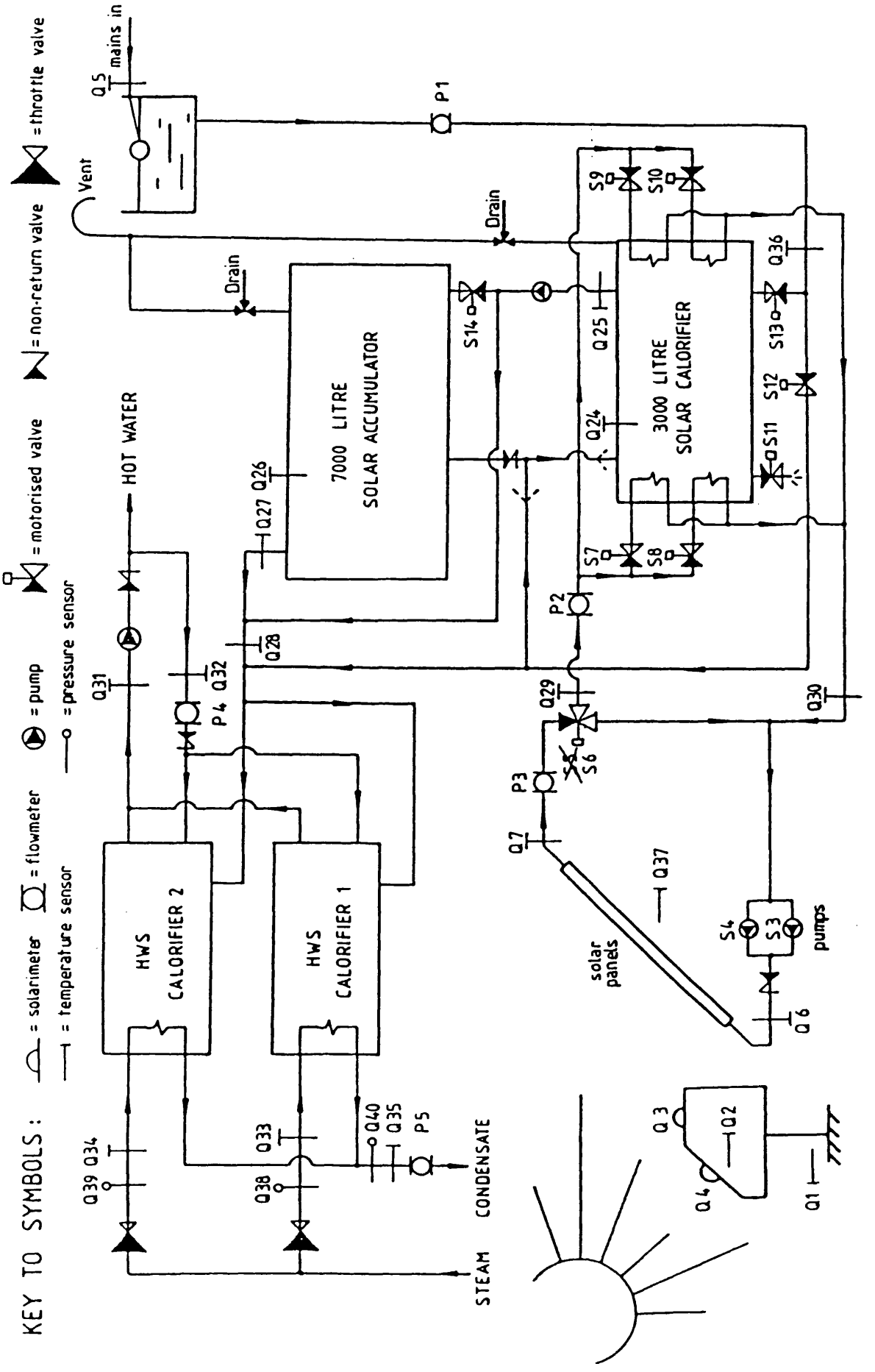

APPENDIX IV

ANALOGUE SIGNAL ATTENUATION

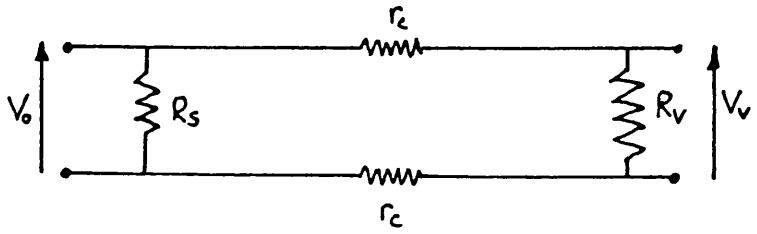

The measurement circuit for analogue signals is basically as shown above where

$2r_c$ is the total circuit resistance including all cable; contacts and reed relay scanner.

Rs is the sensor resistance.

Rv is the resistance of the voltmeter.

Vo is the voltage output of the sensor.

Vr is the voltage read by the voltmeter.

Hence $Vv = \frac{Vo\ Rv}{Rv + 2r_c}$

Now for furthest sensor, measured value of $2r_c = 15\Omega$

For voltmeter Rv = 10 MΩ

Hence attenuation = $\frac{2r_c}{Rv+2r_c} = \frac{15}{10^7} = 1.5$ ppm

i.e. attenuation is negligible.

APPENDIX V

This appendix contains the FORTRAN77 source code for the following analysis programs, subroutines and functions:

EXECUTABLE FILES

datastrip.or.plot.ec (dsop.ec)

MAIN PROGRAMS

channel.search
datastrip
function
multi.plot

SUBROUTINES

channel
data.search.and.format
findstart
finput
input
label.plot
plot
pltchan
reduce.data
status.plot
timeaxis
trans
trans2

FUNCTIONS

average
integerdate
integertime
julday
maxfun
minfun
ontime
sectime
switches
total

There are a number of subroutines called by the above analysis programs which are not listed in this Appendix. These are standard library graphics subroutines available with the Honeywell Multics system.

```
&version 2
&-dsop.ec
&-17:JUN:83
&-
&-THIS EC FILE RUNS THE DATA ANALYSIS PROGRAMS:  channel_search, datastrip, function ,multi_plot, and nchannel.
&-IT REQUIRES 4 ARGUMENTS
&-ARG 1 - PROGRAM REQUIRED:  datastrip, function, plot (for multi_plot), search (for channel_search) , or nchannel
&-ARG 2 - INSTRUCTION DATA INPUT SOURCE FOR FORTRAN PROGRAMS:  terminal OR A FILE NAME
&-ARG 3 - NAME OF DATA SOURCE FILE
&-ARG 4 - NAME OF OUTPUT FILE  *** SEE NOTES BELOW ***
&-FILE NAMES USED IN ARG 2, 3 AND 4 MUST BE FULL PATH NAMES
&-FOR PLOT OUTPUT FILE ARG 4 DO NOT ENTER  .graphics  SUFFIX (THIS IS ATTACHED AUTOMATICALLY)
&-
&trace &command off
&ready off
&if &[io opened file70] &then io close file70
&if &[io opened file80] &then io close file80
&if &[io attached  file70] &then io detach file70
&if &[io attached file80] &then io detach file80
&-
&-IF terminal NOT SPECIFIED IN ARG 2 INSTRUCTION DATA FOR FORTRAN PROGRAMS WILL BE TAKEN
&-FROM THE FILE NAMED BY ARG 2 INSTEAD.
&-IO_CALLS THAT FOLLOW ATTACH AND OPEN file05 CONNECTING IT TO vfile_  NAMED BY ARG 2
&-
&if &[equal &2 terminal]
&then &goto attach_file70
&if &[io opened file05] &then io close file05
&if &[io attached file05] &then io detach file05
io attach file05 vfile_ &2
io open file05 si
&-
&label attach_file70
&-
&-ATTACH DATA SOURCE FILE ARG 3 TO IO_SWITCH file70
&-
io attach file70 vfile_ &3
```

```
&-
&-UNLESS multi_plot PROGRAM REQUIRED (IN WHICH CASE GO AND RUN IT)
&-DELETE SEGMENT THAT MIGHT EXIST ALREADY NAMED FOR OUTPUT FILE (ARG 4)
&-RECREATE THAT SEGMENT AND ALSO ATTACH IT TO IO_SWITCH file80
&-THEN GO AND RUN PROGRAM SPECIFIED BY ARG 1
&-
&if &[equal &1 plot] &then &goto plot
&if &[exists file &4] &then dl &4
cr &4
io attach file80 vfile_ &4
&if &[equal &1 datastrip] &then &goto datastrip
&if &[equal &1 function] &then &goto function
&if &[equal &1 search] &then &goto search
&if &[equal &1 nchannel] &then &goto nchannel
&-
&-INCORRECT PROGRAM SPECIFIED BY ARG 1
&-DELETE FILE NAMED ARG 4 AND QUIT WITH ERROR MESSAGE
&-
dl &4
&print Specified program &1 not implemented by this version of dsop.ec
&goto end
&-
&-
&label datastrip
&-
&-DATA STRIPPING PROGRAM PRODUCES REDUCED DATA BLOCK IN SAME FORM AS RAW DATA
&-REDUCED DATA BLOCK IS OUTPUT TO FILE NAMED BY ARG 4
&-
on storage "" -bf -rt >udd>BABSEE>Reynell>analysis_programs>datastrip
&goto end
&-
&label plot
&-
&-PLOTTING PROGRAM USES SOURCE DATA FROM FILE ARG 3 AND PRODUCES
&-GRAPHICS OUTPUT FILE NAMED ARG 4 WITH SUFFIX .graphics
&-
&if &[exists file &4.graphics] &then dl &4.graphics
sy -of &4
on storage "" -bf -rt >udd>BABSEE>Reynell>analysis_programs>multi_plot
abc &4.graphics
&goto end
```

```
&-
&label search
&-
&-CHANNEL SEARCH PROGRAM USES SOURCE DATA FROM FILE ARG 3
&-FORMATTED DATA IS OUTPUT TO FILE NAMED BY ARG 4
&-
on storage "" -bf -rt >udd>BABSEE>Reynell>analysis_programs>channel_search
&goto end
&-
&label function
&-
&-FUNCTION PROGRAM USES SOURCE DATA FROM FILE ARG 3.
&-FORMATTED OUTPUT DATA FILE IS THAT NAMED BY ARG 4.
&-
on storage "" -bf -rt >udd>BABSEE>Reynell>analysis_programs>function
&goto end
&-
&label nchannel
&-
&-NCHANNEL PROGRAM USES SOURCE DATA FROM FILE ARG3.
&-OUTPUT DATA FILE IS THAT NAMED BY ARG4.
&-
on storage "" -bf -rt >udd>BABSEE>Reynell>analysis_programs>nchannel
&goto end
&-
&label end
&-
&-END OF EC FILE, RESET SYSTEM AND EXIST AFTER PRINTING "finished"
&-IF terminal INPUT OF INSTRUCTION DATA FOR FORTRAN PROGRAMS REQUESTED
&-THEN JUMP TO THE FINISH
&-ELSE CLOSE AND DETACH THE FILE05 SWITCH
&-
io detach file70
&if &[io attached file80] &then io detach file80
&if &[equal &2 terminal]
&then &goto finish
io close file05
io detach file05
&label finish
&print finished
&quit
```

```
* channel_search.fortran
* 09:MAR:83
*
* PRODUCES A FORMATTED BLOCK OF DATA (file80)
* WHICH IS A SUBSET OF THE INPUT DATA (file70)
*
      character*3 chan(50)
      character*10 job
      integer datefound,timefound,date1,date2,numchan,time1,time2
      logical failed
      call input(job,chan,numchan,date1,date2,time1,time2)
      call findstart (date1,time1,date2,time2,datefound,timefound,failed)
      if (failed) goto 10
      call data_search_and_format (chan,numchan,datefound,date2,timefound,time2)
      stop
10    continue
      end
```

datastrip.fortran 09/14/83 1413.0 bst Wed

```
* datastrip.fortran
* 09:MAR:83
*
* PRODUCES A BLOCK OF DATA (file80) WHICH IS A
* SUBSET OF THE INPUT DATA (file70)
*
      character*3 chan(50)
      character*10 job
      integer datefound,timefound,date1,date2,numchan,time1,time2
      logical failed
      call input(job,chan,numchan,date1,date2,time1,time2)
      call findstart (date1,time1,date2,time2,datefound,timefound,failed)
      if (failed) goto 10
      call reduce_data (chan,numchan,datefound,date2,timefound,time2)
      stop
10    continue
      end
```

```
+ function.fortran
+ 16:MAY:83
+
+ COMPUTES UPTO FIVE FUNCTIONS OF THE PARAMETERS SPECIFIED IN THE INPUT MODULE "finput".
+ FUNCTIONS ARE:    time average (average)
+                           total of readings (total)
+                           status on time (ontime)
+                           number of status changes (switches)
+                           maximum and minimum values (maxfun,minfun)
+ UPTO TO A FIVE CHARACTER KEYWORD MUST BE ENTERED AFTER EACH PARAMETER NAME TO INDICATE WHICH
+ FUNCTIONS ARE REQUIRED.  THE KEYWORD MUST CONTAIN THE LETTERS A, T, O, S, AND/OR M (IN ANY ORDER)
+ TO INDICATE THE FUNCTIONS:  Average, Total, Ontime, Switches, Maxfun_and_Minfun
+
+ E.G.    Q64,A   will yield  the time average of parameter Q64
+                   S 3,SO  will yield the number of status changes and the on time for parameter S 3
+
        character*1 fred
        character*3 chan(50)
        character*5 key(50),dummy,acchar
        character*10 job
+
        character*61 form
        integer date1,date2,time1,time2,numchan,integerdate,integertime,julday,sectime,numpts,ichan,flag(5),count
+
        real x(10000),y(10000),average,total,ontime,switches,datavalue(5),maxfun,minfun
+
        fred=" "
        acchar="ATOSM"
        call finput (job,chan,numchan,date1,date2,time1,time2,key)
+
+ THE FOLLOWING DO-LOOP PERFORMS THE REQUIRED FUNCTIONS FOR
+ EACH PARAMETER IN TURN, WRITING THE FORMATTED RESULTS TO FILE 80
+
        write (80,1000) integertime(time1),integerdate(date1),integertime(time2),integerdate(date2)
        write (80,1001) fred
        do 100 ichan=1,numchan
        call channel (chan(ichan),date1,date2,time1,time2,x,y,numpts)
```

```
      dummy=key(ichan)
*
* SET FLAG FOR EACH FUNCTION REQUIRED
* i.e flag(i)=1 if time average required , etc
*
      do 10 i=1,5
10    flag(i)=0
      do 20 i=1,5
      do 20 j=1,5
20    if (dummy(i:i).eq.acchar(j:j)) flag(j)=1
*
* CALL APPROPRIATE SUBROUTINE FOR EACH FUNCTION REQUIRED, ADJUST FORMAT
* STATEMENT "FORM" READY FOR PRINTOUT, AND INCREMENT "COUNT" TO EQUAL
* THE TOTAL NUMBER OF FUNCTIONS REQUIRED.
*
      form="(2x,a3,3x,12x  ,5x,12x  ,3x,12x  ,4x,12x  ,4x,12x  ,4x,12x  )"
      count=0
      if (flag(1).ne.1) goto 30
      form(11:15)="f12.4"
      count=count+1
      datavalue(count)=average(x,y,numpts)
30    if (flag(2).ne.1) goto 40
      form(20:24)="f12.4"
      count=count+1
      datavalue(count)=total(x,y,numpts)
40    if (flag(3).ne.1) goto 50
      form(29:33)="f12.2"
      count=count+1
      datavalue(count)=ontime(x,y,numpts)
50    if (flag(4).ne.1) goto 60
      form(38:42)="f12.0"
      count=count+1
      datavalue(count)=switches(y,numpts)
60    if (flag(5).ne.1) goto 70
      form(47:51)="f12.4"
      form(56:60)="f12.4"
      count=count+2
      datavalue(count-1)=maxfun(y,numpts)
      datavalue(count)=minfun(y,numpts)
70    continue
```

```
          write (80,form) chan(ichan),(datavalue(i),i=1,count)
100       continue
1000 format (3x,"DATA IS FOR PERIOD FROM ",i6,x,"HRS ON ",i6,4x,"TO ",i6,x,"HRS ON ",i6/)
1001 format ("CHANNEL",4x,"TIME AVERAGE",8x,"TOTAL",10x,"TIME ON",6x,"NO.OF SWITCHES",4x,"MAX VALUE",6x,"MIN VALUE"/a1)
          stop
          end
```

multi_plot.fortran 09/14/83 1413.0 bst Wed

```
* multi_plot.fortran
* 09:MAR:83
*
* INITIALISES THE MULTICS GRAPHICS SYSTEM PRIOR TO CALLING
* SUBROUTINE "PLOT", WHICH PLOTS THE GRAPH REQUIRED.
* TERMINAL INPUT OF NUMBER OF GRAPHS.
*
      print,"ENTER NUMBER OF GRAPHS TO BE PLOTTED."
      read (5,1000) numgraph
      call pltsta
      do 10 i=1,numgraph
      call plot
10    continue
      call pltend
1000  format (v)
      stop
      end
```

```
* 23:JUN:83
*
* INCLUDES SUBROUTINES:       channel
*                             data_search_and_format
*                             findstart
*                             finput
*                             input
*                             label_plot
*                             plot
*                             pltchan
*                             reduce_data
*                             status_plot
*                             timeaxis
*                             trans
*                             trans2
```

```
      subroutine channel (chan,date1,date2,time1,time2,x,y,numpts)
*
* EXTRACTS THE RELEVANT DATA (SECTIMES AND VALUES) FOR PARAMETER CHAN
* AND STORES IT IN ARRAYS X AND Y READY FOR PLOTTING
* THE TOTAL NO. OF POINTS RECORDED IS STORED IN "NUMPTS"
*
      character*1 k(2)
      character*3 chan
      character*15 indata
      character*10 form
      integer intdate,inttime,julday,sectime,date1,date2,time1,time2,numpts,datefound,timefound
      real x(10000),y(10000),daysec
      logical failed
*
      data k/"D","T"/
      daysec=3600.0*24.0
      form='(3x,f12.4)'
      if (chan(1:1).eq."S") form='(3x,f1.0)'
*
* CALLS SUBROUTINE "FINDSTART" WHICH LOCATES THE READING HEAD AT THE REQUIRED STARTPOINT
*
      call findstart (date1,time1,date2,time2,datefound,timefound,failed)
      if (failed) return
      intdate=datefound
      inttime=timefound
*
* NOW BEGIN EXTRACTION OF RELEVANT DATA FROM FILE 70
*
      numpts=1
10    read (70,1000,end=50) indata
      if (indata(1:1).eq.k(1)) goto 60
      if (indata(1:1).eq.k(2)) goto 20
      if (indata(1:3).ne.chan) goto 10
*
* DATA IS FOR CHANNEL OF INTEREST. RECORD VALUE IN Y(NUMPTS).
* ALSO RECORD THE CURRENT TIME (in hours measured from start time ) IN X(NUMPTS)
*
      numpts=numpts+1
      if (numpts.gt.10000) goto 40
      decode (indata,form) y(numpts)
```

```
          x(numpts)=(daysec*float(intdate-date1)+float(inttime-time1))/3600.0
          goto 10
20        decode (indata,1001) inttime
          inttime=sectime(inttime)
*
* THE FOLLOWING FOUR LINES TEST WHETHER THE ENDPOINT HAS BEEN REACHED
*
          if (intdate.lt.date2) goto 10
          if (intdate.gt.date2) goto 100
          if (inttime.le.time2) goto 10
          goto 100
40        print,"NUMBER OF POINTS EXCEEDED 10000."
          return
50        print,"END POINT NOT REACHED."
          return
60        decode (indata,1001) intdate
          intdate=julday(intdate)
          goto 10
100       if (numpts.eq.1) print,"NO DATA FOUND FOR CHANNEL OF INTEREST."
          x(numpts+1)=(daysec*float(date2-date1)+float(time2-time1))/3600.0
          y(numpts+1)=y(numpts)
          numpts=numpts+1
          x(1)=0.0
          y(1)=y(2)
1000      format (a15)
1001      format (x,i6)
          return
          end
```

```
      subroutine data_search_and_format (chan,numchan,date1,date2,time1,time2)
*
* READS LINES OF RAW DATA FROM FILE 70, AND OUTPUTS ALL RELEVANT DATA TO FILE 80
* IN FORMATTED SEQUENCE, WITH TIMES AND VALUES FOR EACH CHANNEL OF INTEREST REQUESTED.
*
      character*1 k(2)
      character*2 nchan,nspace
      character*20 form2,form3
      character*15 indata,lndate,lntime
      character*35 form1
      character*3 chan(50),xchan
      integer count,numchan,integerdate,date1,date2,olddate,integertime,time1,time2,timesec,julday,sectime,intdate,inttime
      integer oldtime,printchan(50),ispace,iprint
      logical dateprint,timeprint,dataprint
      real datavalue(50)
*
      open (80,defer=.true.,form="formatted")
      data k/"D","T"/
*
* SET OLD DATE AND OLD TIME EQUAL TO START DATE AND START TIME
*
      dateprint=.false.
      timeprint=.false.
      olddate=integerdate(date1)
      intdate=olddate
      oldtime=integertime(time1)
*
* WRITE HEADER LINE EVERY 30 OUTPUT LINES
*
      encode (nchan,1005) numchan
      form1='(/x,"DATE",4x,"TIME",  (5x,a3)/)'
      form1(21:22)=nchan
      write (80,form1) (chan(i),i=1,numchan)
*
* READ A LINE OF RAW DATA
*
10    read (70,1000,end=60) indata
*
* TEST IF DATA IS A DATE
*
```

APPENDIX V

```
14        if (indata(1:1).ne.k(1)) goto 15
          decode (indata,1003) intdate
          goto 10
*
* TEST IF DATA IS A TIME
*
15        if (indata(1:1).ne.k(2)) goto 19
          decode (indata,1003) inttime
          if ((inttime.eq.oldtime).and.(intdate.eq.olddate)) goto 10
*
* NEW TIME HAS BEEN FOUND.
*
          if (dataprint) goto 90
          if (dateprint) goto 89
          write (80,1001) olddate
          iprint=iprint+1
          dateprint=.true.
*
*  WRITE DATA LINE (PRECEDED BY HEADER LINE IF NECESSARY)
*
89        if (iprint.ge.30) then
                    write (80,form1) (chan(i),i=1,numchan)
                    iprint=0
          end if
          write (80,1002) oldtime
          iprint=iprint+1
          ispace=1
          do 90 i=1,numchan
          if (printchan(i).ne.1) goto 85
          form3='(  x,f7.2)'
          xchan=chan(i)
          if (xchan(1:1).eq."S") form3(9:9)="0"
          encode (nspace,1005) ispace
          form3(2:3)=nspace
          write (80,form3) datavalue(i)
          ispace=1
          printchan(i)=0
          goto 90
85        ispace=ispace+8
90        continue
```

```
          dataprint=.true.
          oldtime=inttime
          if (olddate.eq.intdate) goto 95
          olddate=intdate
          dateprint=.false.
*
* TEST WHETHER END POINT HAS BEEN REACHED
*
95        if (julday(intdate).lt.date2) goto 10
          if (julday(intdate).gt.date2) goto 70
          if (sectime(inttime).le.time2) goto 10
          goto 70
*
* TEST IF DATA IS FOR CHANNEL OF INTEREST
*
19        count=0
20        count=count+1
          if(indata(1:3).eq.chan(count)) goto 80
          if (count.eq.numchan) goto 10
          goto 20
*
* A DATA VALUE HAS BEEN FOUND FOR CHANNEL OF INTEREST No CHAN(COUNT).
* WRITE THIS VALUE INTO DATAVALUE(COUNT) USING APPROPRIATE FORMAT FORM2
* AND SET DATA_TO_PRINT FLAGS.  (Printchan(count)=1, and dataprint=.true.)
*
80        xchan=chan(count)
          form2='(3x,f12.4)'
          if (xchan(1:1).eq."S") form2='(3x,f1.0)'
          decode (indata,form2) datavalue(count)
          printchan(count)=1
          dataprint=.false.
          goto 10
60        print,"END NOT FOUND ON THIS DATA FILE"
70        close (80)
          return
1000      format (a15)
1001      format (/i6)
1002      format (/8x,i6)
1003      format (x,i6)
1004      format (a1,i6)
1005      format (i2)
          end
```

```
      subroutine findstart (date1,time1,date2,time2,datefound,timefound,failed)
*
* READS LINES OF RAW DATA SEQUENTIALLY UNTIL STARTDATE AND STARTTIME ARE FOUND
*
      character*1 k(2)
      character*15 indata
      integer date1,date2,datefound,time1,time2,timefound,inttime,julday,sectime
      logical failed
*
      failed=.false.
      inttime=time1
      datefound=date1-1
      data k/"D","T"/
      rewind 70
*
* READ NEXT LINE OF DATA
*
10    read (70,1000,end=20) indata
*
* TEST IF DATA IS A DATE OR TIME
* IF DATA IS A TIME CURRENT DATE FOUND MUST BE EQUAL TO OR GREATER THAN START DATE FOR TEST OF TIME DATA
*
      if (indata(1:1).eq.k(1)) goto 14
      if (datefound.lt.date1) goto 10
      if (indata(1:1).eq.k(2)) goto 19
      goto 10
*
* DATE DATA TEST.  UPDATES CURRENT DATE FOUND
* IF DATE IS GREATER THAN END DATE FINDSTART HAS FAILED
* IF DATE IS GREATER THAN START DATE THEN START TIME FOR SEARCH IS CHANGED TO 00.00HRS
*
14    decode (indata,1001) datefound
      datefound=julday(datefound)
      if (datefound.lt.date1) goto 10
      if (datefound.gt.date2) goto 20
      if (datefound.gt.date1) inttime=0
      goto 10
```

```
*
* TEST OF TIME DATA
* FINDSTART SUCCESSFUL PROVIDED CURRENT TIME FOUND IS GREATER THAN OR EQUAL TO START TIME, AND...
* CURRENT TIME FOUND IS LESS THAN END TIME IF CURRENT DATE EQUALS END DATE
*
19        decode (indata,1001) timefound
          timefound=sectime(timefound)
          if (inttime.gt.timefound) goto 10
          if (datefound.lt.date2) goto 40
          if (timefound-time2) 40,20,20
*
* FINDSTART UNSUCCESSFUL, OUTPUTS ERROR MESSAGE AND RETURNS THE failed PARAMETER AS TRUE
*
20        failed=.true.
          print,"START  NOT FOUND ON THIS FILE."
1000      format (a15)
1001      format (x,i6)
40        return
          end
```

```
      subroutine finput (job,chan,numchan,date1,date2,time1,time2,key)
*
* READS INPUT FROM THE TERMINAL FOR THE function PROGRAM
*
* 27th May 1982
*
      character*10 job
      character*3 chan(50),ans
      character*5 key(50)
      integer i,numchan,startdate,starttime,enddate,endtime,date1,date2
      integer julday,sectime,date,time,time1,time2
*
5     print,"JOB?"
      read (5,1004) job
      print,"Enter startdate,starttime,enddate,endtime"
      read (5,1000) startdate,starttime,enddate,endtime
      date1=julday(startdate)
      date2=julday(enddate)
      if (starttime.ne.240000) goto 6
      starttime=0
      date1=date1+1
6     if (endtime.ne.240000) goto 7
      endtime=0
      date2=date2+1
7     time1=sectime(starttime)
      time2=sectime(endtime)
      i=0
10    i=i+1
      print,"CHANNEL IDENTIFIER AND KEYWORD ?"
      read (5,1001) chan(i),key(i)
      if (chan(i).eq."0  ") goto 20
      if (i.ge.50) goto 20
      goto 10
20    numchan=i-1
      write (6,1002) job,integerdate(date1),starttime,integerdate(date2),endtime,date1,date2,time1,time2
      write (6,1003) (chan(i),i=1,numchan)
      print,"IS DATA CORRECT?"
      read (5,1001) ans
      if (ans.eq."no ") goto 5
1000  format(v)
```

```
1001      format (a3,x,a5)
1002      format (2x,"JOB",13x,"STARTDATE",4x,"STARTTIME",5x,"ENDDATE",3x,"ENDTIME",4x,
&         "JULDAY(start)",4x,"JULDAY(end)",4x,"SECTIME(start)",4x,"SECTIME(end)"/2x,a10,3(7x,i6),4x,i6,7x,i8,9x,i8,9x,i6,11x,i6)
1003      format (4x,"CHANNELS FOR WHICH INFORMATION HAS BEEN REQUESTED"/50(3x,a3))
1004      format (a10)
          return
          end
```

```
      subroutine input (job,chan,numchan,date1,date2,time1,time2)
*
* READS INPUT DATA FROM THE TERMINAL FOR THE channel_search, datastrip AND multi_plot PROGRAMS
*
      character*10 job
      character*3 chan(50),ans
      integer i,numchan,startdate,starttime,enddate,endtime,date1,date2
      integer julday,sectime,integerdate,integertime,time1,time2
*
5     print,"JOB?"
      read (5,1004) job
      print,"Enter startdate,starttime,enddate,endtime"
      read (5,1000) startdate,starttime,enddate,endtime
      date1=julday(startdate)
      date2=julday(enddate)
      if (starttime.ne.240000) goto 6
      starttime=0
      date1=date1+1
6     if (endtime.ne.240000) goto 7
      endtime=0
      date2=date2+1
7     time1=sectime(starttime)
      time2=sectime(endtime)
      i=0
10    i=i+1
      print,"CHANNEL IDENTIFIER?"
      read (5,1001) chan(i)
      if (chan(i).eq."0  ") goto 20
      if (i.ge.50) goto 20
      goto 10
20    numchan=i-1
      write (6,1002) job,integerdate(date1),starttime,integerdate(date2),endtime,date1,date2,time1,time2
      write (6,1003) (chan(i),i=1,numchan)
      print,"IS DATA CORRECT?"
      read (5,1001) ans
      if (ans.eq."no ") goto 5
1000  format(v)
1001  format (a3)
1002  format (2x,"JOB",13x,"STARTDATE",4x,"STARTTIME",5x,"ENDDATE",3x,"ENDTIME",4x,
     &  "JULDAY(start)",4x,"JULDAY(end)",4x,"SECTIME(start)",4x,"SECTIME(end)"/2x,a10,3(7x,i6),4x,i6,7x,i8,9x,i8,9x,i6,11x,i6)
```

```
1003    format (4x,"CHANNELS FOR WHICH INFORMATION HAS BEEN REQUESTED"/50(3x,a3))
1004    format (a10)
        return
        end
```

```
      subroutine label_plot (itxt)
*
* THIS SUBROUTINE IS CALLED ONCE ONLY BY SUBROUTINE "TIMEAXIS".
* IT PLOTS THE VARIOUS TEXT STRINGS IN ITXT(5) TO LABEL THE TIME AXIS.
*
      character*20 itxt(5)
      integer ichar(20),nchrs(5),ipos
      real xpos,ypos,ix
      common /grfblk/nxic,nyic,xsc,x0,cdx,xoyax,ysc,y0,cdy,yoxax,xlc,ylc
*
      cdx=cdx*float(nxic)/15.0
      ix=((15.0*cdx)-x0)*xsc
      do 100 i=1,5
      if (i.eq.1) goto 20
      if (i.eq.2) goto 21
      if (i.eq.3) goto 22
      if (i.eq.4) goto 23
      if (i.eq.5) goto 24
20              xpos=0.0
                ypos=-0.6
                ipos=3
      goto 30
21              xpos=0.0
                ypos=-1.2
                ipos=3
      goto 30
22              xpos=0.0
                ypos=-1.5
                ipos=3
      goto 30
23              xpos=ix
                ypos=-1.2
                ipos=9
      goto 30
24              xpos=ix
                ypos=-1.5
                ipos=9
      goto 30
30    call trans2 (itxt(i),ichar,nchrs(i))
      call plttxt (ichar,nchrs(i),xpos,ypos,ipos,0)
100   continue
      return
      end
```

```
      subroutine plot
*
* THIS SUBROUTINE PLOTS DATA FOR UP TO SIX PARAMETERS ON A COMMON TIME AXIS.
* EACH PARAMETER HAS A SEPARATELY SCALED AND LABELLED Y-AXIS
*
      character*3 chan(50)
      character*10 job
      integer julday,integerdate,sectime,integertime,numchan,ichan,numpts,date1,date2,time1,time2,nxinc
      logical timeday,failed
      real x(10000),y(10000),dx
*
* CALLS SUBROUTINE INPUT WHICH READS INPUT DATA FROM FILE 60 (OR TERMINAL)
*
      call input (job,chan,numchan,date1,date2,time1,time2)
*
* CALLS SUBROUTINE TIMEAXIS WHICH PLOTS THE COMMON TIME AXIS
* (NOTE: TIME AXIS INTERVALS DEPEND ON TOTAL TIME PERIOD)
*
      call axlen (10.0,7.0)
      call timeaxis (date1,date2,time1,time2,dx,nxinc,numchan,timeday)
*
* A DO-LOOP IS NOW INITIATED SO THAT EACH PARAMETER (IN CHAN) IS PLOTTED IN TURN,
* WITH A SEPARATELY SCALED AND LABELLED Y-AXIS, SUPERIMPOSED ON THE COMMON TIME AXIS.
*
      do 10 ichan=1,numchan
*
* CALLS SUBROUTINE CHANNEL WHICH EXTRACTS DATA (TIMES AND VALUES) FROM FILE 70 FOR THE PARAMETER IDENTIFIED
* BY CHAN(ichan) , AND STORES IT IN ARRAYS X AND Y.
*
      call channel (chan(ichan),date1,date2,time1,time2,x,y,numpts)
*
* CALLS SUBROUTINE PLTCHAN WHICH PLOTS THE PARAMETER IDENTIFIED BY CHAN(ichan)
*
10    call pltchan (numpts,x,y,ichan,chan(ichan),timeday)
      call pltoff
      return
      end
```

```
      subroutine pltchan(numpts,x,y,ichan,chan,timeday)
*
* THIS SUBROUTINE PLOTS THE NUMBERS IN ARRAYS X AND Y ON A COMMON TIME AXIS PREVIOUSLY DRAWN.
* A NEW Y-AXIS IS CREATED BY EACH CALL TO PLTCHAN.
*
      character*1 fred
      character*3 chan
      character*256 ity
      integer nxc,nchy,ichan,numpts,ichar(256),nyinc,isym
      real x(10000),y(10000),dy,ymax,ymin
      logical mirror,timeday
*
      mirror=.false.
      isym=ichan-1
      fred=" "
      encode (ity,1001) fred
*
* IF TIMEAXIS UNITS ARE DAYS, (logical timeday=.true.) DIVIDE EVERY X VALUE BY 24.0
*
      if (.not.timeday) goto 20
      do 10 i=1,numpts
10    x(i)=x(i)/24.0
20    continue
*
* ENTER SCALING FOR Y-AXIS
*
      encode (ity,1000) chan
      call trans (ity,ichar,nchy)
      print,"Enter minimum and maximum values for parameter."
      read (5,1002) ymin,ymax
      dy=(ymax-ymin)/10.0
      nyinc=(ymax-ymin)/dy
*
* DETERMINE POSITION OF Y-AXIS RELATIVE TO TIME AXIS. (NXC)
*
      if ((ichan.eq.2).or.(ichan.eq.4).or.(ichan.eq.6)) mirror=.true.
      if (ichan.eq.1) nxc=0
      if (ichan.eq.2) nxc=15
      if (ichan.eq.3) nxc=-3
      if (ichan.eq.4) nxc=18
```

```
          if (ichan.eq.5) nxc=-6
          if (ichan.eq.6) nxc=21
*
* PLOT Y-AXIS BY CALLING SUBROUTINE YAX
*
          call yax (ymin,dy,nyinc,nxc,ichar,nchy,.false.,mirror,isym)
*
* PLOT PARAMETER.   A SIMPLE CURVE IS PLOTTED THROUGH THE POINTS UNLESS (CHAN) IS A STATUS CHANNEL.
* IF (CHAN) IS A STATUS CHANNEL, SUBROUTINE STATUS_PLOT IS CALLED.
* THIS SUBROUTINE RE-ARRANGES ARRAYS X AND Y TO GIVE A SQUARE-WAVE TYPE GRAPH.
* NO SYMBOLS ARE PLOTTED FOR STATUS CHANNELS.
*
          if (chan(1:1).ne."S") goto 30
          call status_plot (x,y,numpts)
          isym=-1
30        call pltfn (x,numpts,y,numpts,0,0,isym)
          return
1000      format (a3)
1001      format (255(1h ),a1)
1002      format (v)
          end
```

```
      subroutine reduce_data (chan,numchan,date1,date2,time1,time2)
*
* READS LINES OF RAW DATA FROM FILE 70, SAVING ALL RELEVANT DATA IN FILE 80, UNTIL ENDPOINT IS REACHED
*
      character*1 k(2)
      character*15 indata,lndate,lntime
      character*3 chan(50)
      integer count,numchan,integerdate,date1,date2,datefound,integertime,time1,time2,timefound,julday,sectime,intdate,inttime
      logical dateprint,timeprint,end
*
      data k/"D","T"/
*
* ENCODE STARTDATE AND TIME READY FOR WRITING TO FILE80
*
      encode (lndate,1002) "D",integerdate(date1)
      dateprint=.false.
      encode (lntime,1002) "T",integertime(time1)
      timeprint=.false.
      datefound=date1
      timefound=time1
      end=.false.
*
* READ A LINE OF RAW DATA
*
10    read (70,1000,end=60) indata
*
* TEST IF DATA IS A DATE
*
14    if (indata(1:1).ne.k(1)) goto 15
      decode (indata,1001) intdate
      intdate=julday(intdate)
      if (intdate.eq.datefound) goto 10
      datefound=intdate
      lndate=indata
      dateprint=.false.
      goto 10
*
* TEST IF DATA IS A TIME
*
```

```
15        if (indata(1:1).ne.k(2)) goto 19
          decode (indata,1001) inttime
          inttime=sectime(inttime)
          if (inttime.eq.timefound) goto 10
          timefound=inttime
          intime=indata
          timeprint=.false.
          if (date2.gt.datefound) goto 10
          if (timefound.le.time2) goto 10
          end=.true.
          goto 80
*
* TEST IF DATA IS FOR CHANNEL OF INTEREST
*
19        count=0
20        count=count+1
          if(indata(1:3).eq.chan(count)) goto 80
          if (count.eq.numchan) goto 10
          goto 20
*
* PRINT DATA PRECEDED BY DATE AND TIME IF NECESSARY INTO FILE 80
*
80        if (dateprint) goto 81
          write (80,1003) indate
          dateprint=.true.
81        if (timeprint) goto 82
          write (80,1003) intime
          timeprint=.true.
          if (end) goto 70
82        write (80,1000) indata
          goto 10
60        print,"END NOT FOUND ON THIS DATA FILE"
          stop
1000      format (a15)
1001      format (x,i6)
1002      format (a1,i6)
1003      format (a7)
70        return
          end
```

```
      subroutine status_plot (x,y,numpts)
*
* THIS SUBROUTINE RE-ARRANGES ARRAYS X AND Y IN ORDER
* TO GIVE A SQUARE-WAVE TYPE PLOT IN SUBSEQUENT CALL TO "PLTFN".
*
      real x(10000),y(10000),xnew(10000)
      integer numpts,ynew(10000)
*
* FIRST ENSURE THAT ALL Y VALUES ARE INTEGER 0 OR 1.
*
      do 10 i=1,numpts
10    y(i)=int(y(i)+0.5)
*
* THE FOLLOWING LINES INSERT EXTRA POINTS INTO ARRAYS X AND Y AT EACH CHANGE OF STATE.
*
      i=1
      j=1
      xnew(1)=x(1)
      ynew(1)=y(1)
20    i=i+1
      if (i.gt.numpts) goto 30
      if (y(i).eq.ynew(j)) goto 20
      ynew(j+1)=ynew(j)
      ynew(j+2)=y(i)
      xnew(j+1)=x(i)
      xnew(j+2)=x(i)
      j=j+2
      goto 20
30    ynew(j+1)=ynew(j)
      xnew(j+1)=x(numpts)
      numpts=j+1
      do 40 i=1,numpts
      y(i)=ynew(i)
      x(i)=xnew(i)
40    continue
      return
      end
```

```
      subroutine timeaxis (date1,date2,time1,time2,dx,nxinc,numchan,timeday)
*
* THIS SUBROUTINE PLOTS THE COMMON TIME AXIS FOR SUBSEQUENT GRAPH PLOTS.
* IF TIME PERIOD IS LESS THAN OR EQUAL TO 24 HRS, TIME AXIS INTERVALS = 1 HR.
* IF TIME PERIOD IS GREATER THAN 24 HRS BUT LESS THAN OR EQUAL TO 3 x 24 HRS, TIME AXIS INTERVALS = 6 HRS.
* IF TIME PERIOD IS GREATER THAN 72 HRS, TIME AXIS INTERVALS = 24 HRS.
* THIS SUBROUTINE ALSO CALLS SUBROUTINE "LABEL_PLOT" WHICH USES TEXT
* STRINGS ITXT (1 to 5) TO LABEL THE AXES AND PROVIDE A KEY TO SUBSEQUENT OVERPLOTS.
*
      character*256 itx
      character*20 itxt(5)
      character*1 fred
      integer date1,date2,time1,time2,nxinc,nxc,nchx
      integer integerdate,integertime,ichar,startdate,starttime,enddate,endtime
      real timesec,daysec,dx
      common /grfblk/nxic,nyic,xsc,x0,cdx,xoyax,ysc,y0,cdy,yoxax,xlc,ylc
      dimension ichar(256)
      logical timeday
      timeday=.false.
      ysc=7.0
      y0=0
      cdy=0
      nyic=0
      nxc=0
      daysec=3600.0*24.0
      fred=" "
*
* THE FOLLOWING 17 LINES ENCODE THE START DATE, STARTTIME, ENDDATE,AND END TIME VALUES
* INTO TEXT STRINGS READY FOR THE LABELLING OF THE AXIS.
*
      startdate=integerdate(date1)
      starttime=integertime(time1)
      enddate=integerdate(date2)
      endtime=integertime(time2)
      do 70 i=1,5
70    encode (itxt(i),1005) fred
      encode (itxt(2),1001) startdate
      encode (itxt(3),1002) starttime
      encode (itxt(4),1003) enddate
      encode (itxt(5),1004) endtime
```

```
*
* SETS TIME AXIS INTERVALS (dx) ACCORDING TO TOTAL TIME PERIOD
*
          timesec=(float(date2-date1)*daysec)+float(time2-time1)
          if (timesec.le.(daysec/2.)) goto 10
          if (timesec.le.daysec) goto 15
          if (timesec.le.(3.0*daysec)) goto 20
*
* TIME PERIOD GREATER THAN 72 HRS
*
          dx=1.0
          timeday=.true.
          itxt(1)="TIME - DAYS"
          goto 50
*
* TIME PERIOD LESS THAN OR EQUAL TO 12 HRS
*
10        dx=1.0
          itxt(1)="TIME - HOURS"
          goto 50
*
* TIME PERIOD GREATER THAN 12 HRS BUT LESS THAN OR EQUAL TO 24 HRS.
*
15        dx=3.0
          itxt(1)="TIME - HOURS"
          goto 50
*
* TIME PERIOD GREATER THAN 24 HRS BUT LESS THAN OR EQUAL TO 72 HRS
*
20        dx=6.0
          itxt(1)="TIME - HOURS"
          goto 50
*
* TIME AXIS INTERVAL (DX) HAS BEEN DECIDED.  ENTER TITLE OF GRAPH.
*
50  if (.not.timeday) goto 60
          timesec=timesec/24.0
60        nxinc=int(timesec/(dx*3600.0))
          xoyax=xlc*float(nxc)/float(nxinc)
          print,"ENTER TITLE FOR TIME AXIS"
          read (5,1000) itx
```

```
*
* CALLS SUBROUTINE "TRANS" WHICH TRANSLATES THE CHARACTER STRING
* IN ITX INTO AN INTEGER ARRAY FOR MULTICS PLOTTING
*
      call trans (itx,ichar,nchx)
*
* PLOT AXIS BY CALLING SUBROUTINE XAX
*
      call xax (0.0,dx,nxinc,0,ichar,nchx,.false.)
*
* CALLS SUBROUTINE "LABEL_PLOT" WHICH ENCODES AND PLOTS VARIOUS TEXT STRINGS
* TO LABEL THE AXES AND PROVIDE A KEY TO SUBSEQUENT PLOTTING.
*
      call label_plot (itxt)
      return
1000  format (a256)
1001  format ("START DATE = ",i6)
1002  format ("START TIME = ",i6)
1003  format ("END DATE = ",i6)
1004  format ("END TIME = ",i6)
1005  format (19(1h ),a1)
      end
```

```
      subroutine trans (itx,ichar,nchx)
*
* THIS SUBROUTINE TRANSLATES THE CHARACTER STRING IN "ITX"
* INTO AN INTEGER ARRAY "ICHAR", IN ORDER TO MAKE IT
* INTELLIGIBLE TO "MULTICS" PLOTTING PROGRAMS.
* STRING "ITX" UPTO 256 CHARACTERS LONG
*
      character*256 itx
      integer ichar(256),nchx
*
      decode (itx,1000) (ichar(i),i=1,256)
      do 10 i=1,256
      nchx=257-i
      if (ichar(nchx).ne.1h ) return
10    continue
      nchx=0
      return
1000  format (256a1)
      end
*
*****************************************************************************
*
      subroutine trans2 (itx,ichar,nchx)
*
* THIS SUBROUTINE TRANSLATES THE CHARACTER STRING IN "ITX"
* INTO AN INTEGER ARRAY "ICHAR", IN ORDER TO MAKE IT
* INTELLIGIBLE TO "MULTICS" PLOTTING PROGRAMS.
* STRING "ITX" UPTO 20 CHARACTERS LONG
*
      character*20 itx
      integer ichar(20),nchx
*
      decode (itx,1000) (ichar(i),i=1,20)
      do 10 i=1,20
      nchx=21-i
      if (ichar(nchx).ne.1h ) return
10    continue
      nchx=0
      return
1000  format (20a1)
      end
```

```
* 16:MAY:83
*
* INCLUDES FUNCTIONS:        average
*                            integerdate
*                            integertime
*                            julday
*                            maxfun
*                            minfun
*                            ontime
*                            sectime
*                            switches
*                            total
```

```
      function average (x,y,numpts)
*
* RETURNS THE TIME-AVERAGED VALUE OF THE NUMBERS
* IN ARRAY Y, AGAINST THE TIMES IN ARRAY X.
* EACH Y VALUE Y(n) IS ASSUMED TO BE VALID FOR THE TIME PERIOD X(n) TO X(n+1).
* THE LAST Y VALUE IS DISREGARDED.
*
      integer numpts
      real x(10000),y(10000),average,yp
      average=0.0
      do 10 i=2,numpts
      yp=y(i)*(x(i)-x(i-1))
10    average=average+yp
      average=average/(x(numpts)-x(1))
      return
      end
*
*
*****************************************************************************************
*
*
      function integerdate(julday)
*
* CALCULATES THE DATE AS AN INTEGER WITH FORMAT ddmmyy
* FROM THE JULIAN DAY (julday).
* THE CENTURY IS SET AND SUBTRACTED FROM THE CALCULATED
* YEAR A.D. (y1) TO GIVE yy IN THE DATE.
*
      integer julday,integerdate,day,month,year,d1,d2,m1,y1,century
      parameter (century=1900)
      d1=julday-1720997
      y1=int((d1-121.5)/365.2425)
      d2=d1-int(365.25*y1)+int(y1/100.0)-int(y1/400.0)
      m1=int(d2/30.6001)
      day=d2-int(30.6001*m1)
      if(m1.gt.13) m1=m1-12
      month=m1-1
      if(month.lt.3) y1=y1+1
      year=y1-century
      integerdate=10000*day+100*month+year
      return
      end
```

```
      function integertime(sectime)
*
* CALCULATES THE TIME AS AN INTEGER WITH FORMAT hhmmss
* FROM THE TIME IN SECONDS FROM MIDNIGHT (sectime).
*
      integer integertime,sectime
      integertime=mod(sectime,60)+100*mod(int(sectime/60.0),60)+10000*int(sectime/3600.0)
      return
      end
*
*
*****************************************************************************
*
*
      function julday(integerdate)
*
* CALCULATES THE JULIAN DAY FROM THE DATE IN INTEGER FORMAT ddmmyy (integerdate).
* THE CENTURY IS SET AND ADDED TO yy TO GIVE THE YEAR A.D. (y1).
*
      integer julday,date,day,month,year,m1,y1,century
      parameter (century=1900)
      year=mod(integerdate,100)+century
      month=mod(int(integerdate/100.0),100)
      day=int(integerdate/10000.0)
      y1=year
      m1=month+1
      if(month.lt.3) m1=m1+12
      if(month.lt.3) y1=y1-1
      julday=int(365.25*y1)-int(y1/100.0)+int(y1/400.0)+int(30.6001*m1)+day+1720997
return
end
```

```
      function maxfun (y,numpts)
*
* RETURNS THE MAXIMUM VALUE OF THE NUMBERS IN ARRAY (Y)
*
            real y(10000),maxfun
            maxfun=-100.0
            do 10 i=1,numpts
            if (y(i).gt.maxfun) maxfun=y(i)
10          continue
return
end
*
*****************************************************************************
*
            function minfun (y,numpts)
*
* RETURNS THE MINIMUM VALUE OF THE NUMBERS IN ARRAY (Y)
*
            real y(10000),minfun
            minfun=100000.0
            do 10 i=1,numpts
            if (y(i).lt.minfun) minfun=y(i)
10          continue
            return
end
*
*****************************************************************************
*
            function ontime (x,y,numpts)
*
* RETURNS THE TOTAL TIME IN HOURS FOR WHICH THE STATUS VALUE IS 1
* THIS FUNCTION APPLIES ONLY TO A STATUS CHANNEL WHOSE STATUS (0 or 1)
* IS RECORDED IN ARRAY Y, WITH TIMES (in hours) IN ARRAY X.
*
            real x(10000),y(10000),ontime
            integer numpts
            ontime=0.0
             do 10 i=1,numpts
10          if ((int(y(i)+0.5)).eq.1) ontime=ontime+(x(i+1)-x(i))
            return
            end
```

```
      function sectime(integertime)
*
* CALCULATES THE TIME IN SECONDS FROM MIDNIGHT
* FROM THE TIME IN INTEGER FORMAT hhmmss (integertime).
*
      integer sectime,integertime,hour,minute,second
      second=mod(integertime,100)
      minute=mod(int(integertime/100.0),100)
      hour=int(integertime/10000.0)
      sectime=(hour*60+minute)*60+second
      return
      end
*
*
*****************************************************************************
*
*
      function switches (y,numpts)
*
* RETURNS THE NUMBER OF CHANGES OF STATE OF THE NUMBERS IN ARRAY Y.
* THE NUMBERS ARE FIRST CONVERTED TO INTEGER FORM, USUALLY 0 OR 1.
*
      integer numpts
      real y(10000),switches
      switches=0.0
      do 20 i=2,numpts
20    if ((int(y(i)+0.5)).ne.int(y(i-1)+0.5)) switches=switches+1.0
      return
      end
```

```
      function total (x,y,numpts)
*
* SUMS ALL THE RECORDED VALUES IN ARRAY Y.
*
      integer numpts
      real x(10000),y(10000),total
      total=0.0
*
* ONLY THE NUMBERS y(2) to y(numpts-1) ARE TOTALLED, TO ALLOW FOR
* SUBROUTINE "channel" WHICH INSERTS EXTRA POINTS x(1), y(1)
* AND x(numpts),y(numpts) FOR PLOTTING PURPOSES.
*
      do 10 i=3,(numpts-1)
10    total=total+y(i)
*
* POINTS (2) AND (numpts) WILL NOT BE USED IN THE TOTAL IF THEY ARE MERELY
* THE "DUMMY" POINTS INSERTED BY THE "channel" SUBROUTINE.   THE FOLLOWING TWO
* IF STATEMENTS ENSURE THIS.
*
      if (x(2).ne.x(1)) total=total+y(2)
      if (x(numpts).ne.x(numpts-1)) total=total+y(numpts)
      return
      end
```

modout.fortran

```
1,$P
      1             program modout
      2     c
      3     c  This program reads output files as generated by the solar modelling program
      4     c  suite, and produces an alternative output file in the same format as the data
      5     c  logger, so that graphical comparisons between measured and predicted performance can be made.
      6     c  Note:  Day numbers are valid for 1983 only.  Readings are converted to MJ where necessary.
      7     c
      8     c  The following parameters are extracted and written to unit file80, in data logger
      9     c  format, for each hour:
     10     c
     11     c  F 1    Solar energy incident on collectors        MJ/m2          SUN3
     12     c  F 2    Solar energy input to store                 MJ             C3 - S3
     13     c  F 3    Solar energy output to HWS                  MJ             TO HW2
     14     c  F 4    Auxiliary energy to HWS                     MJ              FROM AUX2
     15     c  F 5    Hot water load                              MJ              QHOT2
     16     c  F 6    Store temperature                          deg C            STORE 3
     17     c
     18             real para(6,24)
     19             character*132 indata
     20             character*11 test
     21             integer today,hour,count,integerdate,julday1
     22             logical lastday
     23     c
     24     10      read(70,1000,end=80) indata
     25     c
     26     c  Test for new day number.  When found, write out old day's data and update "today"
     27     c
     28             read(indata(84:86),1009)test
     29     1009    format(a3)
     30             if (indata(84:86).eq.'DAY') then
     31                     count=count+1
     32                     if (count.gt.1) then
     33     c
     34     c  Write out the day's data in desired format
     35     c
     36     45                          write(80,1006)today
     37                                 do 50 hour=1,23
```

```
c  Decode second part of daily output
c
          read(indata(3:13),1010)test
          if(indata(3:13).eq.'HOUR  COLL3') then
                    do 30 hour=1,24
                    read(70,1000) indata
                    read(indata(14:20),1004) para(6,hour)
30        continue
          end if
c
c  Decode third part of daily output
c
          read(indata(2:12),1010)test
          if(indata(2:16).eq.'HOUR    INCOLL3') then
                    do 40 hour =1,24
                    read(70,1000) indata
                    read(indata(2:12),1010) test
                    read(indata(16:26),1010) test
                    read(indata(38:48),1010)test
                    read(indata(27:37),1010)test
                    read(indata(16:26),1005) para(2,hour)
                    read(indata(38:48),1005) para(4,hour)
                    read(indata(27:37),1005) para(3,hour)
40        continue
          end if
          goto 10
1000      format (a132)
1001      format (i3)
1002      format (v)
1003      format (v)
1004      format (f6.2)
1005      format (v)
1006      format ('D',i6)
1007      format ('T',i6)
1008      format ('F ',i1,x,f11.4)
80        lastday=.true.
          goto 45
100       stop
          end
```

```
c  Write out the day's data in desired format
c
45                              write(80,1006)today
                                do 50 hour=1,23
                                write(80,1007) hour*10000
                                do 50 ii=1,6
                                if(ii.lt.6)para(ii,hour)=para(ii,hour)*3.6*0.001
                                if(ii.eq.1)para(ii,hour)=para(ii,hour)/270.0
                                write(80,1008) ii,para(ii,hour)
50                              continue
                                write(80,1006)integerdate(julday1+1)
                                write(80,1007)0
                                do 60 ii=1,6
                                if(ii.lt.6)para(ii,24)=para(ii,24)*3.6*0.001
                                if(ii.eq.1)para(ii,24)=para(ii,24)/270.0
60                              write(80,1008)ii,para(ii,24)
                        end if
                                if(lastday)goto 100
                        read(indata(88:90),1009)test
                        read(indata(88:90),1001) today
                        julday1=today+2445335
                        today=integerdate(julday1)
                        goto 10
                end if
c
c  Decode first part of daily output
c
                read(indata(1:11),1010)test
1010            format(a11)
                if(indata(1:10).eq.'HOUR  TAIR') then
                        do 20 hour=1,24
                        read(70,1000) indata
                        read(indata(46:56),1010)test
                        read(indata(64:74),1010)test
                        read(indata(46:56),1002) para(1,hour)
                        read(indata(64:74),1003) para(5,hour)
20              continue
                end if
c
c  Decode second part of daily output
c
                read(indata(3:13),1010)test
                if(indata(3:13).eq.'HOUR  COLL3') then
                        do 30 hour=1,24
                        read(70,1000) indata
                        read(indata(14:20),1004) para(6,hour)
```

```
1,$P
     1              program merge
     2    c
     3    c  This program reads two simultaneous data files (70,75) in data
     4    c  logger format, and merges them into one (file80).
     5    c  File70 is the normal raw data file, file75 is the output
     6    c  from program "modout". (F channels)
     7    c
     8              character*15 indata
     9              integer day1,day2,time1,time2,julday1,julday2,sectime1,sectime2,julday,sectime
    10              integer lastday,lasttime
    11    c
    12    c  Set up start date and time values
    13    c
    14              read(70,1000)indata
    15              read(indata(2:7),1001)day1
    16              write(80,1000)indata
    17              julday1=julday(day1)
    18              read(70,1000)indata
    19              read(indata(2:7),1001)time1
    20              write(80,1000)indata
    21              sectime1=sectime(time1)
    22              read(75,1000)indata
    23              read(indata(2:7),1001)day2
    24              julday2=julday(day2)
    25              read(75,1000)indata
    26              read(indata(2:7),1001)time2
    27              sectime2=sectime(time2)
    28    c
    29    c  Start merging, reading first from file70
    30    c
    31    5         if(julday1.gt.lastday)then
    32                        write(80,1002)day1
    33                        lastday=julday1
    34              end if
    35              if(time1.ne.lasttime)then
    36                        write(80,1003)time1
    37                        lasttime=time1
    38              end if
    39    10        read(70,1000,end=40)indata
    40              if(indata(1:1).eq.'D')then
```

```
35              if(time1.ne.lasttime)then
36                      write(80,1003)time1
37                      lasttime=time1
38              end if
39    10        read(70,1000,end=40)indata
40              if(indata(1:1).eq.'D')then
41                      read(indata(2:7),1001)day1
42                      sectime1=0
43                      julday1=julday(day1)
44                      goto 20
45              end if
46              if(indata(1:1).eq.'T')then
47                      read(indata(2:7),1001)time1
48                      sectime1=sectime(time1)
49                      goto 20
50              end if
51    30        write(80,1000)indata
52              goto 10
53    c
54    c  Test whether date/time1.ge.date/time2
55    c
56    20        if((julday1.gt.julday2).or.((julday1.eq.julday2).and.(sectime1.ge.sectime2)))goto 35
57              goto 30
58    c
59    c  Start reading from file75
60    c
61    35        if(julday2.gt.lastday)then
62                      write(80,1002)day2
63                      lastday=julday2
64              end if
65              if(time2.ne.lasttime)then
66                      write(80,1003)time2
67                      lasttime=time2
68              end if
69    40        read(75,1000,end=10)indata
70              if(indata(1:1).eq.'D')then
71                      read(indata(2:7),1001)day2
72                      sectime2=0
73                      julday2=julday(day2)
74                      goto 50
75              end if
76              if(indata(1:1).eq.'T')then
77                      read(indata(2:7),1001)time2
78                      sectime2=sectime(time2)
79                      goto 50
80              end if
```

```
57              goto 30
58      c
59      c  Start reading from file75
60      c
61      35      if(julday2.gt.lastday)then
62                      write(80,1002)day2
63                      lastday=julday2
64              end if
65              if(time2.ne.lasttime)then
66                      write(80,1003)time2
67                      lasttime=time2
68              end if
69      40      read(75,1000,end=10)indata
70              if(indata(1:1).eq.'D')then
71                      read(indata(2:7),1001)day2
72                      sectime2=0
73                      julday2=julday(day2)
74                      goto 50
75              end if
76              if(indata(1:1).eq.'T')then
77                      read(indata(2:7),1001)time2
78                      sectime2=sectime(time2)
79                      goto 50
80              end if
81      60      write(80,1000)indata
82              goto 40
83      c
84      c  Test whether date/time2.gt.date/time1
85      c
86      50      if((julday2.gt.julday1).or.((julday2.eq.julday1).and.(sectime2.ge.sectime1)))goto 5
87              goto 60
88      1000    format(a15)
89      1001    format(i6)
90      1002    format('D',i6)
91      1003    format('T',i6)
92              end
```

APPENDIX VI

Calculation of collector heat capacity (including water content).

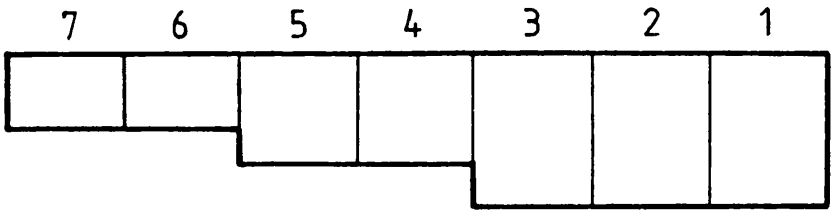

The collector array consists of seven banks, as shown, each of width six metres. Banks 1 to 3 have a riser length of 8 metres, banks 4 and 5 have a riser length of 6 metres, and banks 6 and 7 have a riser length of 4 metres.

The total area of absorber fin, A, is therefore:

$A = (18 \times 8) + (12 \times 6) + (12 \times 4)$

$= 264\ m^2$

The copper fin is 0.254mm thick, and the density of copper is 8960 Kg/m3. The mass of copper in the fin is therefore:

$8960 \times 264 \times 0.000254 = 600.8\ Kg$

APPENDIX VI

Each bank of panels contains 24 water-filled riser pipes which are standard 15mm copper tubes having an average wall thickness of 0.57mm. The total length of riser pipe, L, is therefore:

$$L = (72 \times 8) + (48 \times 6) + (48 \times 4)$$

$$= 1056 \text{ metres}$$

The mass of copper in the riser pipes is therefore:

$$8960 \times \pi \times 0.015 \times 1056 \times 0.00057 = 254 \text{ Kg}$$

The mass of water in the riser pipes is:

$$1000 \times \pi \times (0.0075)^2 \times 1056 = 187 \text{ Kg}$$

The specific heat capacity of copper is 0.38 kJ/Kg°K. The specific heat capacity of water is 4.18 kJ/Kg°K (at 20°C). The combined heat capacity of the fin, tube and water combination is therefore:

$$0.38 (600.8 + 254) + 4.18 (187) = 1106 \text{ kJ/°K}$$

Dividing this total figure by the collector aperture area of 270 m^2, we obtain a figure for the heat capacity per unit area of collector, C:

$$\underline{C = 4.1 \text{ kJ/m}^2\text{°K}}$$